Molecular and functional analysis of the gene *snoo* in *Drosophila melanogaster*

DISSERTATION ZUR ERLANGUNG DES
DOKTORGRADES DER NATURWISSENSCHAFTEN (DR. RER. NAT.)
DER FAKULTÄT FÜR BIOLOGIE UND VORKLINISCHE MEDIZIN
DER UNIVERSITÄT REGENSBURG

vorgelegt von
Matthias Josef Schramm

aus
Freyung

im Jahr
2020

Das Promotionsgesuch wurde eingereicht am:
16.10.2020

Die Arbeit wurde angeleitet von:
Prof. Dr. Stephan Schneuwly

Unterschrift:

Table of contents

Abstract

The gene *snoo* forms part of the Ski/Sno protein family, which is characterised by a conserved SAND domain and a Dachshund homology domain. Snoo interacts with the Dpp/Activin signalling pathways. However, there are serious doubts on some of the published experimental evidence of *snoo* mutants.

By combining the CRISPR/Cas9 system with homology directed repair two mutant lines with precisely defined deletions in the gene *snoo* and two Gal4 driver lines for this gene were generated. Using these driver lines, it could be revealed that *snoo* has a relatively broad expression pattern. During almost all stages of development, *snoo* is expressed in many different tissues and organs, including the central nervous system.

Furthermore, it was revealed that a knockdown of *snoo* reduces lifespan and negative geotaxis and that the deletion impairs locomotion in general. By specifically inducing a CRISPR/Cas9 dependent conditional knockout in different cell types using the Gal4/UAS system, it could be shown that these phenotypes are most likely caused by the lack of Snoo in neurons.

Finally, the transcriptomic analysis in the brains of the generated deletion lines by RNAseq and qPCR led to the identification of a set of possible target genes or interaction partners of *snoo*. These include genes that are involved in metabolic homeostasis, circadian rhythm or the resistance to xenobiotics.

1. Introduction

1.1. The TGFβ signalling pathway

As cancer is one of the major causes of death worldwide, the understanding of the mechanisms responsible for tumorigenesis is of fundamental interest for improving diagnosis and treatment of this disease. Cytokines of the Transforming Growth Factor β (TGFβ) family and the processes that are regulated by the signalling pathways that rely on these ligands are known to play crucial roles in the development of different types of tumours (Miyazono *et al*, 2003; Waite & Eng, 2003; Pot & Bonni, 2008). The members of this family are important for normal development and homeostasis (Massagué, 1990). Their ability to inhibit cell proliferation has widely been studied and the loss of this antiproliferative effect might contribute to the progression of different tumours (Derynck *et al*, 2001; Chen *et al*, 2002; Ten Dijke *et al*, 2002; Jakowlew, 2006).

Examples for ligands of the TGFβ superfamily are Bone Morphogenetic Protein (BMP), whose orthologue in *Drosophila melanogaster* is Decapentaplegic (Dpp), and Activin (Deheuninck & Luo, 2009). They signal by binding to the extracellular domain of their membrane bound receptors, which in turn form complexes consisting of two type I and two type II receptors (Wrana *et al*, 1994; Pot & Bonni, 2008). These receptors are serin/threonine kinases. Ligand binding activates the type II receptors, which activate the type I receptors by phosphorylating them (Macías-Silva *et al*, 1996; Abdollah *et al*, 1997; Kretzschmar *et al*, 1997; Souchelnytskyi *et al*, 1997; Brummel *et al*, 1999). The activated type I receptors phosphorylate the receptor associated Smad (R-Smad) proteins. The phosphorylated R-Smads form heterotrimeric complexes with the common mediator Smad (Co-Smad) Smad4, which is called Medea in *Drosophila melanogaster* (Wrana *et al*, 1992; Lagna *et al*, 1996). These complexes are transferred into the nucleus and regulate gene expression by interaction with different co-factors (Ng & Bird, 2000; Chan & La Thangue, 2001). The different TGFβ signalling pathways involve different receptors and R-Smads but share the single Co-Smad.

The TGFβ signalling pathways interact with other pathways and can be influenced by different factors like the members of the Ski/Sno family (Takaesu *et al*, 2006; Barrio *et al*, 2007; Ramel *et al*, 2007; Shravage *et al*, 2007; Jahchan & Luo, 2010; Djabrayan & Casanova, 2016; Pot & Bonni, 2008). These proteins can bind to the R-Smad/Co-Smad complexes and disrupt their formation. This interaction can especially be observed if Ski/Sno proteins are overexpressed. At more physiological levels some of these proteins seem to even stabilise the R-Smad/Co-Smad complexes or shift the affinity of the cell from one signalling pathway to another.

1.2. The Ski/Sno family

This family of transcription factors is defined by the similarities they share with the protein Sloan-Kettering Institute (Ski). The cellular gene *c-ski* coding for this protein was originally identified by its close homology to the transforming component of the avian Sloan-Kettering retrovirus *v-*

ski (Li *et al*, 1986; Nomura *et al*, 1989; Barrio *et al*, 2007; Pot & Bonni, 2008; Deheuninck & Luo, 2009). The Ski/Sno family can be further divided into three subfamilies. The Dachshund Homolog (Dach) subfamily consists of the orthologues of the *Drosophila melanogaster* gene *dachshund* (*dac*), like the human genes *dach1* and *dach2* (Mardon *et al*, 1994; Caubit *et al*, 1999; Heanue *et al*, 1999; Wu *et al*, 2003). Examples for members of the Functional Smad Suppressing Element (Fussel) subfamily are the human genes *fussel-15* and *fussel-18* and their *Drosophila melanogaster* orthologue *fussel* (Arndt *et al*, 2005, 2007; Fischer *et al*, 2012; Takaesu *et al*, 2012; Rass *et al*, 2019). The Ski/Sno subfamily consists of *ski* itself and the mammalian Ski novel gene (SnoN). The gene *sno* coding for this protein was originally identified by its high sequence homology to *ski* (Nomura *et al*, 1989). The protein Sno oncogene (Snoo) is the orthologue of the mammalian proteins SnoN and Ski in *Drosophila melanogaster* (Graca *et al*, 2004; Barrio *et al*, 2007).

The members of the Ski/Sno family show both, prooncogenic and antioncogenic activities, depending on the protein levels and stages of cancer. They have been shown to induce cell growth by antagonising TGFβ dependent cell cycle arrest if they are overexpressed and at early stages of cancer (Pot & Bonni, 2008; Bonni & Bonni, 2012; Tecalco-Cruz *et al*, 2018). At lower physiological levels they might even promote TGFβ dependent transcription and act as tumour suppressors by inhibiting tumour invasion at later stages of cancer (Deheuninck & Luo, 2009; Jahchan & Luo, 2010).

The proteins of the Ski/Sno family share an evolutionary conserved domain structure (Jahchan & Luo, 2010). The N-terminally located Dachshund homology domain (DHD) has a globular structure consisting of five β-sheets and four α-helices (Pearson-White & Crittenden, 1997; Kozmik *et al*, 1999; Wu *et al*, 2003; Pot & Bonni, 2008; Deheuninck & Luo, 2009; Bonni & Bonni, 2012; Tecalco-Cruz *et al*, 2018). It contains a groove with an open and a closed conformation that might act as a platform for the interaction with other proteins, especially with transcriptional co-regulators. Furthermore, the DHD contains a Destruction Box (D-Box). This motif mediates the ubiquitin-proteasomal dependent degradation by which the protein levels of the members of the Ski/Sno family are regulated (Pot & Bonni, 2008).

Another conserved domain at the N-terminus is the Sp100, AIRE1, NucP41/75 and DEAF1 (SAND) domain (Pot & Bonni, 2008; Deheuninck & Luo, 2009; Bonni & Bonni, 2012; Walldén *et al*, 2017; Tecalco-Cruz *et al*, 2018; Ji *et al*, 2019). Unlike the SAND domain found in chromatin remodelling proteins, the domain of Ski/Sno proteins is not able to directly bind DNA. Instead it contains a C2H2 zinc finger motif, which contributes to its structural stability, and an interaction loop motif that mediates the interaction with the Co-Smad.

The C-terminus of the Ski/Sno family is less conserved than the N-terminus. The members Ski/Sno subfamily contains Coiled-coil motifs at their C-terminus. In the case of the mammalian

proteins SnoN and Ski, these motifs were shown to mediate homo- and heterodimerisation (Pot & Bonni, 2008; Deheuninck & Luo, 2009).

1.3. Snoo is a member of the Ski/Sno family

Snoo is encoded by the gene *snoo* (sequence location on 2L: 7,984,196 – 7,891,187) which is transcribed into four different mRNAs that only differ in their untranslated regions (Takaesu *et al*, 2006; Barrio *et al*, 2007). It consists of two translated exons that are separated by a 78,434 bp long intron (Fig 1). The first exon (sequence location on 2L: 7,976,190 – 7,975,189) is 1,002 bp long and contains the DHD and the SAND domain. Therefore, this exon contains both functionally important domains. The second exon (sequence location on 2L: 7,896,754 – 7,894,085) is 2,670 bp long.

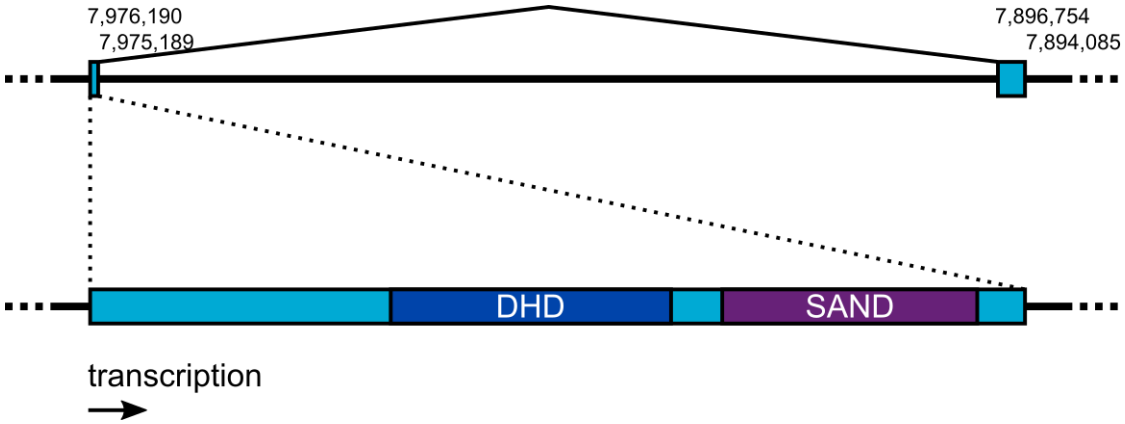

Fig 1. Schematic overview of the *snoo* locus.

snoo is located on the second chromosome and consists of 2 exons which are separated by a 78,434 bp long intron. The first exon (7,976,190 – 7,975,189) is 1,002 bp long, the second exon (7,896,754 – 7,894,085) consists of 2,670 bp (top). Both known functionally important and evolutionary conserved domains reside within the first exon (bottom). DHD: Dachshund homology domain; SAND: Sp100, AIRE1, NucP41/75 and DEAF1 domain.

The members of the Ski/Sno family are known to interact with the TGFβ signalling pathway (Takaesu *et al*, 2006; Barrio *et al*, 2007; Ramel *et al*, 2007; Shravage *et al*, 2007; Jahchan & Luo, 2010; Djabrayan & Casanova, 2016; Pot & Bonni, 2008). If they are overexpressed, Snoo and its mammalian orthologues interfere with the TGFβ signalling pathway (Barrio *et al*, 2007; Pot & Bonni, 2008; Jahchan & Luo, 2010; Walldén *et al*, 2017). Especially Ski has been shown to disrupt the heteromeric Smad complexes. In contrast to these results, SnoN seems to even stabilise the Smad complexes and therefore positively interact with the TGFβ signalling pathway if it is expressed at physiological levels. In this regard, Snoo seems to share more similarities with SnoN than Ski, as it has been proposed that Snoo shifts the affinity of the Co-Smad Medea from the R-Smad of the Dpp signal Mother Against Dpp (Mad) towards Smad on X (Smox), which is the R-Smad of the Activin signalling pathway (Brummel *et al*, 1999; Raftery & Sutherland, 1999; Takaesu *et al*, 2006).

1.4. Functions of *snoo*

Previous studies have shown that the interaction of Snoo with the TGFβ signalling plays important roles during development. In particular, this includes the formation of wing veins, tracheae and the eggshell (Ramel *et al*, 2007; Shravage *et al*, 2007; Djabrayan & Casanova, 2016). The vertebrate orthologues of Snoo have also been shown to be important for the formation of different organs and tissues. For example, SnoN is required for the proliferation of granule neuron precursors in the postnatal mammalian cerebellum and promotes the differentiation of adipocyte progenitor cells during adipogenesis (Zhu *et al*, 2018; Chen *et al*, 2019).

The expression of Snoo has been shown to start at embryonal stage 14 (Takaesu *et al*, 2006). It is increased with further onset of embryogenesis. At embryonal stage 17 *snoo* expression was found to be restricted to the central nervous system (CNS). At the end of the embryogenesis Snoo seems to be expressed in the whole organism. This ubiquitous expression continues during all postembryonic stages. Like the ubiquitous *snoo* expression, the mammalian *ski* can also be found to be expressed in all embryonic and adult tissues at low levels (Jahchan & Luo, 2010; Deheuninck & Luo, 2009). During different stages *ski* expression is increased in specific tissues. The first peak of *ski* expression correlates with neural tube closure during embryogenesis. This is in concordance with the first peak of *snoo* expression in *Drosophila melanogaster* that seems to appear with the formation of the CNS.

Some null mutations of the *snoo* gene were found to be lethal or have reduced viability and fertility (Takaesu *et al*, 2006). In contrast to this, other studies could not reproduce this observations (Barrio *et al*, 2007; Quijano *et al*, 2010). All the different mutation lines used in these studies consist of relatively large genomic deletions within the *snoo* locus. These deletions not only affect *snoo* but also adjacent genes. It has been proposed that the discrepancies of the phenotypes between the different mutant lines could be explained by the varying conditions in different laboratories, especially regarding the composition of the used food (Quijano *et al*, 2010).

1.5. Genomic engineering using the CRISPR/Cas9 method

The Clustered Regularly Interspaced Short Palindromic Repeats / CRISPR-associated 9 (CRISPR/Cas9) method has become one of the most commonly used techniques for genomic editing (Gasiunas *et al*, 2012; Jinek *et al*, 2012; Gratz *et al*, 2014; Doudna & Charpentier, 2014). The system relies on the endonuclease Cas9 that can be guided to specific target sequences in the genome by single guide RNAs (sgRNAs). These target sequences are 20 bp long and have a 3 nucleotide NGG protospacer adjacent motif (PAM). The Cas9 induces double strand breaks (DSBs) in these target sequences. These DSBs induce cellular repair mechanisms that can result in mutations. The ligation process non-homologous end joining (NHEJ) can induce small insertions or deletions (indels). Such indels can result in a frameshift and thereby disrupt gene function.

By combining the CRISPR/Cas9 system with homology-directed repair (HDR) precise editing of the genomic DNA or the insertion of exogenous sequences is possible. This method relies on the addition of a template sequence that is partly homologous to the sequences upstream and downstream of the DSBs introduced by CRISPR/Cas9. This enables the generation of precise genomic deletions within a gene locus of interest. Furthermore, this method can be used to generate genetic driver lines, for example for the Gal4 / Upstream Activation Sequence (UAS) system.

1.6. Employing CRISPR/Cas9 for conditional knockdown

Many genes can have different functions in different tissues or stages of the development. In these cases, the phenotype of a general knockout can be difficult to explain. Different methods have been developed to specifically disrupt the function of a gene dependent on time and space (Port & Bullock, 2016). These enable to narrow down aspects of the phenotypes of a general knockout to certain tissues or developmental stages. Example for such methods are RNAi based approaches. Using genetic drivers like the Gal4/UAS system these can be specifically induced in the desired tissues. The main disadvantage of these methods is the fact that they often result in incomplete knockdowns and therefore fail to reveal gene functions.

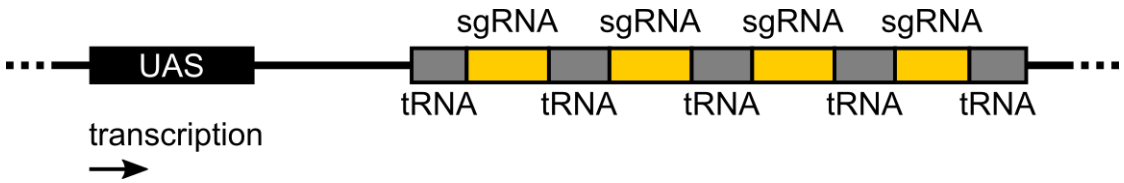

Fig 2. UAS construct used for conditional knockout.

Under the control of the UAS a multiplex of sgRNAs and transfer RNAs (tRNAs) is expressed. The processing of the tRNA sequences liberates the sgRNAs. They interact with the Cas9 protein and guide it to specific target sequences within the genome.

A more reliable approach consists in employing the CRISPR/Cas9 system for conditional mutagenesis. The Gal4/UAS system is used to drive the expression of the Cas9 protein and sgRNAs targeting the gene locus of interest (Port & Bullock, 2016). This was shown to specifically induce indel mutations that result in frameshifts in the Gal4 expressing cells. It was also proven that the expression of at least 4 different sgRNAs is sufficient to achieve almost 100 % mutation efficiency. This method is based on the UAS dependent expression of the sgRNAs as a multiplex. In this multiplex the sgRNAs are interspaced and flanked by transfer RNA (tRNA) sequences (Fig 2). After transcription of the multiplex, the processing of the tRNAs liberates the sgRNAs and they can interact with the Cas9 protein to guide it to their target sequences in the genome.

1.7. The Insulin/IGF signalling (IIS) in *Drosophila melanogaster*

The Insulin / Insulin-like Growth Factor (IGF) signalling (IIS) in *Drosophila melanogaster* relies on eight orthologues of the mammalian Insulin, the Insulin-like peptides (Ilps). These signal

through a single Insulin receptor (InR), which is a receptor tyrosine kinase (Brogiolo *et al*, 2001; Grönke *et al*, 2010; Nässel *et al*, 2015). Most of the different Ilps show great similarities to mammalian Insulin regarding the sequences of their coding genes, processing and protein structure. Only Ilp6 was proposed to show more structural and functional similarities to IGF than to Insulin. Each of the eight Ilps shows a distinct expression pattern that is cell-specific and dependent on the developmental stage. Three of these peptides, Ilp2, Ilp3 and Ilp5, are produced by a set of 14 median neurosecretory cells (mNSCs) within the brain (Cao & Brown, 2001; Broughton *et al*, 2005) that are therefore called Insulin producing cells (IPCs). The IGF-like Ilp6 is produced in the larval and adult fat body (Okamoto *et al*, 2009). The other Ilps are produced in different tissues that include the intestines or the ovaries.

The Ilps also differ in their functional activity. The three Ilps produced in the IPCs are known to regulate the levels of stored energy and circulating carbohydrates (Nässel *et al*, 2015; Broughton *et al*, 2005). Deletion of the genes coding for these peptides or ablation of the IPCs have been shown to increase the storage of lipids and carbohydrates. Ilp5 seems to be involved in the regulation of triacylglyceride (TAG) levels (Semaniuk *et al*, 2018), while especially Ilp2 influences glucose levels in the haemolymph (Broughton *et al*, 2005). Both are involved in the regulation of glycogen synthesis. Furthermore, the lack of these peptides results in an increased lifespan, reduced fecundity and increased stress response. However, it cannot be explained yet, how the Ilps can have different functions even though they signal through a single common receptor.

1.8. Aim of this study

The goal of this project was to gain further insight into both, the protein Snoo and the gene *snoo* coding for it, in *Drosophila melanogaster*. As the discrepancy in previously published results is most likely caused by the fact that they were achieved using mutants which consist of relatively large genomic deletions, new null mutants of *snoo* should be generated first. Combining the CRISPR/Cas9 method with homology directed repair (HDR) it is possible to generate defined deletions. This new deletion lines should be used to address the question if a lack of *snoo* is lethal. Furthermore, the phenotype of a *snoo* null mutation should be analysed.

A similar approach to the generation of null mutants can be employed to generate Gal4 driver lines. By using these to drive the expression of GFP, it is possible to analyse the expression pattern of Snoo.

To further analyse the phenotypes found in the new deletion lines, a conditional knockout line for *snoo* was generated. Inducing this conditional knockout with different driver lines should allow to narrow down the phenotypical effects of a lack of Snoo to certain cell types or tissues.

Additional to this spatial investigation of the phenotype of a *snoo* deletion, an RNA sequencing approach should be used to identify possible targets of this gene. Therefore, RNA should be extracted from brains of one of the deletion lines and sequenced. The results should be validated by qPCR analysis of RNA extracted from brains of both deletion lines.

2. Results

2.1. Generation of *snoo* null mutations

The *snoo* mutant lines used in previous studies consist of relatively large genomic deletions which also affect adjacent genes (Takaesu *et al*, 2006; Shravage *et al*, 2007; Quijano *et al*, 2010). These lines show divergent phenotypes. Most importantly some lines are homozygous lethal, while others are not. To clear this issue, new mutant lines of *snoo* were generated. The CRISPR/Cas9 method was used to generate defined deletions at the gene locus.

To generate the null mutation $snoo^{del1}$ a DSB was introduced 158 bp upstream of the start codon of *snoo* and another one 979 bp downstream (Fig 3). By employing HDR the sequence in between these DSBs was replaced by the fluorescent marker dsRed, which allowed for the selection of the transformed flies. The sequence of dsRed is flanked by two LoxP sites. The Cre-Recombinase can be used to induce the recombination of the two LoxP sites to remove the fluorescence marker from the genome. This mutation lacks almost the complete first exon of *snoo*. As both, the translation start site and the functionally important domains, are absent in this mutant line, there should be no possibility of a functional protein to be expressed.

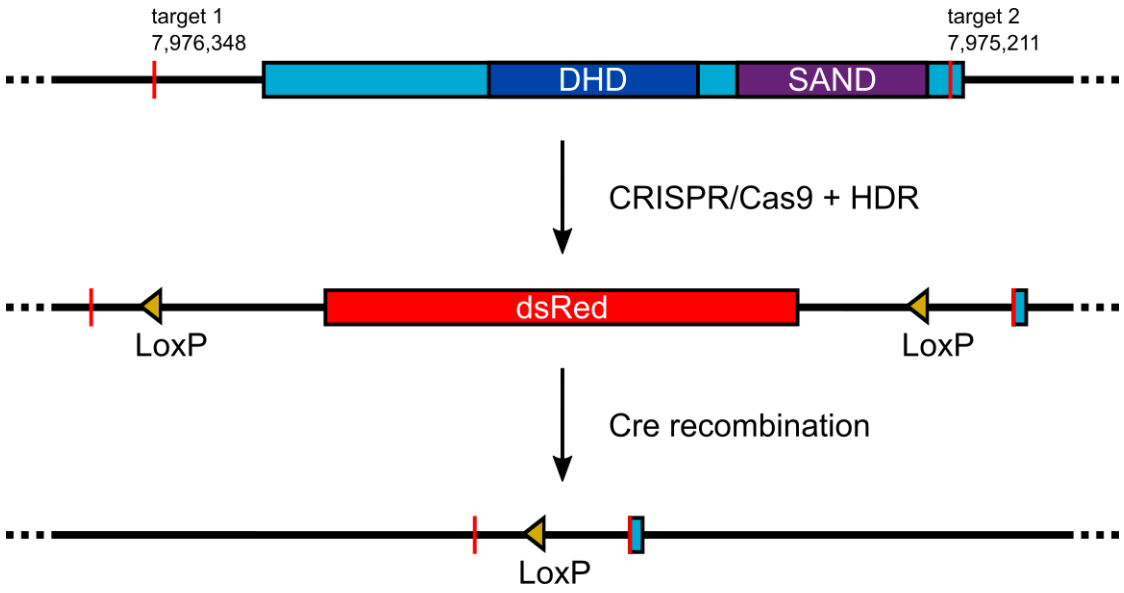

Fig 3. Generation of $snoo^{del1}$.

Two DSBs were introduced at chromosomal positions 7,975,211 (target 2) and 7,976,348 (target 1) using CRISPR/Cas9. The sequence in between the DSBs was replaced with the sequence of dsRed flanked by two LoxP sites by employing HDR. Cre recombinase was used to induce recombination of the two LoxP sites and thereby remove the marker dsRed.

The vectors coding for the sgRNAs targeting the sequences GTGATAGGAGTACGACGATT (target 1) and GCACAAGGCGCAGCGGGAAT (target 2) were cloned by annealing of the corresponding oligonucleotides and ligating them into the vector pU6-BbsI-gRNA. The resulting plasmids were named pU6-$snoo^{target01}$-gRNA and pU6-$snoo^{target02}$-gRNA. To generate the template plasmid for HDR, the sequences homologous to the sequences upstream (homology 1) and

downstream (homology 2) of the edited region were amplified by PCR from genomic DNA and cloned into the vector pHD-DsRed-attP. The resulting plasmid was named pHD-snoo^{hom01}-DsRed-attP-snoo^{hom02}. These plasmids were injected into embryos of the stock *w^{-}; vas-Cas9*. The resulting flies were crossed to the balancer stock *w^{-}; CyO/Sco*. The transformed flies in the offspring of these crosses where identified by the fluorescent signal of dsRed. Transformants were crossed back to the balancer and homozygous stocks of the genotype *w^{1118}; snoo^{del1,dsRed}* were established (labelled as *snoo^{del1}*). This mutation was confirmed using genotyping, sequencing and analysis of the transcriptional activity by qPCR (Fig 4).

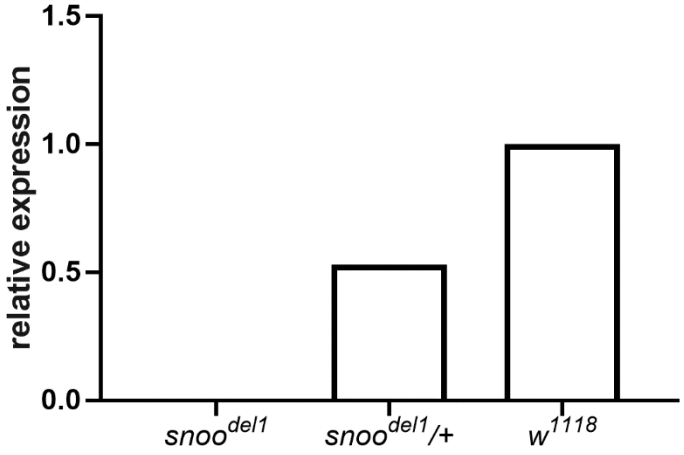

Fig 4. Expression analysis of *snoo^{del1}*.

No expression of *snoo* can be detected in homozygous mutants. Heterozygous flies show half of the *snoo* expression of *w^{1118}*. The RNA of 50 heads from each genotype was extracted and used for cDNA synthesis. qPCR was performed with a primer pair for *snoo*. The relative expression was calculated using the ΔΔCq method.

The null mutation *snoo^{del1}* does not show any visible phenotype except for a marginal deformation of the wing veins. When the mutation was transferred into another genetic background by homologous recombination, this phenotype was lost. Because of this, it was suspected that the phenotype is not caused by the absence of *snoo* but by some other mutation present in the genetic background of the deletion line. To proof this, a second deletion line was generated.

The mutation *snoo^{del2}* was generated by inducing a DSB 379 bp and another one 586 bp downstream of the start codon of *snoo* (Fig 5). Between these DSBs the same sequence was inserted as for the generation of *snoo^{del1}*. The mutation *snoo^{del2}* only lacks 207 bp within the DHD. In this case, translation should be started but be disrupted by a stop codon that was inserted at the site of the deletion. It is unlikely that the produced peptide of 127 amino acids has significant functional activity. Therefore, this line can also be considered a null mutation.

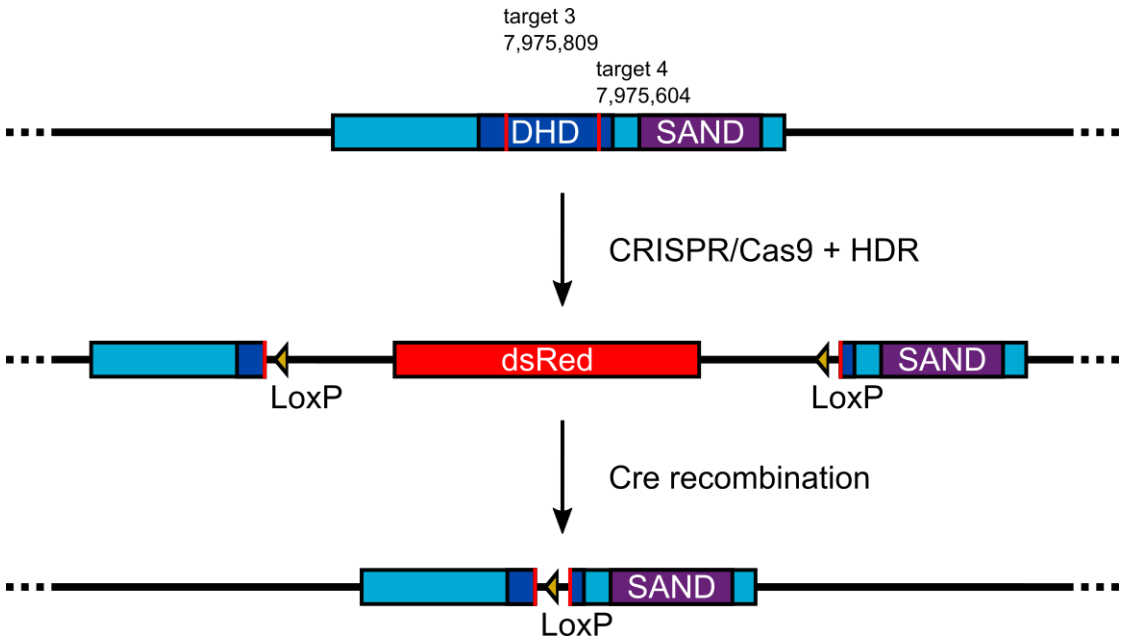

Fig 5. Generation of *snoo*^{del2}.

Using CRISPR/Cas9 two DSBs were introduced at chromosomal positions 7,975,604 (target 4) and 7,975,809 (target 3). Using HDR the deleted sequence was replaced by the marker dsRed flanked by two LoxP sites. Inducing recombination of the LoxP sites with Cre recombinase allowed for the removal of dsRed.

The used sgRNAs targeted the sequences GCCCACGGAGAAGCATCCAA (target 3) and GAGGCGTTCCGCATCGGTTC (target 4). The plasmids coding these sgRNAs were cloned like the ones for *snoo*^{del1} and named pU6-snoo^{target03}-gRNA and pU6-snoo^{target04}-gRNA. This is also the case for the sequences homologous to the regions upstream (homology 3) and downstream (homology 4) of the edited site. The resulting template plasmid was designated pHD-snoo^{hom03}-DsRed-attP-snoo^{hom04}. These three plasmids were injected into embryos of the stock *y*$^{-}$, *w*$^{-}$, *vas-Cas9*. Transformed flies were identified by the fluorescence of dsRed. By backcrossing to the balancer stock *w*$^{-}$*; CyO/Sco* a stock of the genotype *w*^{1118}*; snoo*^{del2,dsRed} was established (labelled as *snoo*^{del2}). This mutation was confirmed using genotyping, sequencing, and analysis of the transcription activity by qPCR (Fig 6).

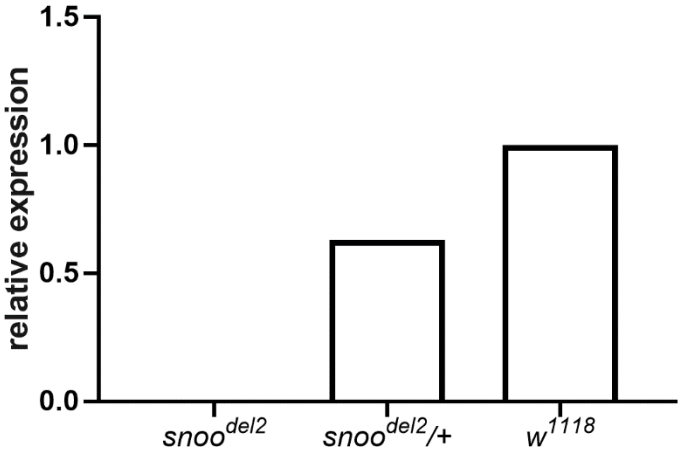

Fig 6. Expression analysis of *snoo^{del2}*.

The homozygous flies of this line also show no *snoo* expression. The *snoo* expression of heterozygous individuals is also reduced to half in comparison to *w^{1118}*. The RNA of 50 heads from each genotype was extracted and used for cDNA synthesis. qPCR was performed with a primer pair for *snoo*. The relative expression was calculated using the ΔΔCq method.

To remove the fluorescence marker dsRed by recombination, *snoo^{del1}* or *snoo^{del2}*, respectively, were crossed to *y^{-}*, *w^{-}; Sco/CyO,Cre*. In the offspring of these crosses individuals showing the phenotype of *CyO* and no fluorescent signal were identified and crossed back to establish homozygous stocks of the genotypes *w^{1118}; snoo^{del1}* (labelled as *snoo$^{del1,-dsRed}$*) and *w^{1118}; snoo^{del2}* (labelled as *snoo$^{del2,-dsRed}$*). Phenotypical analysis revealed no differences between *snoo^{del1}* and *snoo$^{del1,-dsRed}$* or between *snoo^{del2}* and *snoo$^{del2,-dsRed}$*, respectively. Therefore, the stocks *snoo^{del1}* and *snoo^{del2}*, which still contain the fluorescence marker, were used for further experiments to ease the handling of the stocks.

The balancer *w^{-}; CyO/Sco* was crossed several times to Wildtype Berlin (WTB) to exchange all chromosomes except of the second and establish the stock *CyO/Sco*. The stocks *snoo^{del1}* and *snoo^{del2}* were crossed several times to *CyO/Sco* to transfer the mutations from the *w^{1118}* background into the genetic background of WTB.

2.2. Generation of *snoo* Gal4 driver lines

To be able to analyse the expression pattern of *snoo*, two Gal4 driver lines were generated. This was done using a similar approach as for the generation of the deletion lines. The driver line *snoo-Gal4.2* was generated using the same sgRNA coding plasmids that were used for the generation of *snoo^{del1}* (Fig 7). Another template was cloned and additionally to the fluorescent marker dsRed flanked by LoxP sites the sequence of Gal4.2 was inserted into the genome.

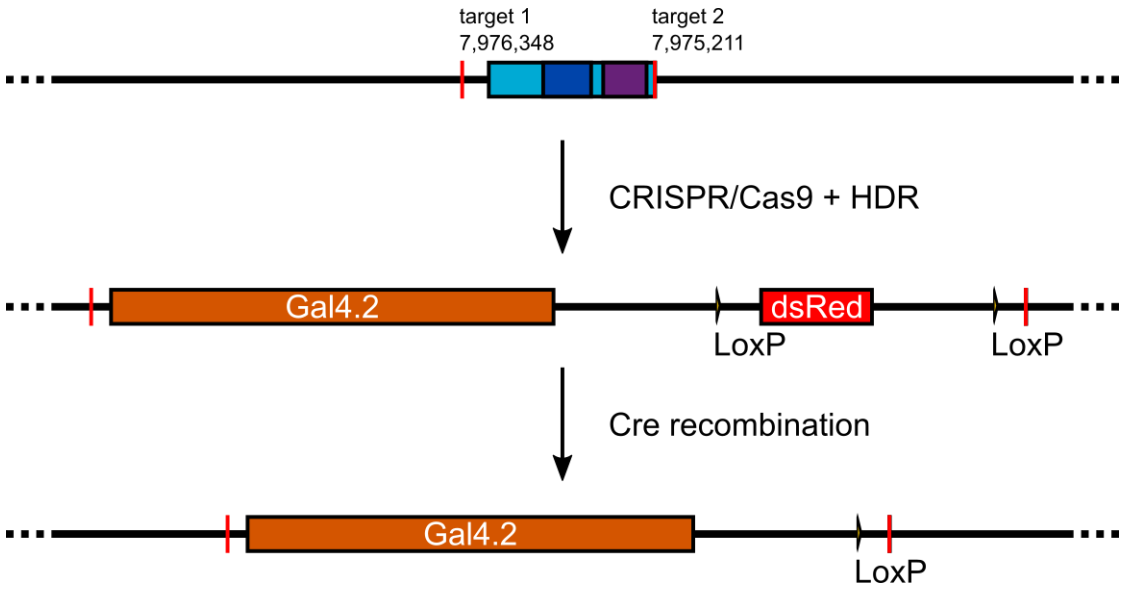

Fig 7. Generation of the line *snoo-Gal4.2*.

The CRISPR/Cas9 method was used to introduce two DSBs at the same chromosomal positions as for the generation of *snoo*^{del1}. Upstream of the marker dsRed the sequence of Gal4.2 was inserted between the DSBs. Cre recombinase was used to induce recombination of the two LoxP sites and thereby remove the marker dsRed.

The sequence of Gal4.2 was amplified by PCR from the plasmid pBPGAL4.2Uw-2 and cloned into pT-GEM(0) to generate the vector pT-GEM-Gal4.2. The same homologous sequences that were used for the generation of *snoo*^{del1} were cloned into this vector. The resulting plasmid was named pT-GEM-snoo^{hom01}-Gal4.2-snoo^{hom02}. It was injected into embryos of the stock *w*$^{-}$*; vas-Cas9* together with the plasmids pU6-snoo^{target01}-gRNA and pU6-snoo^{target02}-gRNA. Transformant flies were identified by the fluorescent signal of dsRed and by crossing to the balancer *w*$^{-}$*; CyO/Sco* a stock with the genotype *w*^{1118}*; snoo-Gal4.2*^{dsRed}*/CyO* was established (labelled as *snoo-Gal4.2*^{dsRed}). The genomic editing was confirmed by genotyping and sequencing.

However, it was not possible to establish a homozygous stock of this driver line, leading to the conclusion that the mutation is homozygous lethal. This was unexpected as both deletion lines, *snoo*^{del1} and *snoo*^{del2}, are homozygous viable. This discrepancy caused doubts about the credibility of the experimental results obtained with this diver line. To double check these results, a second diver line was generated. For the generation of *snoo-T2A-Gal4* a single DSB was induced 294 bp downstream of the start codon of *snoo* (Fig 8). Therefore, no genomic sequences were deleted in this case. The sequences of T2A and Gal4 were inserted in frame with *snoo* at the position of the DSB followed by the fluorescent marker dsRed flanked by two LoxP sites. In this line the first 98 amino acids of *snoo* are translated followed by T2A-Gal4 as one peptide. The autoproteolytic activity of T2A liberates the Gal4 protein.

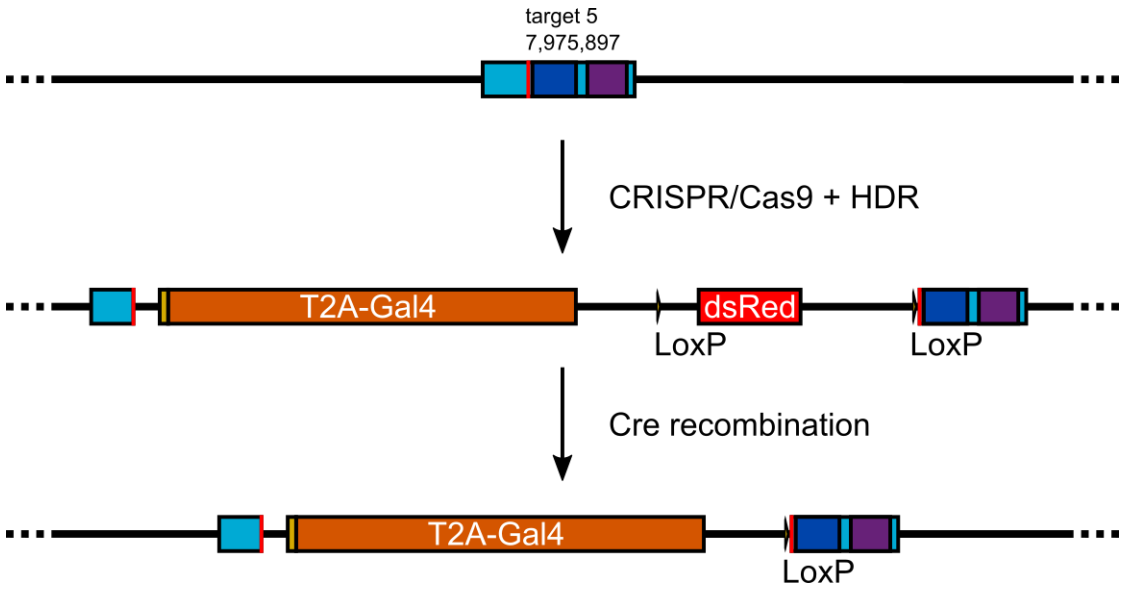

Fig 8. Generation of the line *snoo-T2A-Gal4*.

A DSB was introduced at chromosomal position 7,975,897 (target 5). Upstream of the marker dsRed the sequence of T2A-Gal4 was inserted in frame with the translation start site of *snoo*. Inducing recombination of the LoxP sites with Cre recombinase allowed for the removal of dsRed.

The plasmid pU6-snoo^{target05}-gRNA coding for a sgRNA targeting the sequence GGCTGCGA-TAGTTCACGGGG (target 5) was cloned like the other sgRNA coding plasmids by annealing of oligonucleotides and cloning them into the vector pU6-BbsI-gRNA. The sequences homologous to the sequences upstream (homology 5) and downstream (homology 6) of the induced DSB were cloned into the vector pT-GEM(0). The resulting plasmid was designated pT-GEM-snoo^{hom05}-snoo^{hom06}. Both plasmids were injected into embryos of the stock *w^{-}; vas-Cas9*. The dsRed signal was used for identification of the transformants and by crossing to the balancer *w^{-}; CyO/Sco* a stock with the genotype *w^{1118}; snoo-T2A-Gal4^{dsRed} /CyO* was established (labelled as *snoo-T2A-Gal4^{dsRed}*). The genomic editing was confirmed by genotyping and sequencing. A homozygous stock of *snoo-T2A-Gal4^{dsRed}* could not be established, as it was the case for the other driver line *snoo-Gal4.2^{dsRed}*. As both driver lines are homozygous lethal, it can be assumed that this is a general characteristic of the expression of Gal4 under the control of the *snoo* promotor and most not caused by the absence of Snoo.

To remove the fluorescence marker dsRed by recombination *snoo-Gal4.2^{dsRed}* or *snoo-T2A-Gal4^{dsRed}*, respectively, were crossed to *y^{-}, w^{-}; Sco/CyO,Cre*. In the offspring of this cross individuals showing the phenotype of CyO and no fluorescent signal were identified and crossed back to establish the stocks *w^{1118}; snoo-Gal4.2/CyO* (labelled as *snoo-Gal4.2*) and *w^{1118}; snoo-T2A-Gal4/CyO* (labelled as *snoo-T2A-Gal4*).

2.3. Analysis of the *snoo* expression pattern

To analyse the expression pattern of *snoo snoo-Gal4.2* and *snoo-T2A-Gal4* were used to drive the expression of β-Galactosidase (β-Gal) or derivatives of Green Fluorescent Protein (GFP). The

expression of these proteins was subsequently analysed by microscopy. When investigated with a fluorescent microscope, GFP signals can be observed throughout the whole larva or adult fly. This is the case for both driver lines. In general, they show remarkably similar expression patterns. The most obvious difference consists in the overall stronger expression of *snoo-T2A-Gal4*.

2.3.1. Snoo is expressed during embryogenesis

The line *snoo-Gal4.2* was used to drive the expression of β-Gal. Embryos were stained with antibodies for β-Gal and the neuronal marker Elav (Fig 9).

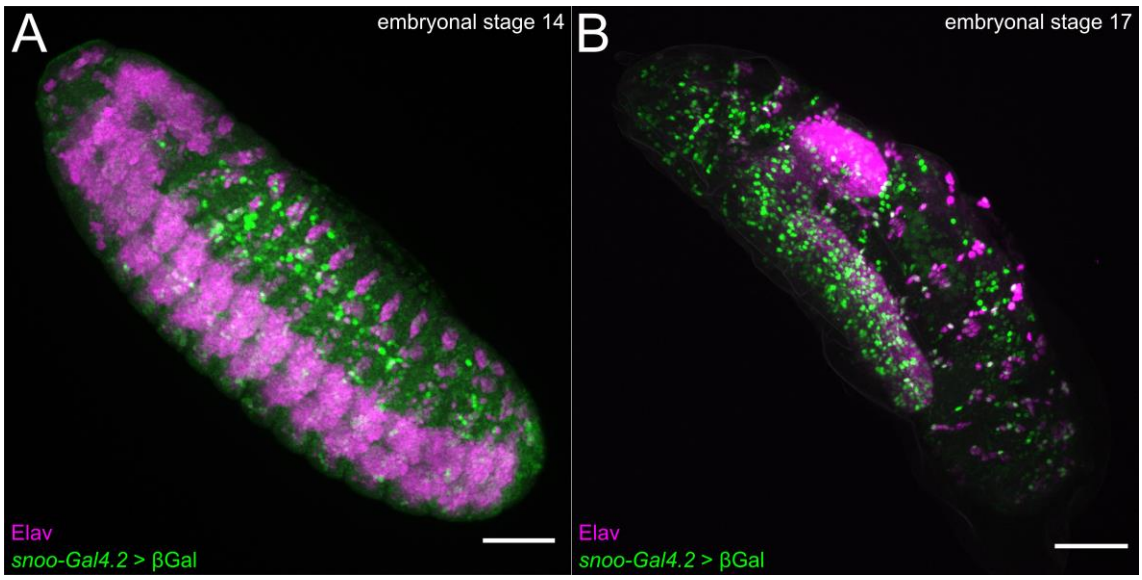

Fig 9. Snoo is expressed in early embryonal stages.

Embryos of stage 14 (A) and stage 17 (B) were stained with antibodies for Elav and β-Gal. Before the establishment of the CNS, a weak and diffused β-Gal signal can be observed throughout the whole embryo. A. Simultaneously with the occurrence of the Elav signal, the first cells appear, which show very strong β-Gal expression. This expression can be observed exclusively outside of the CNS in cells that might be mesodermal. B. After condensation of the CNS, β-Gal expressing cells can be observed throughout the whole embryo but most prominently within the CNS. Scale bars: 50 µm.

β-Gal signal is detectable throughout embryogenesis (Fig 9). At the beginning of embryogenesis, a diffused β-Gal signal is visible all over the embryo (not shown). The first cells that show a very prominent β-Gal expression appear at embryonal stage 14 when the formation of the nervous system begins. These do not seem to be neurons but might be mesodermal cells. With further onset of the development the number of β-Gal expressing cells increases. In the late embryo, immediately before hatching, a strong β-Gal signal can be observed in the now condensed CNS. There are also non-neuronal cells expressing β-Gal at stage 17. However, the signal in the CNS appears to be the most prominent.

2.3.2. Snoo is expressed in Dpp active cells in the larval CNS

As analysis in embryos revealed a prominent expression of *snoo* in the CNS, this tissue was further investigated at later stages of development. The ventral nerve cord (VNC) of 3rd instar larvae expressing GFP with a nuclear localisation sequence (NLS) under the control of *snoo-Gal4.2* was stained using an antibody for Elav (Fig 10).

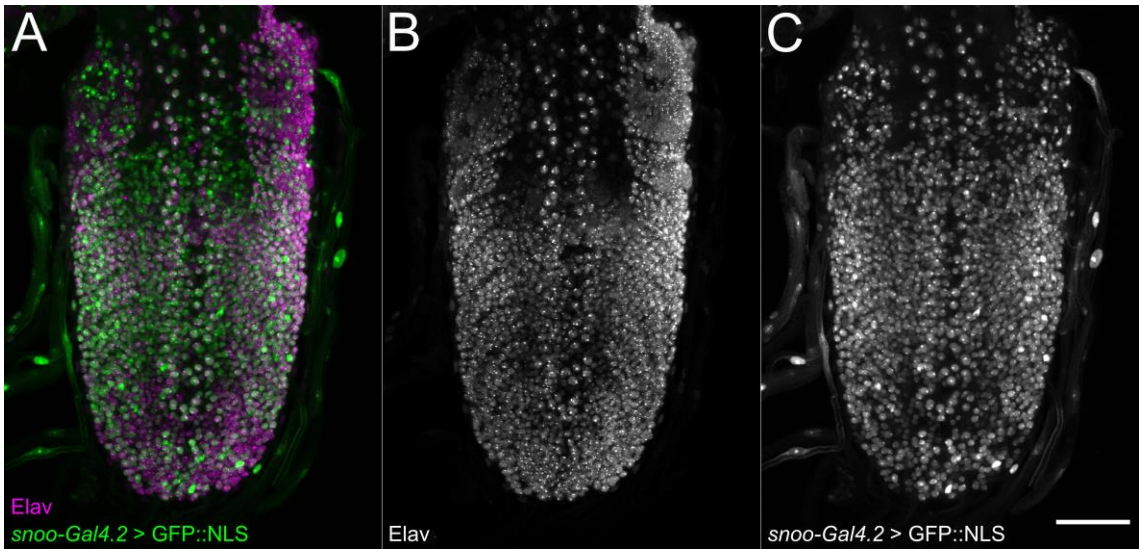

Fig 10. Snoo is expressed throughout the whole larval VNC.

VNCs of 3rd instar larvae expressing GFP::NLS under the control of the driver line *snoo-Gal4.2* were stained with an antibody for Elav. A GFP signal is visible all over the VNC in both, neurons and non-neuronal cells. Scale bar: 50 µm.

snoo-Gal4.2 drives the expression of GFP::NLS all over the VNC of 3rd instar larvae (Fig 10). However, Snoo is not expressed in all neurons. Additionally, *snoo* is also expressed in non-neuronal cells. Staining with an antibody for Repo, which is a marker for glial cells, revealed some of these non-neuronal cells are glia (not shown). It was suspected that the remaining Snoo expressing cells, which appear to be neither neurons nor glia, might be neuroblasts. To address this question brains of 3rd instar larvae were stained with an antibody for phosphorylated Histone 3 (pH3), which is a marker for mitotically active cells (Fig 11).

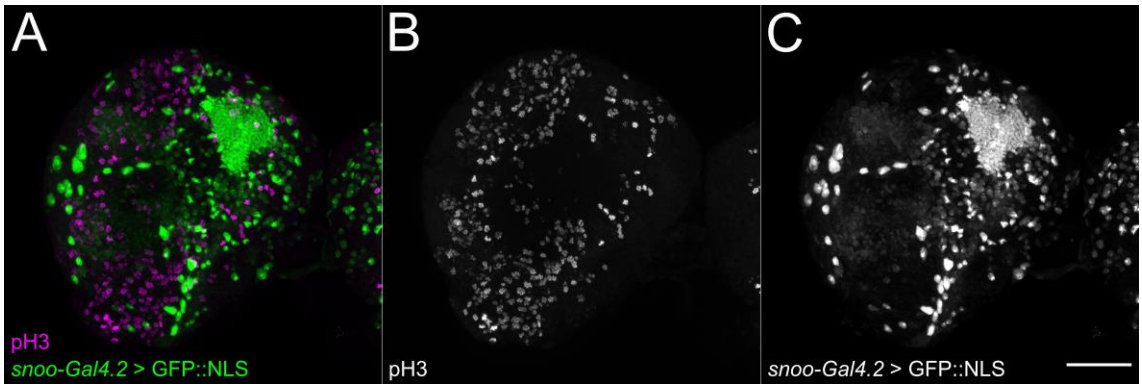

Fig 11. Snoo is not expressed in neuroblasts.

Larval brains were stained with an antibody against pH3, which is a marker for mitotically active cells. No GFP signal is visible in dividing cells. The few cells that seem to show an overlap of the two fluorescent signals are located within different planes. Scale bar: 50 µm.

Snoo is not expressed in cells that are positive for pH3 (Fig 11). It seems that there is pH3 signal within a GFP expressing cluster of cells. However, the figure shown here is a projection of different planes and the pH3 positive cells are not located in the same plane as the GFP expressing cells. Therefore, it can be assumed that *snoo* is not expressed in dividing cells and therefore not in neuroblasts.

As it is known that Snoo can function as a regulator of TGFβ signalling, it was investigated if *snoo* is expressed in cells, in which the Dpp pathway is active. A marker for Dpp active cells is phosphorylated MAD (pMAD). The VNC of 3rd instar larvae was stained using an antibody for pMAD (Fig 12).

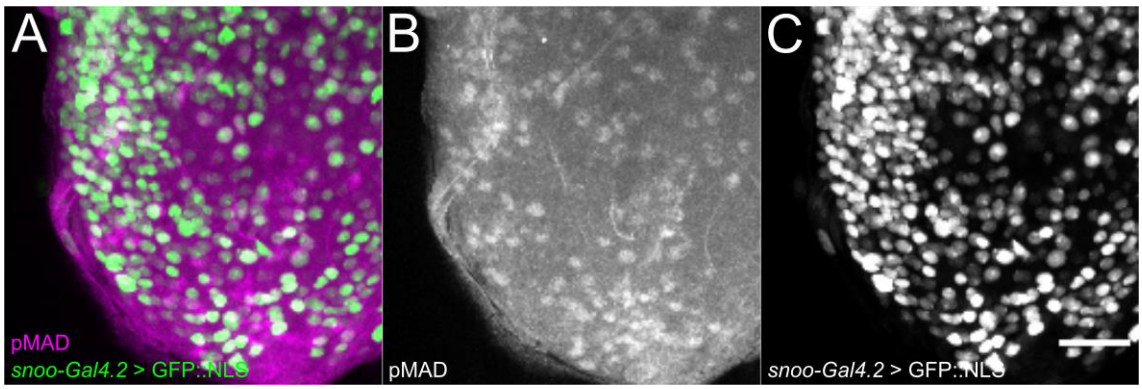

Fig 12. Snoo is expressed in Dpp active cells.

Larval VNCs were stained with an antibody for pMAD, which is a marker for cells with active Dpp signalling. A. Merge of GFP signal and pMAD signal. B. pMAD signal. C. GFP signal. Some cells, in which the Dpp pathway is active, show GFP expression. Scale bar: 25 µm.

Some *snoo* expressing cells were found that are also positive for pMAD (Fig 12). On the one hand, it could be confirmed that *snoo* is expressed in cells where the Dpp signalling pathway is active. This finding is in concordance with previous publications about interactions of *snoo* with this signalling pathway. On the other hand, *snoo* is also expressed in a vast number of cells that

do not show pMAD signal. In these cells, *snoo* must have a function independent from the Dpp signalling pathway.

2.3.3. Snoo shows a broad expression pattern

To further analyse the expression pattern of *snoo* different tissues from 3rd instar larvae expressing GFP::NLS under the control of *snoo-T2A-Gal4* were investigated (Fig 13).

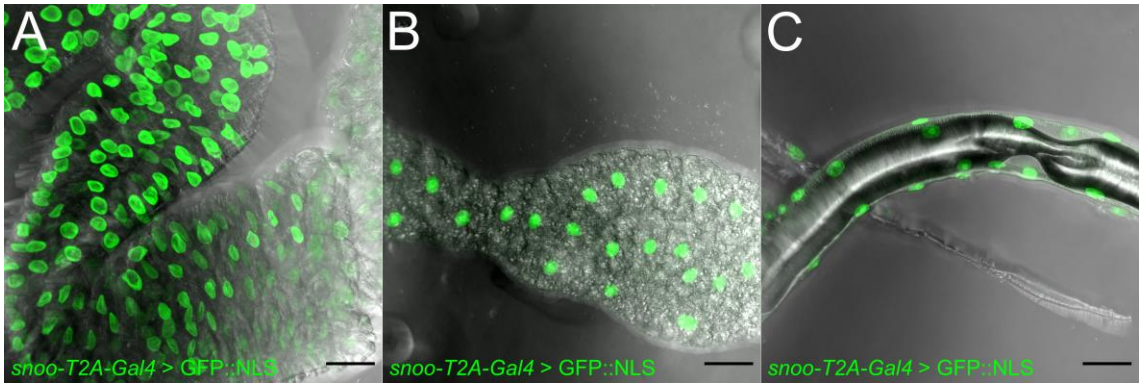

Fig 13. Snoo is expressed in different larval tissues.

Expression of GFP::NLS was induced using *snoo-T2A-Gal4* and different larval tissues were dissected. GFP signal is visible in all cells of the intestines (A), fat body (B) and tracheae (C). Scale bar: 50 µm.

snoo-T2A-Gal4 drives the expression of GFP::NLS in all cells of the larval intestines, fat body and tracheae (Fig 13). It can be assumed that *snoo* has a very broad expression pattern throughout 3rd instar larvae.

For the examination of the expression of *snoo* in muscle tissue, wing muscles of adult flies expressing GFP::NLS under the control of *snoo-T2A-Gal4* were stained with the actin binding compound phalloidin (Fig 14).

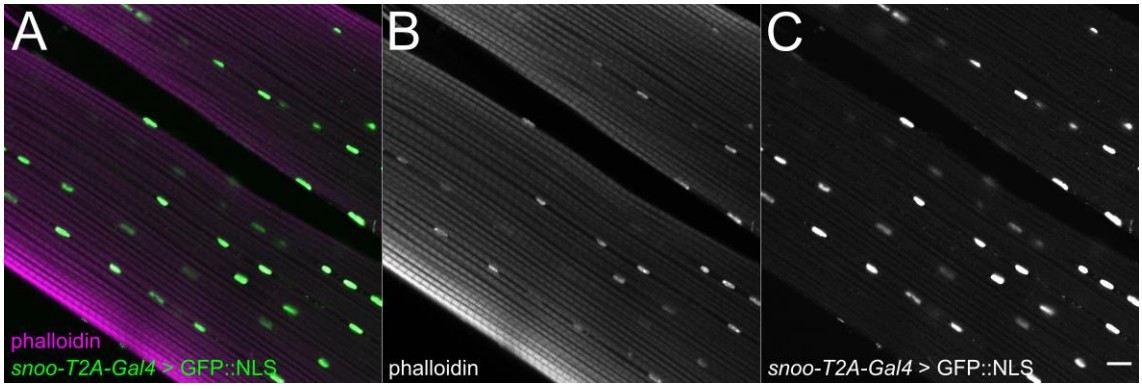

Fig 14. Snoo is expressed in the wing muscles.

Wing muscles were stained using the actin binding compound phalloidin. GFP signal is visible in all nuclei of the muscle cells. Scale bar: 10 µm.

The signal of GFP::NLS driven by *snoo-T2A-Gal4* is visible in nuclei all over the wing muscles (Fig 14). Therefore, *snoo* shows a broad expression pattern in wing muscles. As GFP signals can

be observed all over larvae and flies, it could further be assumed that *snoo* is broadly expressed in different tissues at most postembryonic stages.

2.3.4. Expression pattern of Snoo in the adult CNS

To further study the *snoo* expression in the CNS *snoo-T2A-Gal4* was used to drive the expression of CD8::GFP, which is located within the cell membrane and can be used to visualise whole cell bodies. The brains and VNCs of adult flies were investigated (Fig 15).

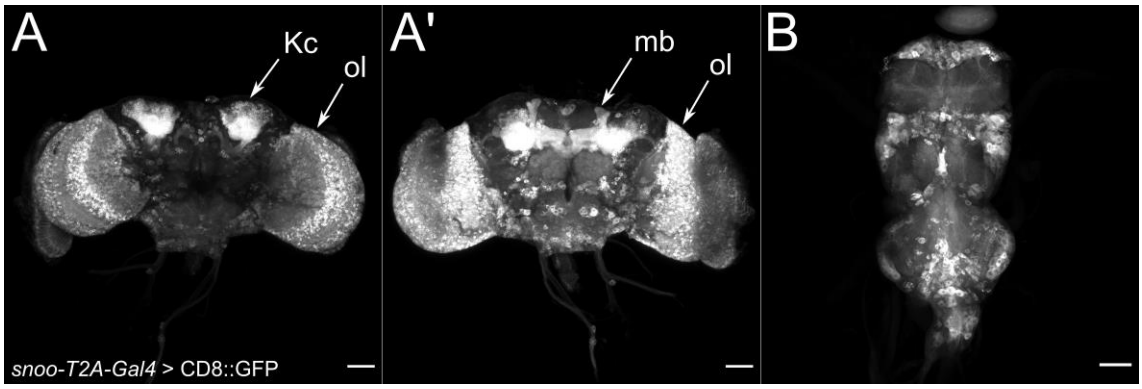

Fig 15. Snoo is expressed in the whole adult CNS.

The brains (A, A') and VNCs (B) of adults expressing CD8::GFP under the control of the driver *snoo-T2A-Gal4* were dissected. GFP signal is visible all over the brain (A, A') and seems to be strongest in the optic lobes (ol) and the mushroom bodies (mb), which are formed by the axons of the Kenyon cells (Kc). Furthermore, all cells of the VNC show GFP expression (B). Scale bar: 50 µm.

The expression of CD8::GFP under the control of *snoo-T2A-Gal4* reveals that *snoo* is expressed all over the adult brain and the VNC (Fig 15). The strongest signal can be observed in the optic lobes and the mushroom bodies. For more detailed investigation, brains of adult flies expressing GFP::NLS under the control of *snoo-Gal4.2* were stained with an antibody for Elav (Fig 16).

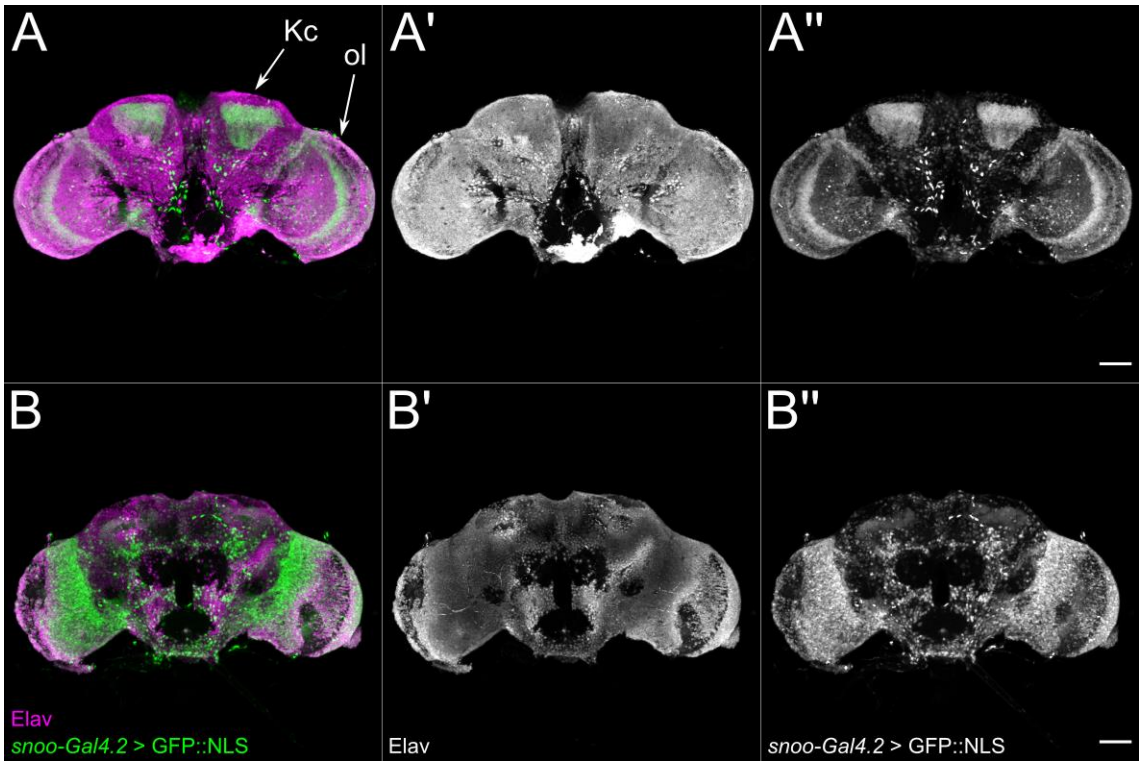

Fig 16. Snoo is expressed all over the adult brain.

Brains of adults expressing GFP::NLS under the control of the driver line *snoo-Gal4.2* were stained with an antibody for Elav. GFP signal is visible in all neurons. The signal is strongest in the optic lobes (ol) and the triangle shaped clusters of Kenyon cells (Kc). Scale bar: 50 µm.

A strong expression of Gal4 can be observed all over the adult brain (Fig 16). The other driver line *snoo-T2A-Gal4* shows a very similar expression pattern in the adult brain (not shown). When comparing both lines, the expression of *snoo-T2A-Gal4* seems to be considerably stronger. A very prominent expression is visible within the optic lobes and the triangle shaped cluster of Kenyon cells, whose axons form the mushroom body.

As the expression of GFP::NLS reveals strong *snoo* expression in the Kenyon cells (Fig 16) and CD8::GFP also seems to show expression in the mushroom bodies (Fig 15), brains of flies expressing CD8::GFP under the control of *snoo-T2A-Gal4* were stained with an antibody for Fasciclin II (FasII), which is expressed in the mushroom body and is a common marker for this part of the brain (Fig 17).

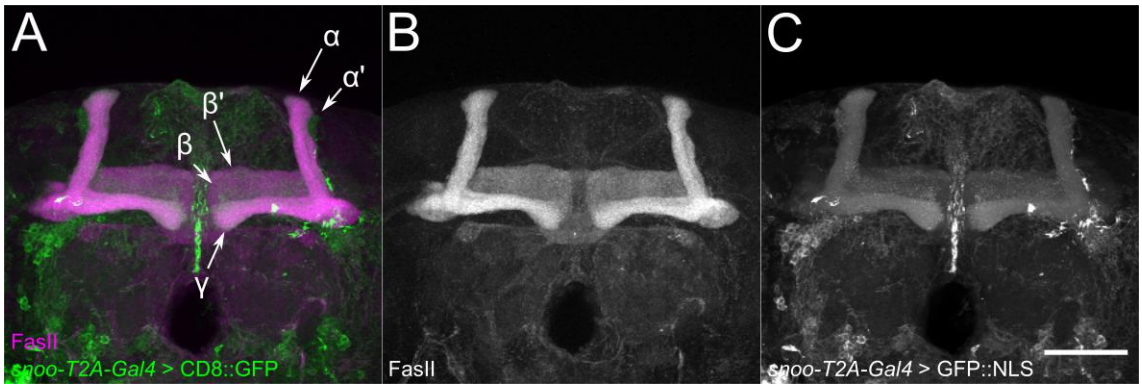

Fig 17. Snoo is expressed in all lobes of the mushroom bodies.

Brains of adults expressing CD8::GFP under the control of the driver *snoo-T2A-Gal4* were stained with an antibody for the mushroom body marker FasII. GFP signal is visible in all lobes (α, α', β, β', γ) of the mushroom body. Scale bar: 50 µm.

A strong Gal4 expression can be found in all lobes (α, α', β, β', γ) of the mushroom body, even in the α' lobe, where the FasII signal is absent (Fig 17). The other driver line *snoo-Gal4.2* shows the same expression pattern in the mushroom body (not shown).

The analysis of the brain also shows *snoo* expression in the pars intercerebralis (Fig 15, Fig 16). This part of the brain contains the IPCs, which are neurosecretory cells that are involved in the regulation of different processes. To investigate if *snoo* is expressed in IPCs, brains of flies expressing GFP::NLS under the control of *snoo-T2A-Gal4* were stained with an antibody against Ilp5 (Fig 18).

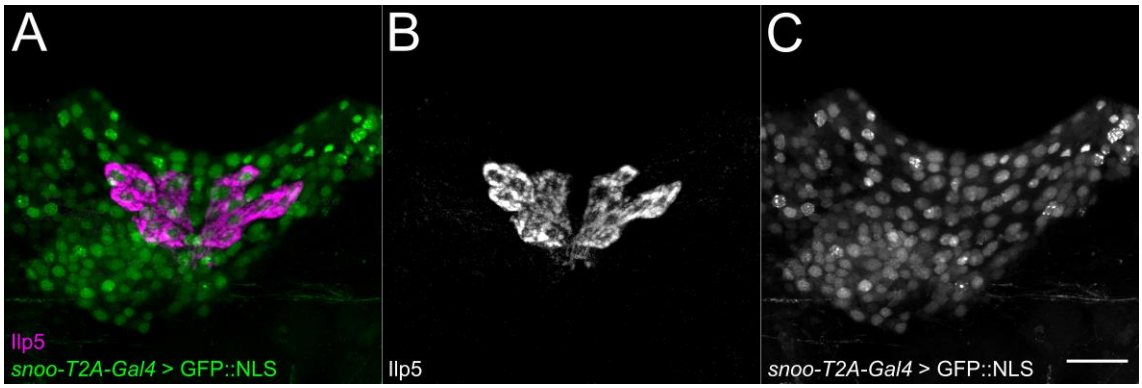

Fig 18. Snoo is expressed in the IPCs.

Brains of adults expressing GFP::NLS under the control of the driver *snoo-T2A-Gal4* were stained with antibody for Ilp5. GFP signal is visible in all IPCs. Scale bar: 20 µm

Staining with the antibody against Ilp5 revealed that *snoo* is expressed in all IPCs (Fig 18).

2.4. Phenotypical analysis of *snoo* deletions

While the generated Gal4 driver lines were used for the analysis of the expression pattern of Snoo, one main purpose of the deletion lines $snoo^{del1}$ and $snoo^{del2}$ was to analyse the phenotype of a *snoo* mutation. On the one hand, it should be investigated if previously published phenotypes could be

reproduced. On the other hand, the phenotypical analysis of functional or developmental defects of the *snoo* deletions might reveal possible functions of the gene.

2.4.1. Deletion of *snoo* has no influence on fertility

As previous studies found a reduced fertility for homozygous *snoo* mutants (Takaesu *et al*, 2006), the fecundity rate of females of $snoo^{del1}$ was analysed as the number of eggs they laid within an hour (Fig 19). As no significant difference could be found between w^{1118} and the heterozygotes $snoo^{del1}/+$, which were generated by crossing $snoo^{del1}$ and w^{1118}, only the results of the heterozygous flies are shown as control.

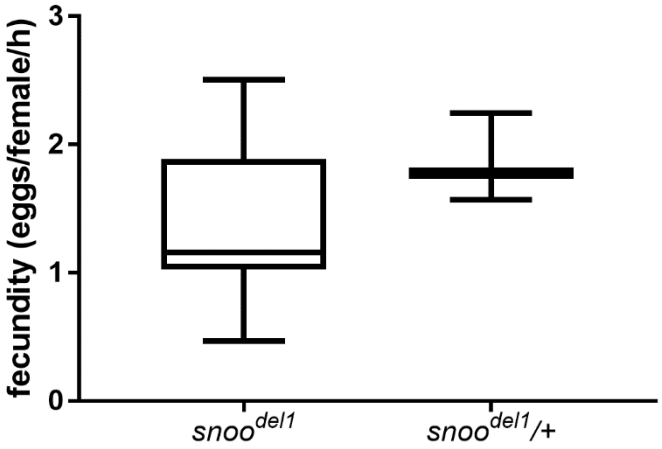

Fig 19. Deletion of *snoo* has no influence on fertility.
The number of eggs laid by a defined number of females in a specific period was counted. The data was analysed using *t*-test. No significant difference was found (*p*-value = 0.231).

There is no significant difference between homozygous $snoo^{de1l}$ and heterozygous $snoo^{de1l}/+$ females (Fig 19). A deletion of *snoo* does not seem to have an influence on fertility.

2.4.2. *snoo* deletion has a weak influence on survival during pupation

The previously proposed lethality of *snoo* mutants was explained by difficulties during pupation (Takaesu *et al*, 2006). In contrast, the generated deletion lines are homozygous viable. It was investigated if the mutants show a reduced survivability during different stages of development (Fig 20). As for the analysis of the fertility rate, no significant difference between the heterozygous control and w^{1118} could be found. Therefore, the control w^{1118} was not included into the analysis.

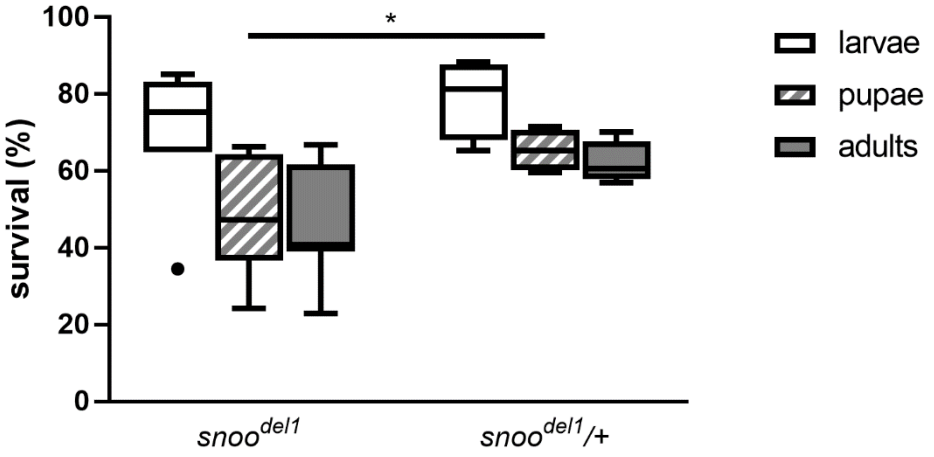

Fig 20. Deletion of *snoo* has a weak effect on survival during development.

Shown is the proportion of eggs that developed up to the indicated developmental stage. The data was analysed using *t*-test. There is a significant difference in the proportion of eggs that developed to pupae between homozygous and heterozygous individuals (*p*-value = 0.0426). No significant difference could be found for eggs that developed into larvae (*p*-value = 0.3312) or adults (*p*-value = 0.0572).

When comparing the mutant line $snoo^{del1l}$ with its corresponding heterozygous control $snoo^{del1}/+$, a significant difference in survivability could only be found for pupae, even though the effect is relatively weak (Fig 20). Analysis of the proportion of larvae developing into pupae also showed a significant reduction (*p*-value = 0.0242). Therefore, a lack of *snoo* seems to have a small effect on survivability during pupation.

2.4.3. Climbing activity is reduced in *snoo* deletion lines

In the context of screening for phenotypes of the *snoo* deletion lines, negative geotaxis assays were performed. When comparing the control w^{1118} with both heterozygous controls, $snoo^{del1}/+$ and $snoo^{del2}/+$, there seems to be no significant difference in the climbing activity of the flies (Fig 21). This is in concordance with the analysis of the fecundity rate and the survivability during the development, as also in these experiments no significant difference between the heterozygous controls and w^{1118} could be found.

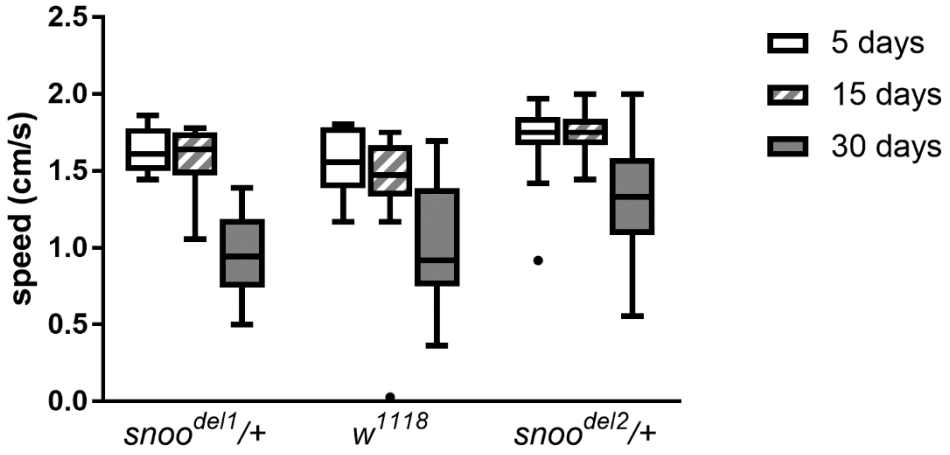

Fig 21. No difference in geotaxis found between heterozygotes and w^{1118}.
ANOVA and Tukey's post hoc test were used to compare w^{1118} with the heterozygous controls. No significant difference between w^{1118} and both heterozygous controls could be found for flies that are 5 (*p*-values: $snoo^{del1}/+$ = 0.9961, $snoo^{del2}/+$ = 0.8771), 15 (*p*-values: $snoo^{del1}/+$ = 0.9818, $snoo^{del2}/+$ = 0.0916) or 30 days old (*p*-values: $snoo^{del1}/+$ = 0.7223, $snoo^{del2}/+$ = 0.0538).

As the heterozygous flies show no phenotypical difference to w^{1118} in this assay, only the heterozygous animals were used as controls in further experiments and the control w^{1118} was not included.

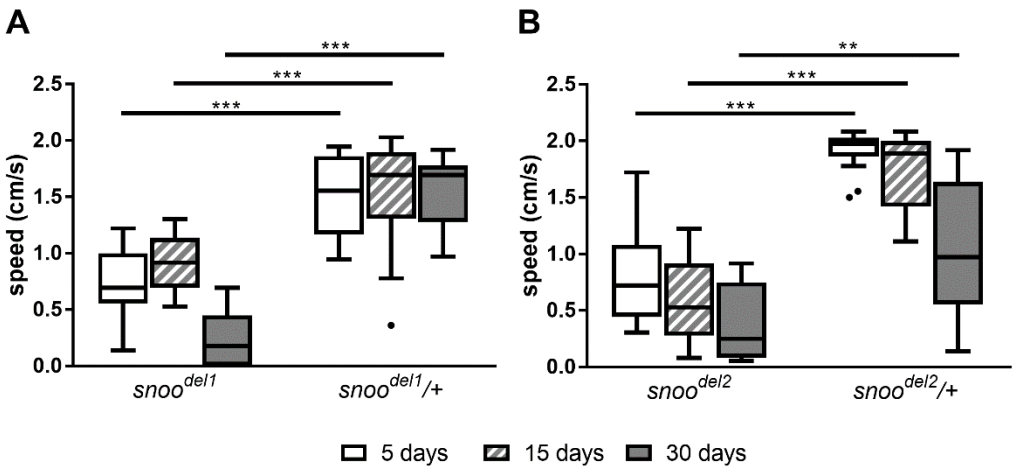

Fig 22. Deletion lines show reduced negative geotaxis.
t-test was used to compare the homozygous mutants with their corresponding heterozygous controls. A. The negative geotaxis of $snoo^{del1}$ is reduced for flies that are 5 (*p*-value < 0.0001), 15 (*p*-value = 0.0004) or 30 days old (*p*-value < 0.0001). B. The negative geotaxis of $snoo^{del2}$ is reduced for flies that are 5 (*p*-value < 0.0001), 15 (*p*-value < 0.0001) or 30 days old (*p*-value = 0.0024).

A comparison between homozygous and heterozygous flies showed significant differences for both deletion lines (Fig 22). The climbing performance of the mutants is reduced at all tested ages. As flies get older, their performance is further reduced.

To confirm the results obtained with the homozygous deletion lines and to minimise the possible influence of the genetic background on the outcome of the experiments, the negative geotaxis assay was repeated using transheterozygous flies, which were generated by crossing virgins of *snoo*^{del2} with males of *snoo*^{del1}. The heterozygosity of the transheterozygous flies can be considered as high as the one of the heterozygous flies that were used as controls.

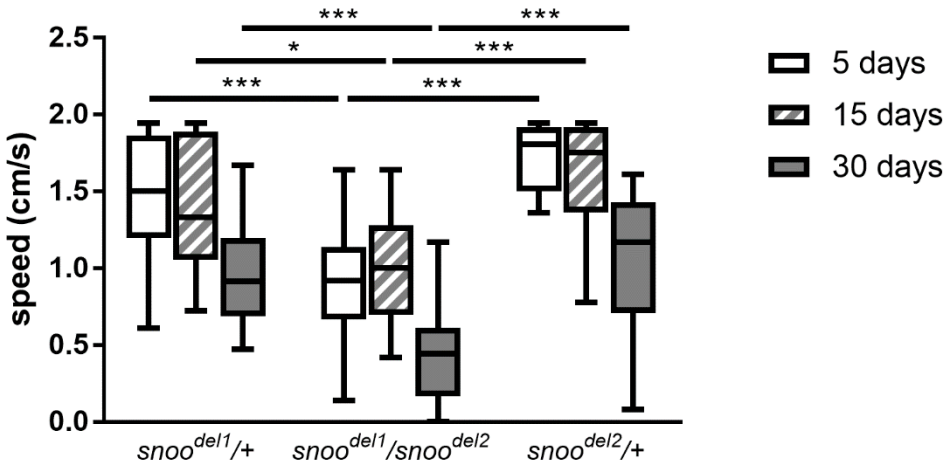

Fig 23. Transheterozygotes confirm geotaxis results.

ANOVA combined with Tukey's post hoc test was used to compare the homozygous mutants with the heterozygous controls. The negative geotaxis of transheterozygotes is significantly reduced in comparison to both heterozygous controls for flies that are 5 (*p*-values: *snoo*^{del1}/+ = 0.0002, *snoo*^{del2}/+ < 0.0001), 15 (*p*-values: *snoo*^{del1}/+ = 0.0261, *snoo*^{del2}/+ = 0.0007) or 30 days old (*p*-values: *snoo*^{del1}/+ = 0.0007, *snoo*^{del2}/+ < 0.0001).

The transheterozygous mutants differ significantly from both heterozygous controls (Fig 23). The climbing performance of the mutants is reduced at all tested ages. Therefore, it could be confirmed that a lack of *snoo* reduces the climbing ability of the flies.

2.4.4. Deletion of *snoo* reduces lifespan

Previous studies found that some *snoo* mutants are homozygous lethal (Takaesu *et al*, 2006). However, the deletion lines generated in this study, *snoo*^{del1} and *snoo*^{del2}, are viable. It was investigated if these two *snoo* mutations have an influence on the lifespan. At first, the heterozygous controls *snoo*^{del1}/+ and *snoo*^{del2}/+ were compared to the control *w*^{1118} (Fig 24), as it was done for the negative geotaxis (Fig 21).

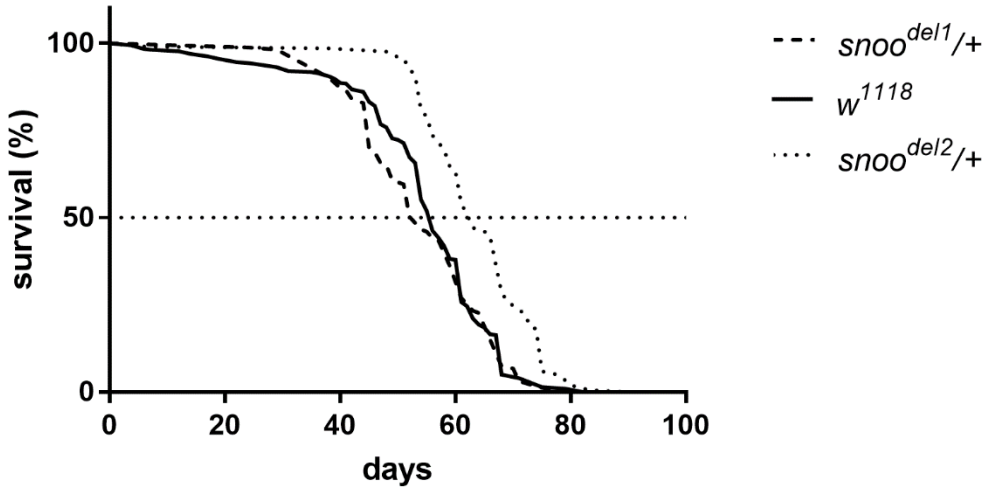

Fig 24. Lifespan of heterozygous controls is not reduced.

The control w^{1118} does not significantly differ from the heterozygous control $snoo^{del1}$/+ (p-value = 0.7649). There is a significant difference between w^{1118} and $snoo^{del2}$/+ (p-value < 0.0001), but heterozygous flies live even longer than w^{1118}. Median survival: w^{1118} = 56 d; $snoo^{del1}$/+ = 54 d; $snoo^{del2}$/+ = 63 d.

In concordance with the results of the negative geotaxis assays, a significant difference between the heterozygous control $snoo^{del1}$/+ and w^{1118} could not be found (Fig 24). However, there is a significant difference between w^{1118} and $snoo^{del2}$/+, but the heterozygous flies tend to live even longer than w^{1118}. Because of this, the heterozygous animals were used as controls in any further experiments and w^{1118} was not included. The homozygous mutants were compared to their corresponding heterozygous controls (Fig 25).

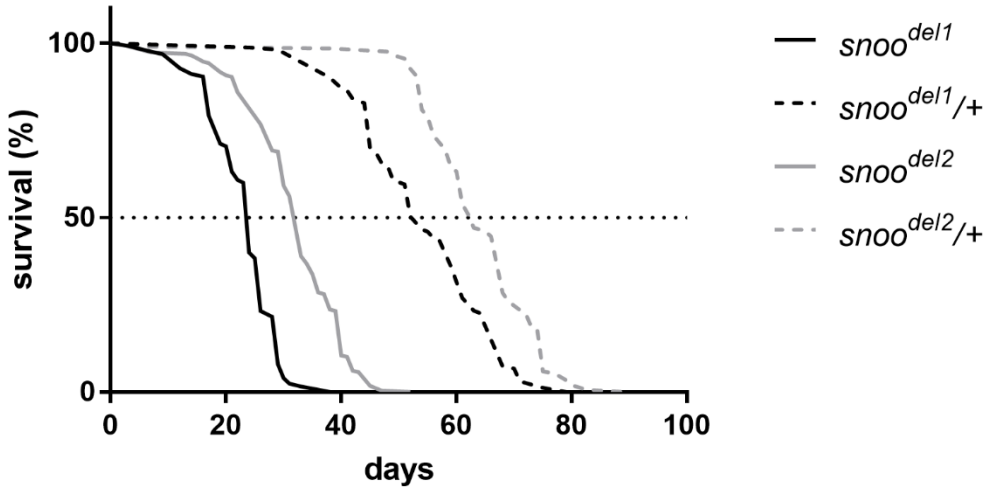

Fig 25. A *snoo* deletion reduces the lifespan.

A significant difference can be found for $snoo^{del1}$ (p-value < 0.0001) and $snoo^{del2}$ (p-value < 0.0001). Median survival: $snoo^{del1}$ = 24 d; $snoo^{del1}$/+ = 54 d; $snoo^{del2}$ = 33 d; $snoo^{del2}$/+ = 63 d.

There is a significant reduction of the lifespan of homozygous flies of the deletion lines *snoo*^{del1} and *snoo*^{del2} when compared to their corresponding heterozygous controls (Fig 25). The median survival of the homozygous animals is shortened by 30 days in both cases. The homozygous and heterozygous flies of the deletion line *snoo*^{del2} survive 9 days longer than the ones of *snoo*^{del1}. This is most likely due to the difference in the genetic background of the deletion lines.
In order to minimise the effects of the genetic background, the deletion lines were crossed to generate transheterozygotes and the lifespan assay was repeated with these flies (Fig 26).

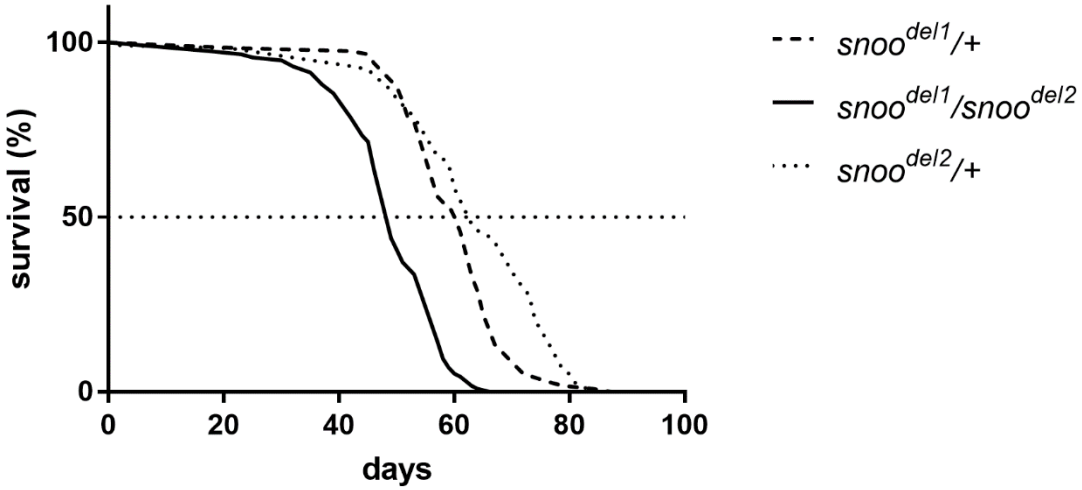

Fig 26. Transheterozygotes confirm lifespan results.
The transheterozygous flies differ significantly from both heterozygous controls (*p*-value < 0.0001 in both cases). Median survival: *snoo*^{del1}/+ = 60.5 d; *snoo*^{del1}/*snoo*^{del2} = 49 d; *snoo*^{del2} = 63 d.

The transheterozygous flies show a significant reduction of their lifespan in comparison to the heterozygous controls (Fig 26). The transheterozygous flies survive 11.5 days less than *snoo*^{del1}/+ and 14 days less than *snoo*^{del2}/+. Therefore, the lifespan of the transheterozygous flies is less reduced than the lifespan of the homozygous animals (Fig 25).

2.4.5. Influence of stress on the lifespan of *snoo* deletions

To gain further insight into the reduced lifespan phenotype of the *snoo* deletion lines, the assay was repeated under stressing conditions (Fig 27). On the one hand, flies were treated with heat stress by keeping them at 30 °C. On the other hand, flies were treated with oxidative stress by keeping them in an atmosphere consisting almost entirely of oxygen.

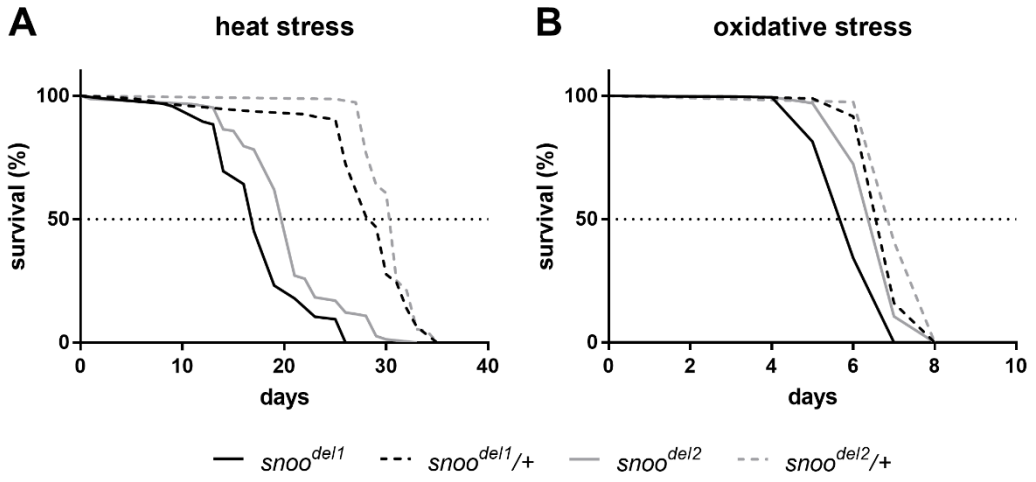

Fig 27. Deletion lines show reduced lifespan under stressing conditions.

A. Rearing conditions: 30 °C. Both mutants, *snoo*^{del1} and *snoo*^{del2}, differ significantly from their corresponding heterozygous controls (*p*-value < 0.0001 in both cases). Median survival: *snoo*^{del1} = 17 d; *snoo*^{del1}/+ = 29 d; *snoo*^{del2} = 21 d; *snoo*^{del2}/+ = 31 d. B. Rearing conditions: 99 % O_2. Both mutants, *snoo*^{del1} and *snoo*^{del2}, differ significantly from their corresponding heterozygous controls (*p*-value < 0.0001 in both cases). Median survival: *snoo*^{del1} = 6 d; *snoo*^{del1}/+ = 7 d; *snoo*^{del2} = 7 d; *snoo*^{del2}/+ = 7 d.

If compared to the standard rearing temperature of 25 °C (Fig 25), the median survival of all flies is reduced under heat stress (Fig 27). Under these conditions the lifespan of the homozygous mutants is significantly reduced in comparison to their corresponding heterozygous controls. The median survival of *snoo*^{del1} is reduced by 12 days and the median survival of *snoo*^{del2} is reduced by 10 days. Oxidative stress also results in an extreme reduction of the median survival of all genotypes. There is a significant difference between the curves, but the difference of the median survival is lost for *snoo*^{del2} and reduced to 1 day for *snoo*^{del1}.

2.5. Analysis of a conditional knockout of *snoo*

In order to resolve how the lack of *snoo* results in the previously described phenotypes, the conditional knockout line *UAS-t::sgRNA-snoo*^{4x} was generated. This line encodes four different sgRNAs with target sequences at the 5' terminus of *snoo* under the control of UAS (Fig 28).

Fig 28. Schematic overview of the target sequences of the conditional knockout.

Target sequences near the N-terminus were chosen with the purpose that the resulting frameshift will affect the gene as much as possible. Previous studies had confirmed that the usage of four sgRNAs is sufficient to achieve an almost 100 % mutation rate (Port & Bullock, 2016).

The plasmid for the generation of the conditional knockout line was generated by amplifying the t::sgRNA scaffold three times from the vector pCFD6 using PCR with specific primer pairs that contained the target sequences within their overhangs. By using Gibson Assembly, the three PCR

products were cloned into the vector pCFD6 that had been linearized using the restriction enzyme BbsI. The resulting plasmid was named pCFD6-t::sgRNA-snoo^{4x} and injected into embryos of the stock *y$^-$, w$^-$, vas-ΦC31; attP*. The resulting flies were crossed to the balancer *w$^-$; D3/TM3* and transformant flies within the offspring of this cross were identified by the mini-white marker of the cloned construct. A homozygous stock of the genotype *w^{1118}; M{UAS-t::sgRNA-snoo^{4x}}ZH-86Fb* was established (labelled as *UAS-t::sgRNA-snoo^{4x}*).

Different Gal4 driver lines were used to drive the expression of the sgRNAs and Cas9 in specific tissues. By crossing *UAS-t::sgRNA-snoo^{4x}* to the double balancer *w$^-$; CyO/Sco; D3/TM3* a stock of the genotype *w^{1118}; CyO/sna^{Sco}; M{UAS-t::sgRNA-snoo^{4x}}ZH-86Fb* was established (labelled as *CyO/Sco; UAS-t::sgRNA-snoo^{4x}*). The stock *UAS-Cas9* was crossed to the double balancer *w$^-$; CyO/Sco; D3/TM3* to establish a stock of the genotype *w*; P{UAS-Cas9.P2}attP40; D3/TM3, Sb^1* (labelled as *UAS-Cas9; D3/TM3*). The stocks *CyO/Sco; UAS-t::sgRNA-snoo^{4x}* and *UAS-Cas9; D3/TM3* were crossed to establish a stock of the genotype *w^{1118}; UAS-Cas9; M{UAS-t::sgRNA-snoo^{4x}}ZH-86Fb* (labelled as *UAS-Cas9; UAS-t::sgRNA-snoo^{4x}*). Males of this stock were crossed to virgins of the desired Gal4 drivers.

2.5.1. Lifespan of a knockout of *snoo* in different cell types

In order to confirm the results obtained with the lifespan assays of the deletion lines (Fig 25) and to show that the conditional knockout is functional, the ubiquitously expressing driver lines *Act-Gal4* and *Da-Gal4* were used to drive the expression of Cas9 and *snoo* targeting sgRNAs. This should result in the induction of indel and frameshift mutations within the *snoo* locus in all cells and thereby reproduce the deletion lines. As controls, the same driver lines were used to drive the expression of the Cas9 protein or the sgRNAs, respectively. Lifespan assays were performed on these flies (Fig 29).

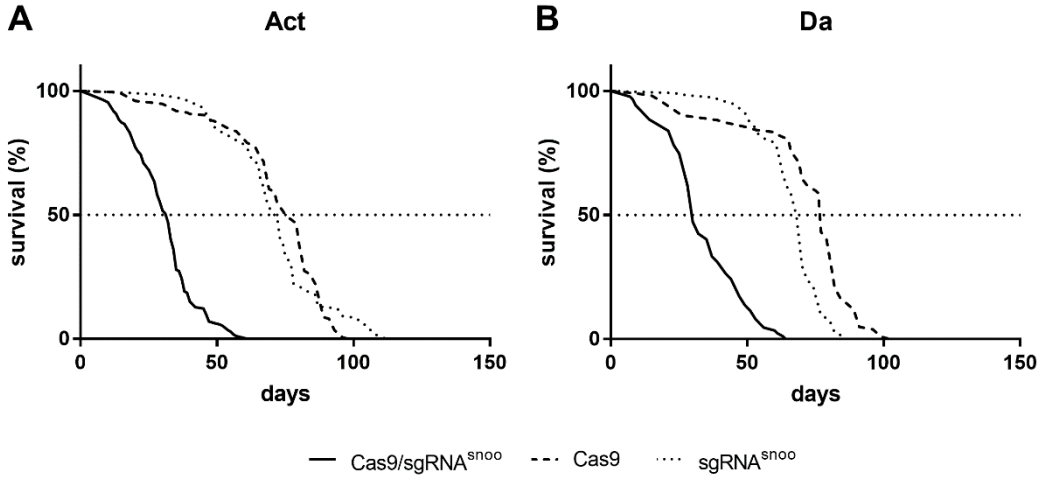

Fig 29. Knockout of *snoo* in all cells reduces lifespan.

Lifespan assay of a conditional knockout of *snoo* in all cells. A. Knockout using *Act-Gal4*. The knockout Act > Cas9/sgRNA^{snoo} shows a significant difference in comparison to both controls, Act > Cas9 and Act > sgRNA^{snoo} (*p*-value < 0.0001 in both cases). Median survival: Act > Cas9/sgRNA^{snoo} = 32 d; Act > Cas9 = 75.5 d; Act > sgRNA^{snoo} = 72 d. B. Knockout using *Da-Gal4*. The knockout Da > Cas9/sgRNA^{snoo} differs significantly from both controls, Da > Cas9 and Da > sgRNA^{snoo} (*p*-value < 0.0001 in both cases). Da > Cas9/sgRNA^{snoo} = 30 d; Da > Cas9 = 77 d; Da > sgRNA^{snoo} = 68 d.

A conditional knockout of *snoo* in all cells results in a significant reduction of the lifespan (Fig 29). The median survival of flies with a knockout of *snoo* in Actin expressing cells is reduced by 43.5 days if compared to the control Act > Cas9 and by 40 days if compared to the other control Act > sgRNA^{snoo}. Flies with a knockout in Daughterless expressing cells survive 47 days less if compared to the control Da > Cas9 and by 38 days if compared to the other control Da > sgRNA^{snoo}. This is in concordance with the results obtained using the deletion lines (Fig 25) and proves that the conditional knockout is functional.

The analysis of the expression pattern of *snoo* had shown that it is expressed in different cell types. Therefore, different driver lines were used to induce a conditional knockout of *snoo* in specific cell types and lifespan assays were performed with these flies. *Repo-Gal4* was used to induce the conditional knockout in glial cells. *Lsp-Gal4* induced the conditional knockout in fat cells. *Mhc-Gal4* induced the conditional knockout in muscle cells (Fig 30).

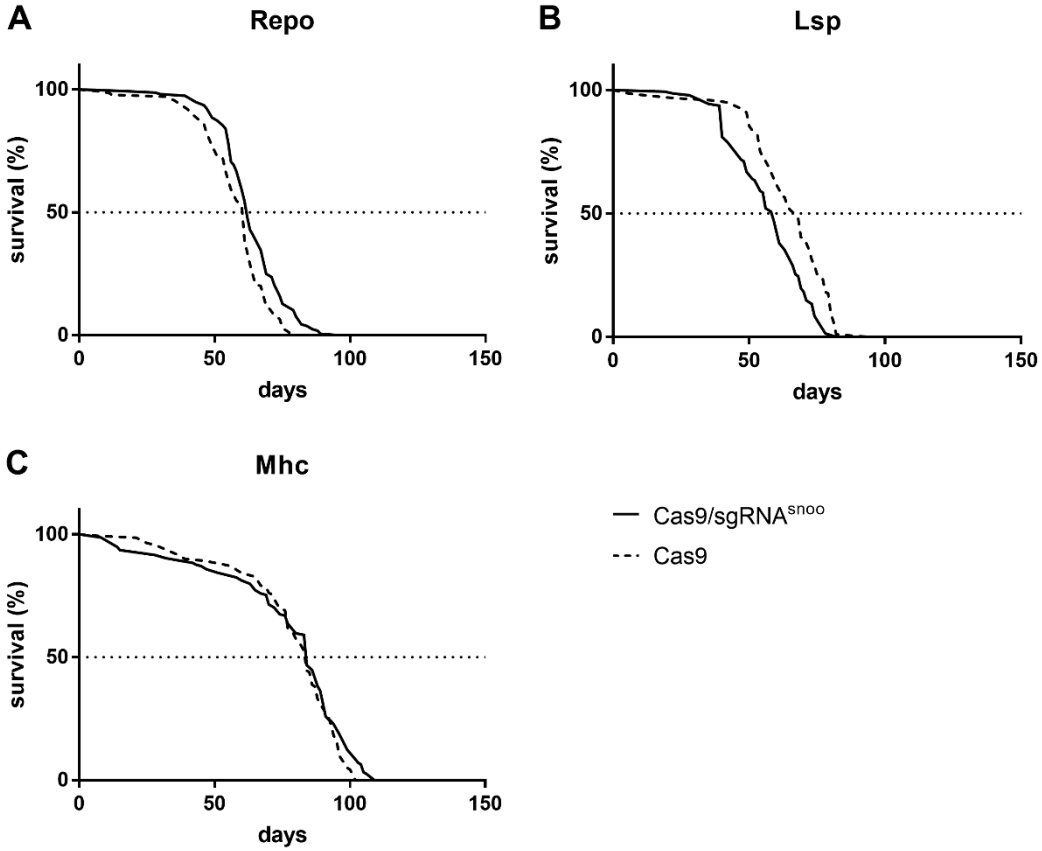

Fig 30. Knockout of *snoo* in fat cells but not in glia or muscle cells reduces lifespan.
Lifespan assay of a conditional knockout of *snoo* in different cell types. A. Knockout in glial cells using *Repo-Gal4*. There is a significant difference (*p*-value < 0.0001). Median survival: Repo > Cas9/sgRNA^{snoo} = 62 d; Repo > Cas9 = 61 d. B. Knockout in fat cells using *Lsp-Gal4*. There is a significant difference (*p*-value < 0.0001). Median survival: Lsp > Cas9/sgRNA^{snoo} = 59 d; Lsp > Cas9 = 67 d. C. Knockout in muscle cells using *Mhc-Gal4*. There is no significant difference (*p*-value = 0.0596). Median survival: Mhc > Cas9/sgRNA^{snoo} = 84 d; Mhc > Cas9 = 84 d.

The lifespan is significantly reduced if *snoo* is knocked out in fat cells (Fig 30). The median survival is reduced by 8 days, which is much less than the effect found for a general knockout (Fig 25, Fig 26, Fig 29). Therefore, it can be assumed that the lack of *snoo* in fat cells is not the main cause of the reduction of the lifespan of a general deletion. A knockout of *snoo* in glia also results in a significant difference of the lifespan (Fig 30). However, the median survival of the flies with a knockdown of *snoo* is even increased by 1 day in comparison to the control. Therefore, it can be assumed that the lack of *snoo* in glial cells does not contribute to the reduction of the lifespan found for a general knockout of *snoo* (Fig 25, Fig 26, Fig 29). A conditional knockout of *snoo* in muscle cells has no significant effect on the lifespan (Fig 30).

As the analysis of the driver lines showed strong *snoo* expression in the CNS, the effect of a specific knockout of *snoo* in neurons was investigated. *Elav-Gal4* was used to drive the expression of t::sgRNA-snoo^{4x} and Cas9 in neurons (Fig 31).

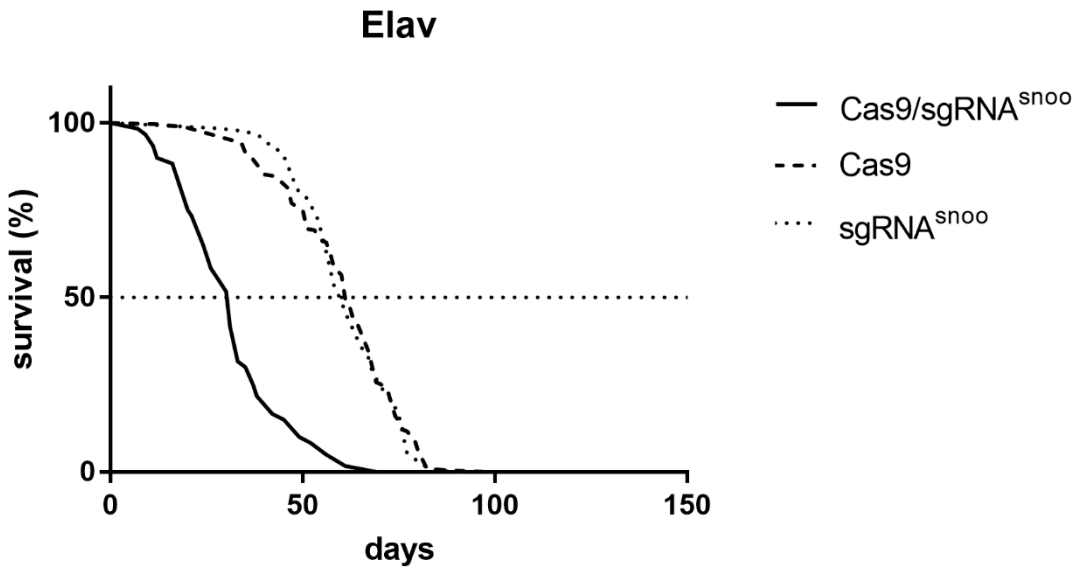

Fig 31. Knockout of *snoo* in neurons reduces lifespan.

Lifespan assay of a conditional knockout of *snoo* in neurons using *Elav-Gal4*. There is a significant difference between the knockout Elav > Cas9/sgRNA^{snoo} and both controls, Elav > Cas9 and Elav > sgRNA^{snoo} (*p*-value < 0.0001 in both cases). Median survival: Elav > Cas9/sgRNA^{snoo} = 31 d; Elav > Cas9 = 61 d; Elav > sgRNA^{snoo} = 60 d.

The conditional knockout of *snoo* in neurons results in a significant reduction of the lifespan (Fig 31). The median survival of the flies is reduced by 30 days if compared to the control Elav > Cas9 and by 29 days if compared to Elav > sgRNA^{snoo}. Therefore, the knockout in neurons reproduces the phenotype of a general knockout (Fig 25, Fig 29) and it can be assumed that the reduction of the lifespan is mainly due to the lack of *snoo* in neurons. Even though the median survival of flies expressing both, the sgRNAs and Cas9, is similar to the observation for *Act-Gal4* and *Da-Gal4* (Fig 29), the controls survive around 10 days less than the controls for *Act-Gal4* and *Da-Gal4*.
As a very prominent *snoo* expression can be found within the brain, the knockout was specifically induced in this organ. This was done by combining *Elav-Gal4* with *Tsh-Gal80*, which expresses Gal80 in the VNC. Gal80 is an inhibitor of Gal4. Therefore, *Elav-Gal4; Tsh-Gal80* specifically drives UAS dependent expression in the brain. This line was used to induce the conditional knock-out of *snoo* (Fig 32).

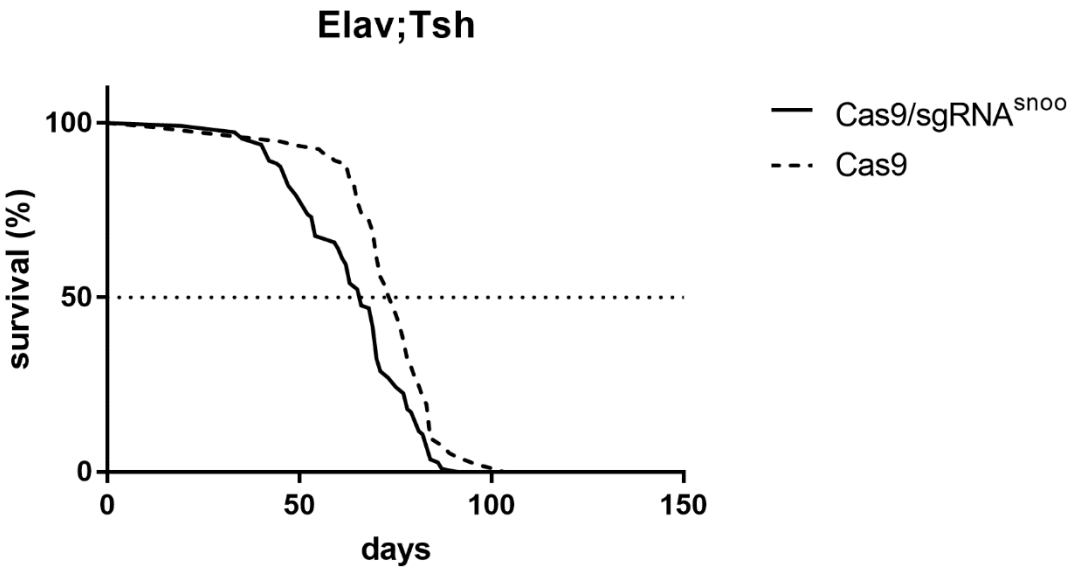

Fig 32. Knockout of *snoo* in the brain only has a weak effect on the lifespan.
Lifespan assay of a conditional knockout of *snoo* in the brain using *Elav-Gal4; Tsh-Gal80*. There is a significant difference (*p*-value < 0.0001). Median survival: Elav;Tsh > Cas9/sgRNA^{snoo} = 66 d; Elav;Tsh > Cas9 = 75 d.

If *snoo* is specifically knocked out in the brain the lifespan is significantly reduced (Fig 32) but this reduction is remarkably weaker than the effect found for a general knockout (Fig 25, Fig 26, Fig 29) or a knockout in all neurons (Fig 31), as the median survival is only reduced by 9 days. Therefore, the effect of a specific knockout of *snoo* in the brain is more comparable to a knockout in fat cells (Fig 30). It can be assumed that the lack of *snoo* in the brain only has a small effect on the lifespan.

To narrow down the phenotype to a specific type of neurons different neuronal driver lines were used to induce a conditional knockout of *snoo* (Fig 33).

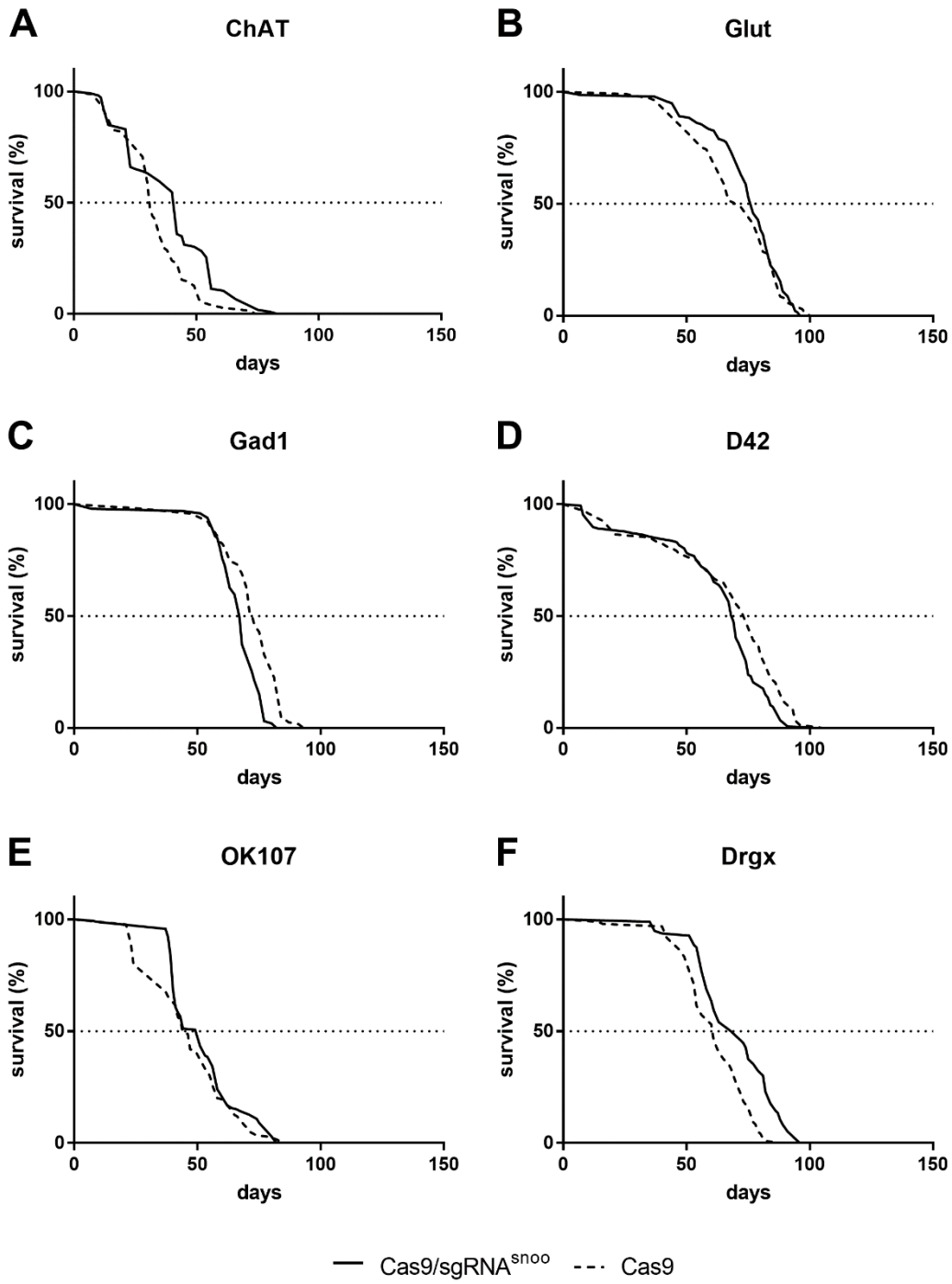

Fig 33. Lifespan reduction could not be attributed to a specific type of neurons.

Lifespan assay of a conditional knockout of *snoo* in different types of neurons. A. Knockout in cholinergic neurons using *ChAT-Gal4*. There is a significant difference (*p*-value < 0.0001). Median survival: ChAT > Cas9/sgRNA^{snoo} = 42 d; ChAT > Cas9 = 31 d. B. Knockout in glutamatergic neurons using *Glut-Gal4*. There is no significant difference (*p*-value = 0.5141). Median survival: Glut > Cas9/sgRNA^{snoo} = 77 d; Glut > Cas9 = 70 d. C. Knockout in GABAergic neurons using *Gad1-Gal4*. There is a significant difference (*p*-value < 0.0001). Median survival: Gad1 > Cas9/sgRNA^{snoo} = 67 d; Gad1 > Cas9 = 73 d. D. Knockout in motor neurons using *D42-Gal4*. There is a significant difference (*p*-value = 0.0002). Median survival: D42 > Cas9/sgRNA^{snoo} = 69 d; D42 > Cas9 = 74 d. E. Knockout in Kenyon cells using *OK107-Gal4*. There is no significant difference (*p*-value = 0.0834). Median survival: OK107 > Cas9/sgRNA^{snoo} = 51 d; OK1017 > Cas9 = 44 d. F. Knockout in neurons of the optic lobe using *Drgx-Gal4*. There is a significant difference (*p*-value < 0.0001). Median survival: Drgx > Cas9/sgRNA^{snoo} = 69 d; Drgx > Cas9 = 61 d.

Glut-Gal4, which drives expression in glutamatergic neurons, shows no significant difference (Fig 33). *ChAT-Gal4* drives the UAS dependent expression in cholinergic neurons and *Gad1-Gal4* in GABAergic neurons. There is a significant difference for a conditional knockout in these neurons. However, the median survival of the conditional knockout in cholinergic neurons is even increased by 11 days if compared to the control and the lifespan is only reduced by 6 days if GABAergic neurons lack Snoo. Therefore, it can be assumed that a specific knockout of *snoo* in cholinergic or glutamatergic neurons does not reduce the lifespan, while a specific knockout in GABAergic neurons has a small effect that is similar to the knockout in the brain (Fig 32).
D42-Gal4 drives the UAS dependent expression in motor neurons, *OK107-Gal4* in the Kenyon cells, which form the mushroom bodies, and *Drgx-Gal4* shows a strong expression in the optic lobes. There is a significant difference in the lifespan of flies with a *snoo* knockout in motor neurons in comparison to the corresponding control but the median survival is only reduced by 4 days (Fig 33). A conditional knockout of *snoo* in Kenyon cells does not have a significant influence on the lifespan. If *snoo* is specifically knocked out in the optic lobes a significant difference in the lifespan can be found. But the median survival of these flies is even increased by 8 days. Therefore, it can be assumed that the lack of *snoo* in the optic lobes does not influence the lifespan.

2.5.2. Climbing assay of a knockout of *snoo* in different cell types

To further confirm the results with the *snoo* deletion lines, negative geotaxis assays were repeated with the conditional knockout driven by *Act-Gal4* and *Da-Gal4* (Fig 34).

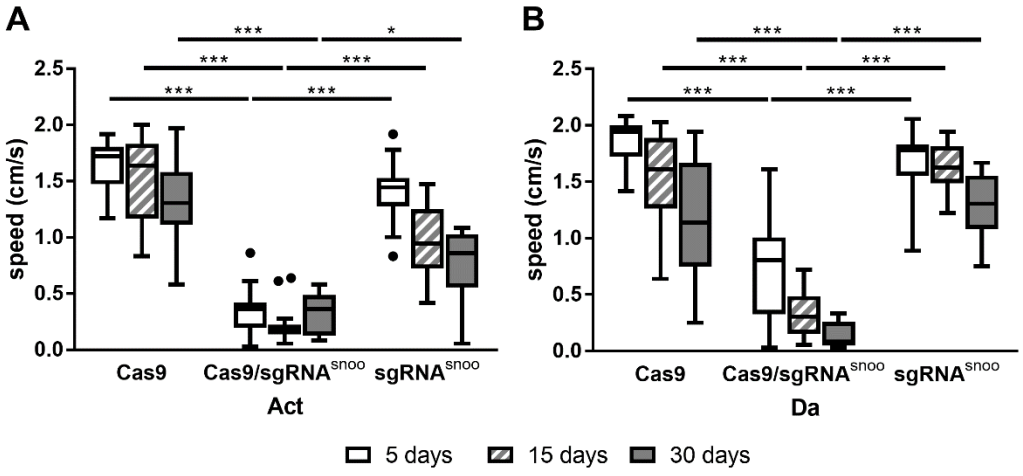

Fig 34. Knockout of *snoo* in all cells reduced negative geotaxis.
Negative geotaxis assay of a conditional knockout of *snoo* in all cells. ANOVA and Tukey's post hoc test were used to compare the knockout flies with the controls. A. Knockout using *Actin-Gal4*. There is a significant difference between the knockout Act > Cas9/sgRNA^{snoo} and both controls, Act > Cas9 and Act > sgRNA^{snoo}, at any age (p-value = 0.0346 for Cas9/gRNA^{snoo} – sgRNA^{snoo} at 30 days old, p-value < 0.0001 for all other cases). B. Knockout using *Da-Gal4*. There is a significant difference between the knockout Da > Cas9/sgRNA^{snoo} and both controls, Da > Cas9 and Da > sgRNA^{snoo}, at any age (p-value < 0.0001 for all cases).

A conditional knockout of *snoo* in both, Actin and Daughterless expressing cells, significantly reduces the performance of the flies in the negative geotaxis assay when compared to the controls (Fig 34). This is the case for all tested ages. The flies with a conditional knockout in all cells perform even worse than the deletion lines (Fig 22, Fig 23).

Negative geotaxis assays were performed on flies with a conditional knockout in glial, muscle or fat cells (Fig 35).

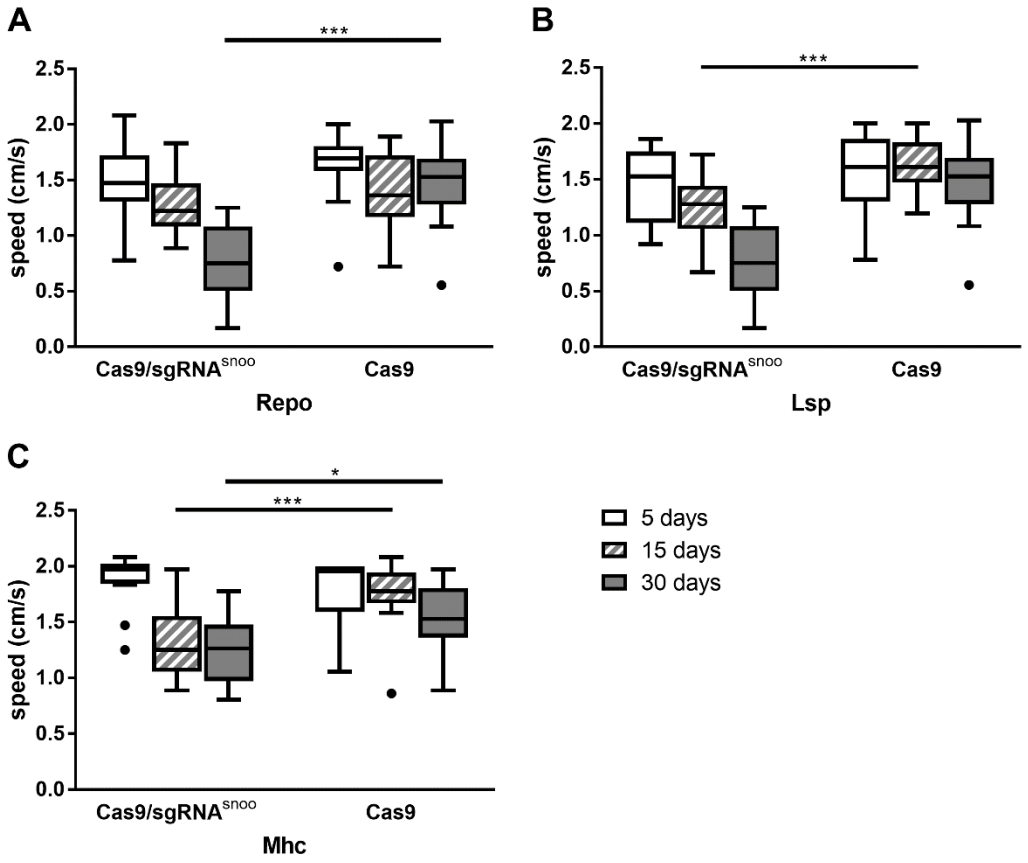

Fig 35. Knockout of *snoo* in glia or muscle cells has a weak effect on the geotaxis.

Negative geotaxis assay of a conditional knockout of *snoo* in different cell types. *t*-test was used to compare the knock-out flies with the controls. A. Knockout in glial cells using *Repo-Gal4*. There is a significant difference for 30 (*p*-value < 0.0001) but not for 5 (*p*-value = 0.2325) or 15 days old flies (*p*-value = 0.1269). B. Knockout in fat cells using *Lsp-Gal4*. A significant difference could be found for 15 (*p*-value = 0.0005) but not for 5 (*p*-value = 0.4833) or 30 days old flies (*p*-value = 0.2612). C. Knockout in muscle cells using *Mhc-Gal4*. There is a significant difference for 15 (*p*-value = 0.0008) and 30 (*p*-value = 0.0145) but not for 5 days old flies (*p*-value = 0.5534).

A conditional knockout of *snoo* in glial cells only results in a significant reduction of performance in the negative geotaxis assay in flies aged for 30 days (Fig 35). If *snoo* is specifically knocked out in fat cells, a significant reduction of the climbing activity could only be found with flies aged for 15 days but not for older or younger individuals. As these differences cannot be found for older flies and one would expect a possible effect to become more prominent with rising age, it

can be assumed that the results for 15 days old flies are a false positive result. If *snoo* is specifically knocked out in muscle cells, a significant reduction of performance in the negative geotaxis assay can be found in flies that were aged for at least 15 days. The observed reduction in all three cell types is considerably weaker than the effect of a general knock out (Fig 22, Fig 23, Fig 34). The driver line *Elav-Gal4* was used to induce the conditional knockout of *snoo* specifically in neurons (Fig 36).

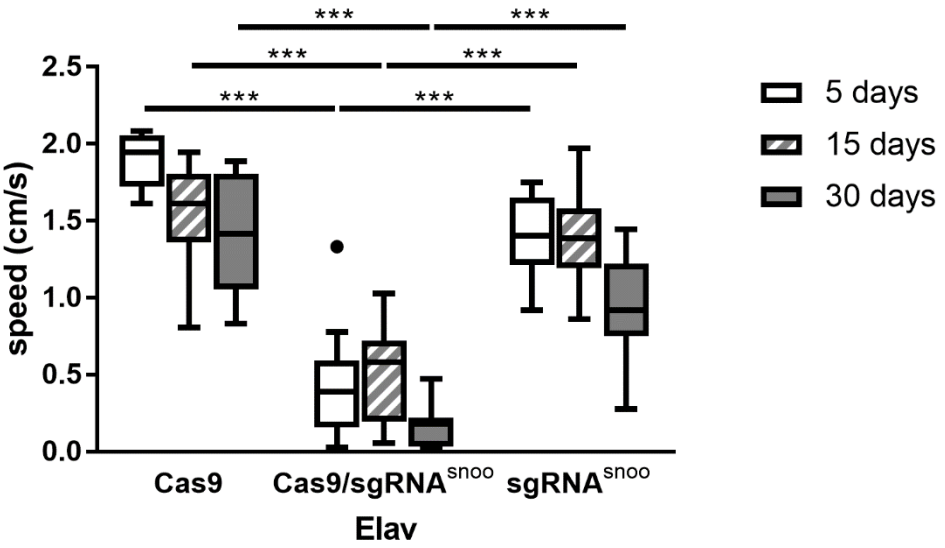

Fig 36. Knockout of *snoo* in neurons reduces negative geotaxis.

Negative geotaxis assay of a conditional knockout of *snoo* in neurons using *Elav-Gal4*. ANOVA and Tukey's post hoc test were used to compare the knockout flies with the controls. There is a significant difference between the knockout Elav > Cas9/sgRNA^{snoo} and both controls, Elav > Cas9 and Elav > sgRNA^{snoo}, at any age (p-value < 0.0001 for all cases).

If *snoo* is specifically knocked out in neurons, the negative geotaxis of the flies is significantly reduced compared to the controls (Fig 36). This is the case for all tested ages. A conditional knockout of *snoo* in neurons reproduces the effect of a general knockout (Fig 22, Fig 23, Fig 34). The negative geotaxis assay was performed on flies with a specific knockout of *snoo* in the brain (Fig 37).

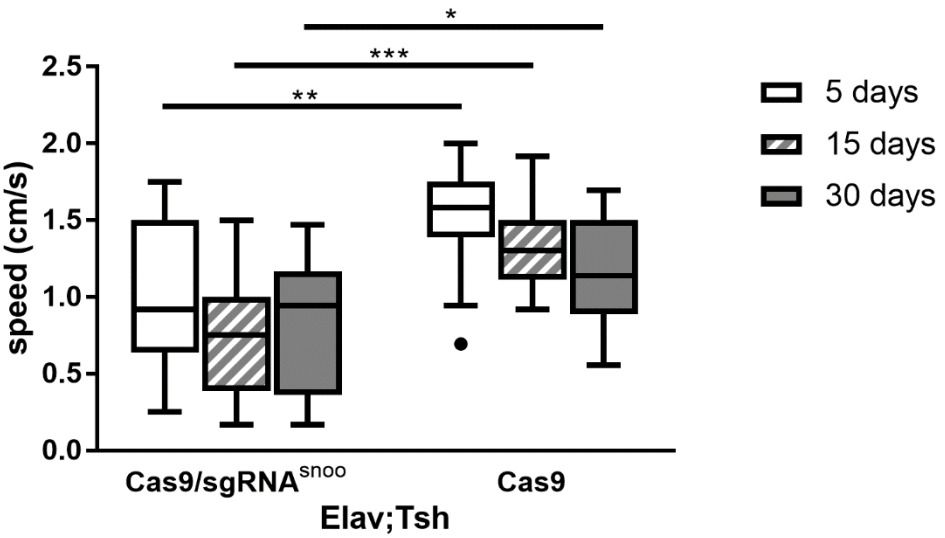

Fig 37. Knockout of *snoo* in the brain reduces negative geotaxis.

Negative geotaxis assay of a conditional knockout of *snoo* in the brains using *Elav-Gal4; Tsh-Gal80*. *t*-test was used to compare the knockout flies with the controls. Significant differences were found for 5 (*p*-value = 0.0038), 15 (*p*-value = 0.0002) or 30 days old flies (*p*-value = 0.0264).

If *snoo* is specifically knocked out in the brain, the negative geotaxis of the flies is significantly reduced when compared to the controls (Fig 37). This is the case for all tested ages. The observed reduction seems to be weaker than the effect of a general knockout (Fig 22, Fig 23, Fig 34). It can be assumed that the negative geotaxis phenotype is mainly due to the lack of *snoo* in the brain. To further narrow down the phenotype to a specific type of neurons, different neuronal driver lines were used to induce a conditional knockout of *snoo* (Fig 38).

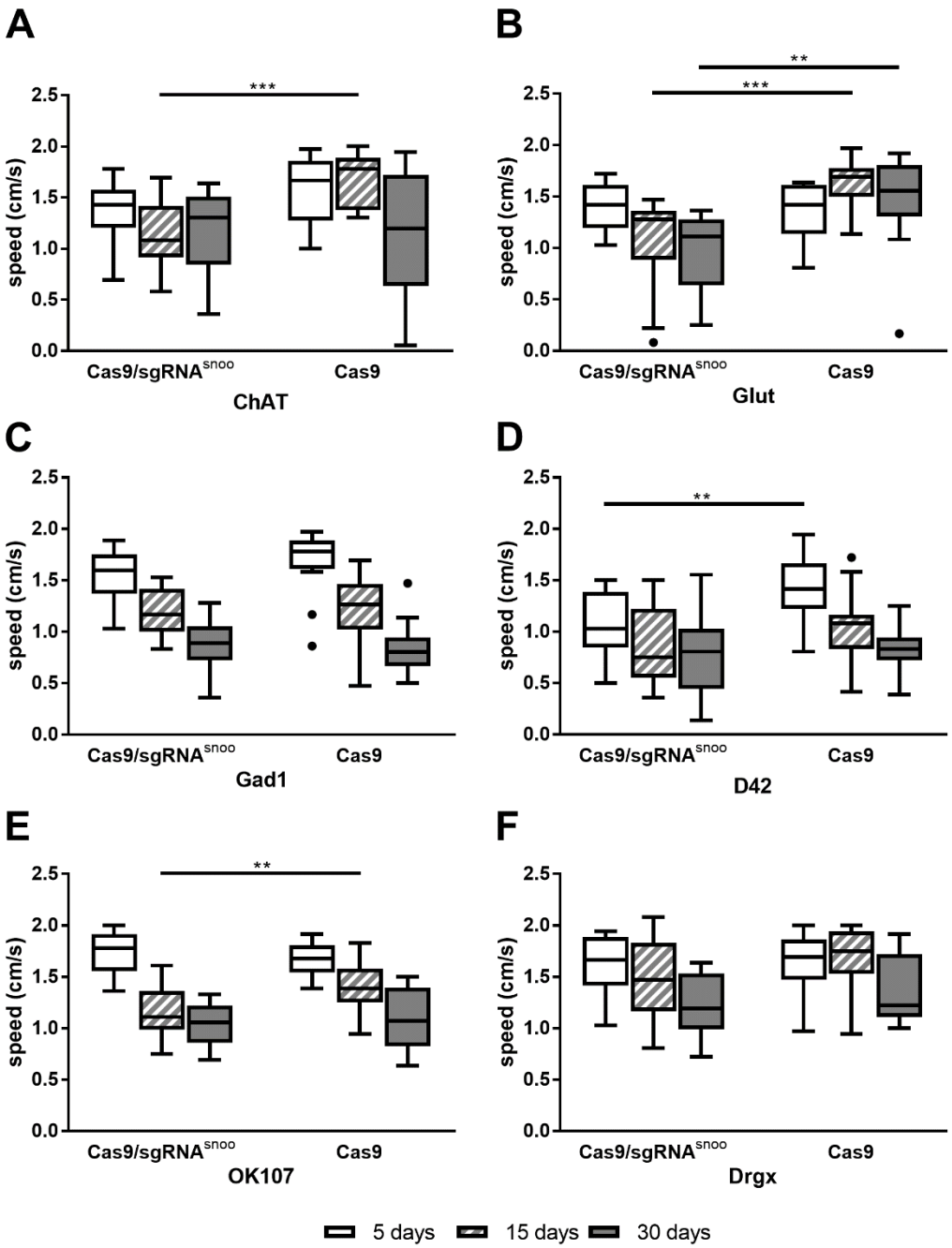

Fig 38. Geotaxis phenotype cannot be attributed to a specific type of neurons.

Negative Geotaxis Assay of a conditional knockout of *snoo* in different types of neurons. *t*-test was used to compare the knockout flies with the controls. A. Knockout in cholinergic neurons using *ChAT-Gal4*. There is a significant difference for 15 (*p*-value = 0.0003) but not for 5 (*p*-value = 0.0872) or 30 days old flies (*p*-value = 0.946). B. Knockout in glutamatergic neurons using *Glut-Gal4*. Geotaxis is significantly reduced in 15 (*p*-value = 0.0003) and 30 (*p*-value = 0.0044) but not in 5 days old flies (*p*-value = 0.666). C. Knockout in GABAergic neurons using *Gad1-Gal4*. No significant difference was found for 5 (*p*-value = 0.2611), 15 (*p*-value = 0.873) or 30 days old flies (*p*-value = 0.5428). D. Knockout in motor neurons using *D42-Gal4*. A significant reduction was found for 5 (*p*-value = 0.0102) but not for 15 (*p*-value = 0.0574) or 30 days old flies (*p*-value = 0.7723). E. Knockout in Kenyon cells using *OK107-Gal4*. Geotaxis is significantly reduced in 15 (*p*-value = 0.0099) but not in 5 (*p*-value = 0.3102) or 30 days old flies (*p*-value = 0.774). F. Knockout in neurons of the optic lobe using *Drgx-Gal4*. No significant difference was found for 5 (*p*-value = 0.8461), 15 (*p*-value = 0.1052) or 30 days old flies (*p*-value = 0.2551).

A conditional knockout of *snoo* in glutamatergic neurons with the driver line *Glut-Gal4* significantly reduces the climbing ability of the flies after 15 and 30 days (Fig 38). The observed reduction is less prominent than for a conditional knockout in all cells (Fig 22, Fig 23, Fig 34) or all neurons (Fig 36) but is similar to the one found in the CNS (Fig 37).

If *snoo* is specifically knocked out in cholinergic neurons using the driver line *ChAT-Gal4*, a significant difference can be found for 15 days old flies (Fig 38). This is also the case for a conditional knockout in Kenyon cells by *OK107-Gal4*. A conditional knockout in motor neurons using *D42-Gal4* results in a significant reduction of negative geotaxis in 5 days old flies. As these differences cannot be found for older flies and one would expect a possible effect to become more prominent with rising age, it can be assumed that the effects found for cholinergic neurons, Kenyon cells and motor neurons are false positive results.

A conditional knockout of *snoo* in GABAergic neurons by employing *Gad1-Gal4* or in the optic lobes using *Drgx-Gal4* has no significant influence on the negative geotaxis (Fig 38).

2.6. Buridan's paradigm assay of *snoo* deletion lines

To investigate the overall locomotor behaviour of the *snoo* deletion lines, a Buridan's paradigm assay was performed. For this assay, the movement of single flies on a platform between two optical cues is tracked via a camera and subsequently analysed (Colomb *et al*, 2012). The software for the analysis of the movement returns a set of different parameters that can be further investigated. Therefore, a single experiment enables the investigation of many different aspect of the locomotion. The tested flies had been crossed into the genetic background of WTB to prevent a possible disturbance of the experimental outcome caused by the optical impairment in w^{1118} (Ferreiro *et al*, 2018). The transition plots represent the density of passage for one tested genotype at any location on the platform and provide an overview of the overall performance of the tested flies (Fig 39).

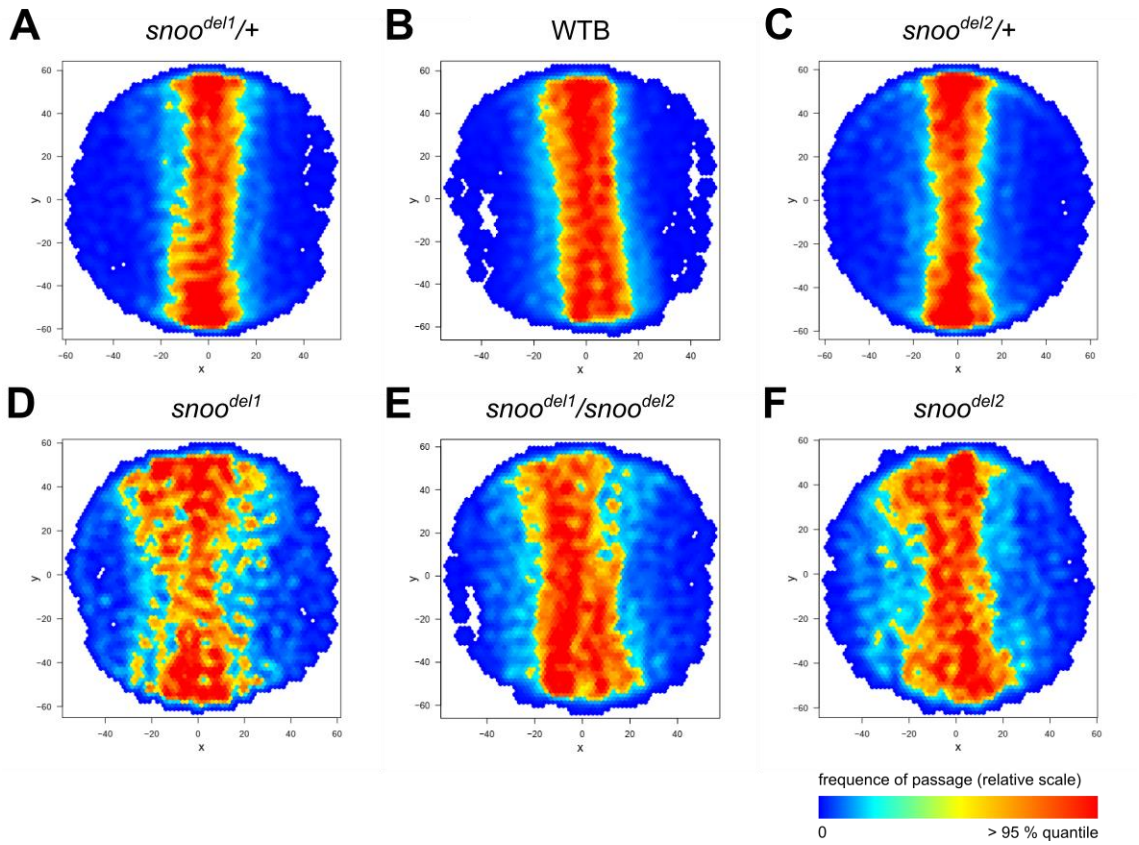

Fig 39. Deletion lines show a phenotype in the Buridan's paradigm assay.

The transition plots show the density of passage of the flies. The heterozygous controls (A, C) and the wildtype (B) are located in the area between the optical cues most of the time. The homozygous (D, F) and transheterozygous (E) *snoo* deletion mutants spend more time in other parts of the platform.

The transition plots show that the homozygous mutants and the transheterozygous flies perform worse than the heterozygous controls and the wildtype in the Buridan's paradigm assay (Fig 39). The controls tend to walk straight from one of the stripes, which function as optical cues, to the other one. If the flies lack *snoo*, their location is more distributed over the whole platform.

The results for the different parameters were analysed using Analysis of variance (ANOVA) and Tukey's post hoc test. A significant difference between the wildtype control and heterozygous flies could not be found for any parameter. Therefore, heterozygotes were used as controls and the wildtype was not included. At first, the parameters regarding the overall activity were analysed (Fig 40).

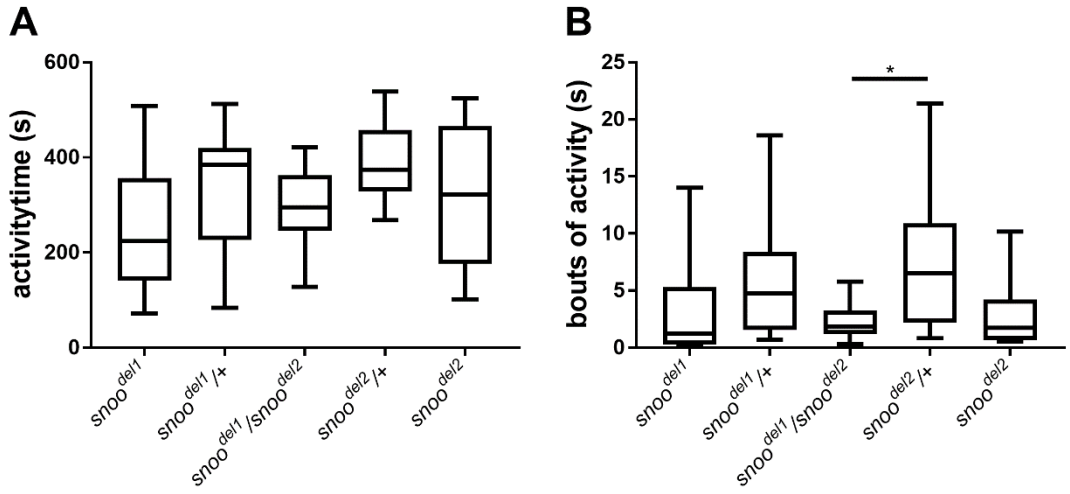

Fig 40. Deletion of *snoo* has no significant influence on the overall activity.

A. Total activity time. No significant differences could be found for the homozygous mutants (*p*-values: $snoo^{del1}$ = 0.5514, $snoo^{del2}$ = 0.8361) or the transheterozygotes (*p*-values: $snoo^{del1}$/+ = 0.9828, $snoo^{del2}$/+ = 0.4542). B. Bouts of activity leading to a larger displacement. There is a significant difference if the transheterozygous flies are compared to the control $snoo^{del2}$/+ (*p*-value = 0.0402) but not to snoo^{del1}/+ (*p*-value = 0.6823). No significant differences could be found for the homozygous mutants (*p*-values: $snoo^{del1}$ = 0.6823, $snoo^{del2}$ = 0.1259).

There is no significant difference in the total activity time of the mutants (Fig 40). The bouts of activity leading to a larger displacement are significantly reduced in transheterozygous flies if compared to the heterozygous control $snoo^{del2}$/+. Even if no other significant differences could be found, the mutant flies seem to show a tendency of reduction for the bouts of activity. Next, it was investigated if the deletion lines show differences in their walking behaviour (Fig 41).

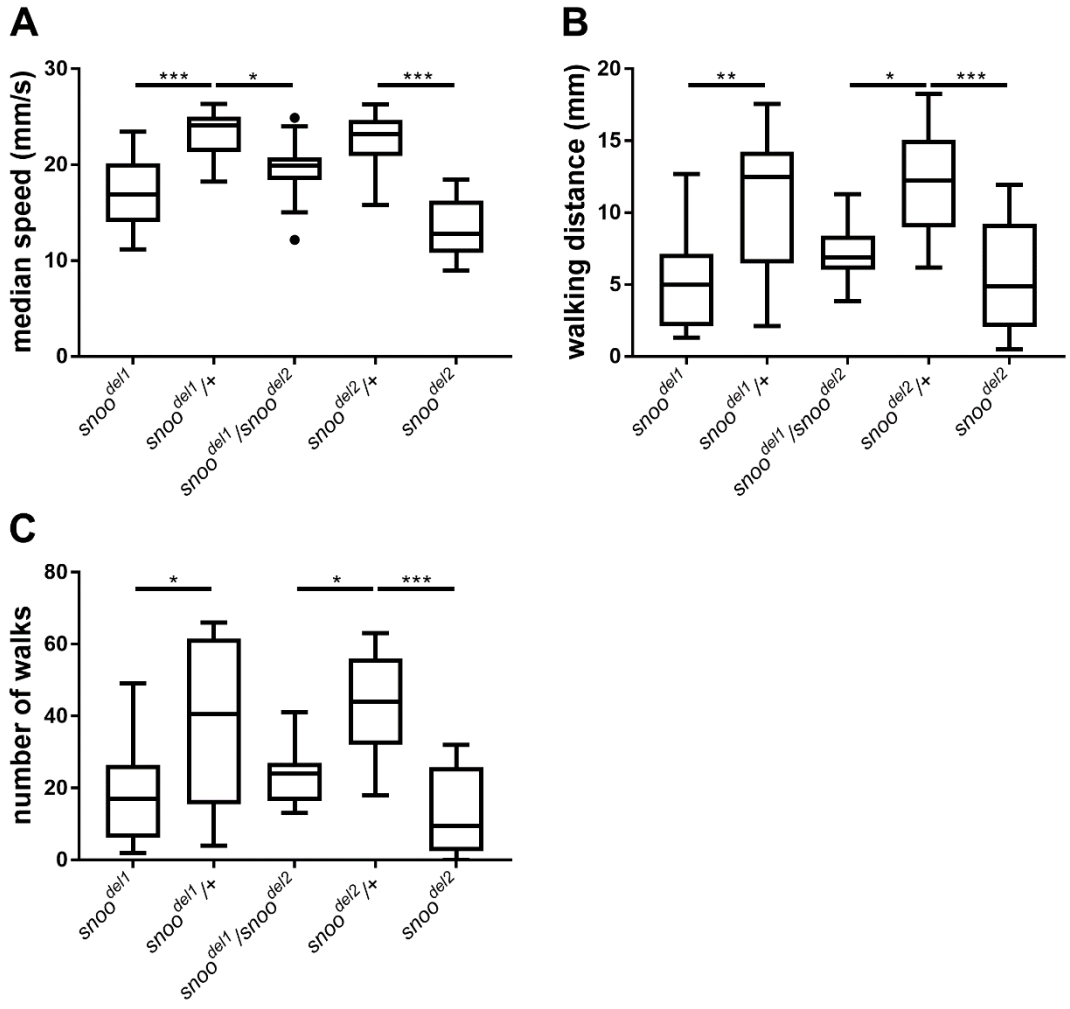

Fig 41. Flies with a deletion of *snoo* walk less.

A. Median speed. Both deletion lines, $snoo^{del1}$ and $snoo^{del2}$, show a significant reduction (p-value < 0.0001 in both cases). The transheterozygotes differ significantly from the control $snoo^{del1}$/+ (p-value = 0.0306) but not from $snoo^{del2}$/+ (p-value = 0.0813). B. Distance travelled by the flies. Both deletion lines show a significant reduction (p-values: $snoo^{del1}$ = 0.0089, $snoo^{del2}$ = 0.0003). Transheterozygotes differ significantly from the control $snoo^{del2}$/+ (p-value = 0.0103) but not from $snoo^{del1}$/+ (p-value = 0.1485). C. Number of times the flies walked from one stripe to the other. Both deletion lines show a significant reduction (p-values: $snoo^{del1}$ = 0.0149, $snoo^{del2}$ < 0.0001). Transheterozygotes differ significantly from the control $snoo^{del2}$/+ (p-value = 0.0113) but not from $snoo^{del1}$/+ (p-value = 0.0954).

The median speed of the mutant flies, the distance they walked per minute and the number of times they walked from one stripe to the other were significantly reduced (Fig 41). For all three parameters a significant difference could only be found if the results for the transheterozygous flies were compared to one of the heterozygous controls but not the other one. In general, the effect in the transheterozygous individuals seems to be weaker than in the homozygous mutants. This can most likely be explained by the fact that the overall fitness of the transheterozygous flies is higher than the one of the homozygous strains as these are more inbred. The parameters regarding the pauses of the flies during the experiments were analysed (Fig 42).

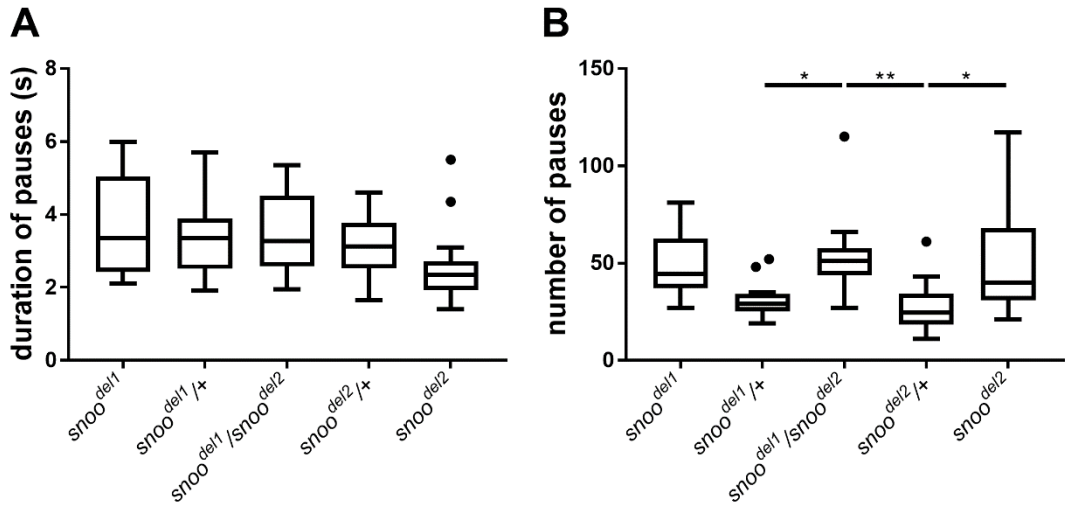

Fig 42. Deletion of *snoo* influences number but not duration of pauses.

A. Duration of pauses in seconds. No significant differences were found (*p*-value = 0.118). B. Number of pauses. A significant increase was found for the deletion line $snoo^{del2}$ (*p*-value = 0.0136) but not for $snoo^{del1}$ (*p*-value = 0.1540). The transheterozygotes differ significantly from both controls (*p*-values: $snoo^{del1}/+$ = 0.0227, $snoo^{del2}/+$ = 0.0058).

No significant differences were found for the duration of pauses but the numbers of pauses were significantly increased for $snoo^{del2}$ and transheterozygous flies (Fig 42). Even if there is no significant difference between $snoo^{del1}$ and its corresponding heterozygous control, the number of pauses also seems to be elevated in this mutant line. Therefore, it can be assumed that the mutant flies tend to make more pauses of the same length. It was analysed if the flies show differences in their turning behaviour while they walk (Fig 43).

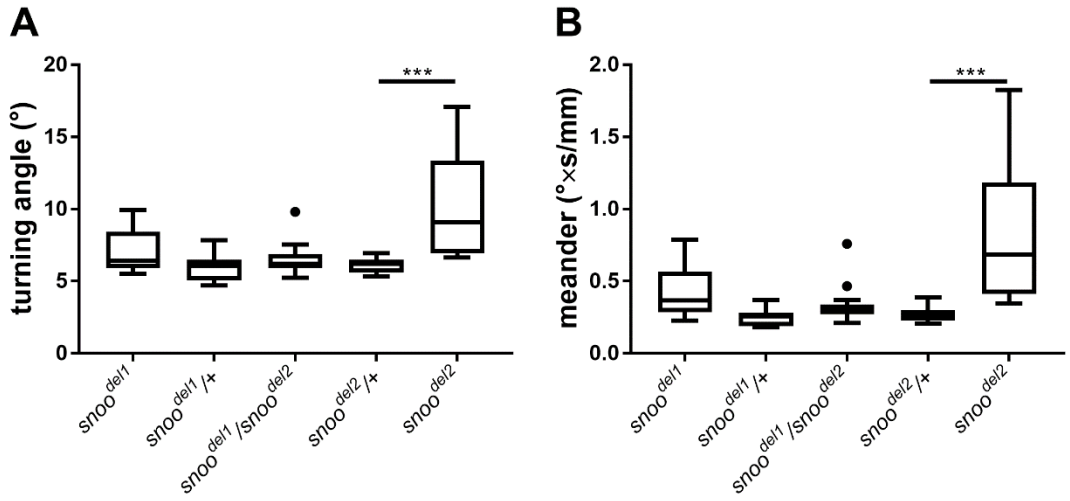

Fig 43. Deletion of *snoo* does not influence turning angle or meander.

A. Median turning angle. A significant difference was found for $snoo^{del2}$ (*p*-value < 0.0001) but not for $snoo^{del1}$ (*p*-value = 0.7215). No significant differences can be found for the transheterozygous flies (*p*-values*:* $snoo^{del1}/+$ = 0.9714, $snoo^{del2}/+$ = 0.9966). B. Tortuosity of trajectories calculated as turning angle divided by instantaneous speed. A significant difference was found for $snoo^{del2}$ (*p*-value < 0.0001) but not for $snoo^{del1}$ (*p*-value = 0.4219). No significant differences can be found for the transheterozygous flies (*p*-values: $snoo^{del1}/+$ = 0.9568, $snoo^{del2}/+$ = 0.9868).

As the only significant difference found for the parameters turning angle and meander are between $snoo^{del2}$ and its corresponding heterozygous control (Fig 43), it can be assumed that this observed effect is due to the genetic background of $snoo^{del2}$. Otherwise, one would expect to find similar results for $snoo^{del1}$ or the transheterozygous flies. Nonetheless, both parameters seem to be slightly elevated for the homozygous mutants and the transheterozygous flies. Finally, the parameters regarding the position of the flies on the platform were analysed (Fig 44).

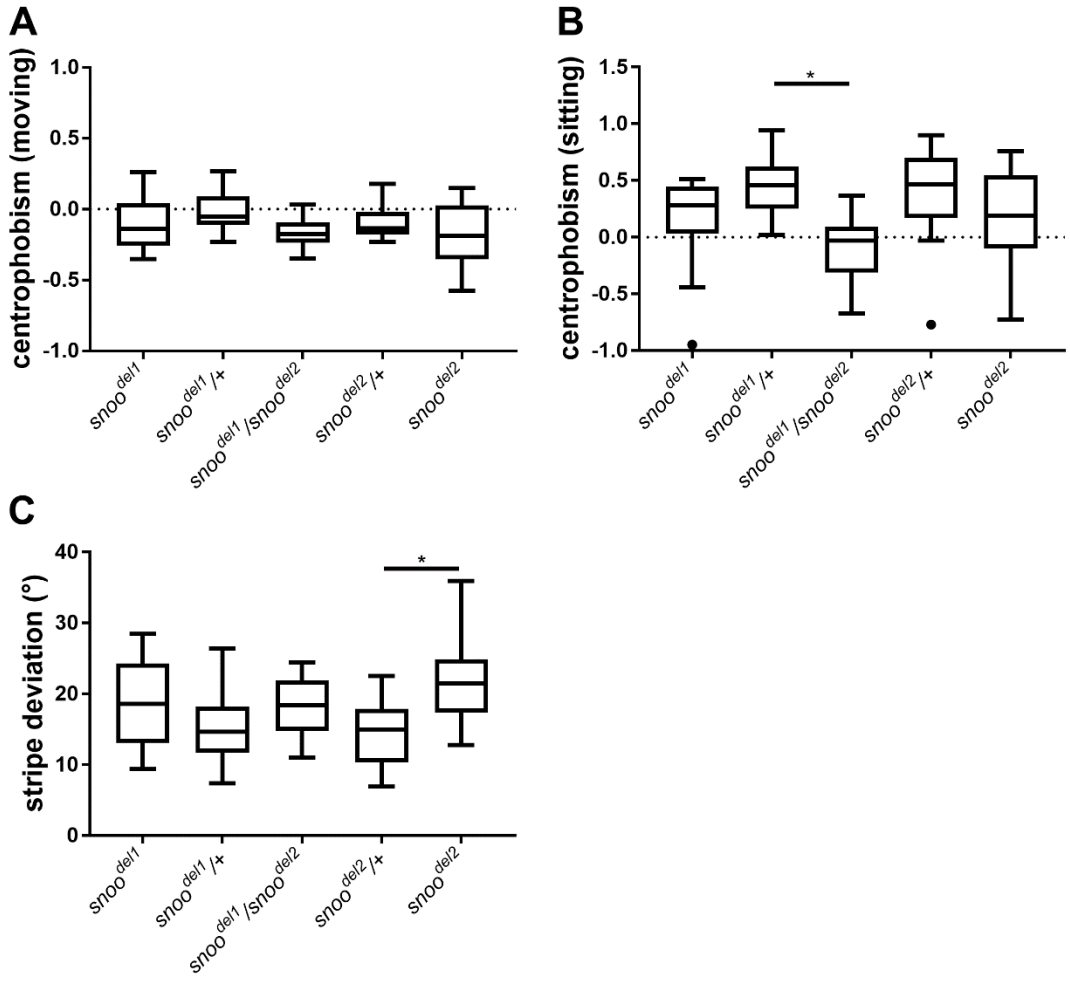

Fig 44. Deletion of *snoo* does not influence centrophobism and stripe deviation.

A. Centrophobism index of moving flies. No significant differences were found for both homozygous deletion lines (*p*-values: $snoo^{del1}$ = 0.9580, $snoo^{del2}$ = 0.6489) or the transheterozygotes (p-values: $snoo^{del1}$/+ = 0.3519, $snoo^{del2}$/+ = 0.9230). B. Centrophobism index of sitting flies. No significant differences were found for both homozygous deletion lines (*p*-values: $snoo^{del1}$ = 0.4578, $snoo^{del2}$ = 0.9188). Transheterozygotes differ significantly from $snoo^{del2}$/+ (*p*-value = 0.0729) but not from $snoo^{del1}$/+ (*p*-value = 0.0116). C. Angle of stripe deviation. A significant difference was found for $snoo^{del2}$ (*p*-value = 0.0301) but not for $snoo^{del1}$ (*p*-value = 0.8294). There is no significant difference between transheterozygous flies and any of both controls (*p*-values: $snoo^{del1}$/+ = 0.8672, $snoo^{del2}$/+ = 0.6699).

Mutant flies seem to tend to spend more time in the inner area of the arena as both centrophobism indices are a bit lower for $snoo^{del1}$, $snoo^{del2}$ and the transheterozygotes (Fig 44). But if there is an effect, it is relatively weak as the only significant difference could be found for the centrophobism index of sitting flies between transheterozygous animals and the heterozygous control $snoo^{del1}$/+. The stripe deviation also seems to be slightly increased (Fig 44). Nonetheless, a significant difference could only be found when comparing $snoo^{del2}$ with its corresponding heterozygous control as it is the case for the parameters turning angle and meander (Fig 43).

2.7. Identification of possible *snoo* target genes by RNAseq

The found phenotypes, like the decreased lifespan, the reduced negative geotaxis and the impaired walking activity in the Buridan's paradigm assay, are not specific enough to enable a detailed genetic or functional analysis of the *snoo* deletions. However, the previous results led to the assumption that *snoo* has a critical function in the nervous system as a conditional knockout in neurons is sufficient to reproduce the lifespan and geotaxis phenotypes of a general knockout. Therefore, an RNAseq of brains of adult flies was performed to compare homozygous mutants with heterozygotes as control. Screening for genes with an altered expression activity in the deletion lines might reveal hints on signalling pathways or cellular processes that could be impaired by the deletion of *snoo*.

Therefore, RNA was extracted from 40 adult brains per replicate and genotype. Two replicates were performed with homozygous mutants of the line $snoo^{del2}$ and heterozygous flies as control. Differential expression analysis was used to compare the read counts of the mutants to the ones of the control (Fig 45). This method calculates the logarithmical fold change of each gene together with the *p*-value.

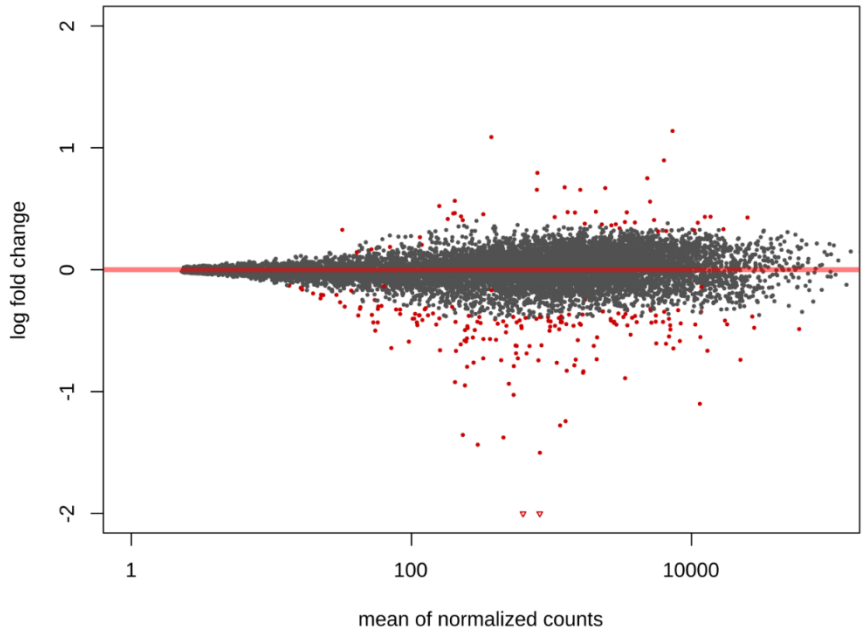

Fig 45. Analysis of RNAseq data revealed 221 differentially expressed genes.

Differential Expression analysis was used to compare the read counts for $snoo^{del2}$ and the control $snoo^{del2}/+$. The red data points belong to genes with an adjusted *p*-value < 0.1 and therefore can be considered significantly different.

If the adjusted *p*-value < 0.1 for a gene, it can be assumed that the expression of this gene is significantly different in the mutants compared to the control. A set of 221 genes was identified with a significantly different expression activity (Fig 45). The logarithmical fold change of 47 of these genes has a positive value, which signifies that the read count of the mutant is higher than the control. Therefore, the transcription of these genes was increased in the mutants in comparison

to the control. The remaining 174 genes have a negative fold change and in assumption, showed less transcription activity in *snoo*^{del2}.

The 27 genes with the highest fold change were selected and qPCR was used to validate the results of the RNAseq. RNA from adult heads was extracted and used to produce cDNA. Homozygous individuals of both deletion lines were compared with heterozygous flies, which were generated by crossing virgins of the homozygous flies with males of the corresponding injection stock. Three biological replicates were performed. ANOVA revealed 12 genes, which showed a significant difference in expression for at least one deletion line.

Some of the genes that are differentially expressed in the *snoo* deletion lines are known to regulate the metabolic homeostasis (Fig 46, Fig 47), while others code for neuropeptides that are for example involved in the regulation of the circadian rhythm or satiety (Fig 48, Fig 49). A further subset codes for enzymes that are important for the resistance to toxins (Fig 50, Fig 51). Furthermore, there are also genes, whose function is still unidentified (Fig 52, Fig 53).

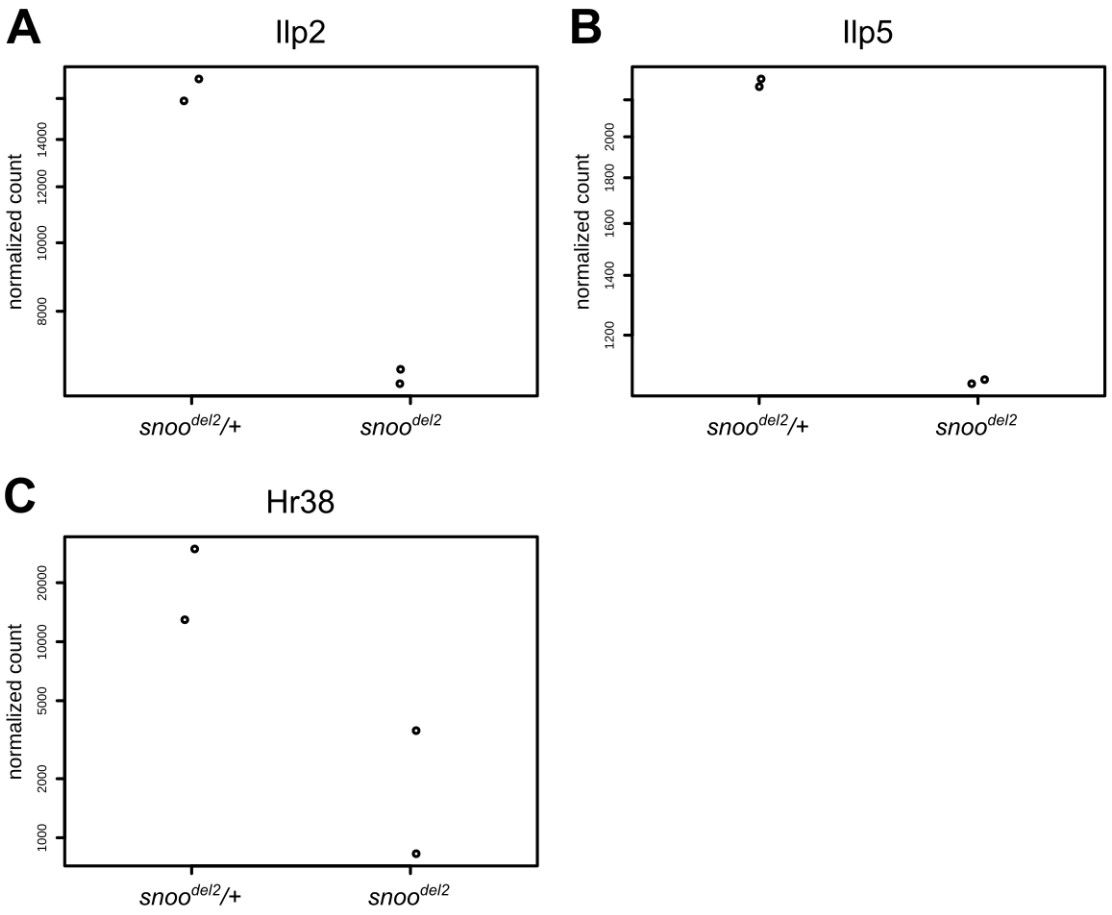

Fig 46. Expression of genes involved in metabolic homeostasis is decreased in *snoo*^{del2}.

The read counts for the genes *ilp2* (fold change = -1.35; adjusted *p*-value < 0.0001), *ilp5* (fold change = -1.11; adjusted *p*-value < 0.0001) and *hr38* (fold change = -3.30; adjusted *p*-value = 0.0926) are significantly lower in the mutant *snoo*^{del2} than in the heterozygous control.

The analysis of the RNAseq found significantly lower read counts in *snoo*^{del2} for some genes that are involved in metabolic homeostasis (Fig 46). These are the Insulin-like proteins Ilp2 and Ilp5 that are ligands of the IIS and Hormone receptor-like 38 (Hr38), which is known to regulate the uptake and storage of glycogen in larvae (Ruaud *et al*, 2011).

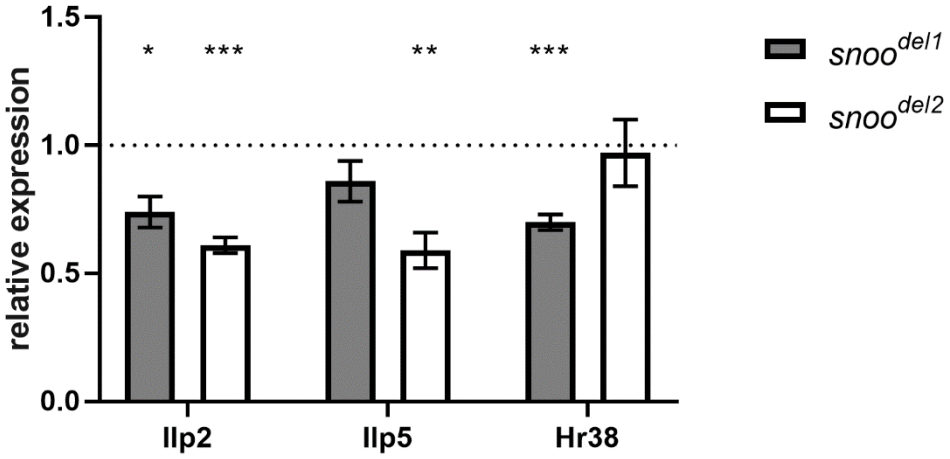

Fig 47. Genes involved in metabolic homeostasis are reduced in both *snoo* deletion lines.
The ΔΔCq method was used to calculate the relative expression of the genes. Mean values of the three replicates and standard error of the mean are shown. *t*-test was used to analyse the data. Significant effects were found for *ilp2* in both deletion lines (*p*-values: *snoo*^{del1} = 0.0123, *snoo*^{del2} = 0.0002). There is a significant difference for *ilp5* in *snoo*^{del2} (*p*-value = 0.0042) but not in *snoo*^{del1} (*p*-value = 0.1550). For *hr38* a significant effect could be found in *snoo*^{del1} (*p*-value = 0.0006) but not in *snoo*^{del2} (*p*-value = 0.8288).

Investigation by qPCR could validate the decreased expression of the genes *ilp2*, *ilp5* and *hr38* for at least one mutant line (Fig 47).

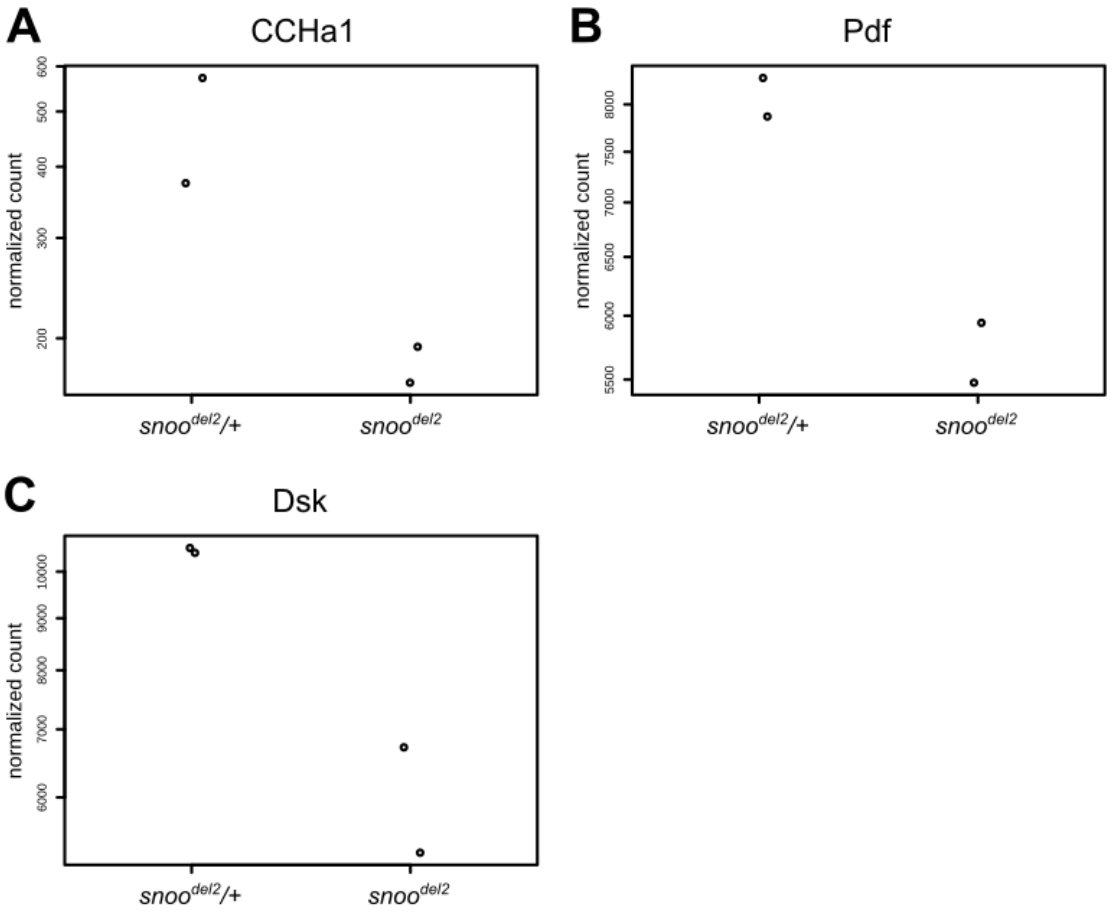

Fig 48. Different neuropeptides are differentially expressed in *snoo^{del2}*.

The analysis of the RNAseq data revealed significantly less reads for CCHa1 (fold change = -1.40; adjusted *p*-value = 0.0012), Pdf (fold change = -0.50; adjusted *p*-value = 0.0108) and Dsk (fold change = -0.80; adjusted *p*-value = 0.0008) in the brains of homozygous *snoo^{del2}* flies than in the heterozygous control.

Other neuropeptides that showed significantly different read counts include *CCHamide1* (*CCHa1*) and *pigment-dispersing factor* (*pdf*), which are both involved in the regulation of the circadian rhythm (Fig 48). The gene *drosulfakinin* (*dsk*) encodes the neuropeptides Dsk1 and Dsk2, which are known to regulate satiety.

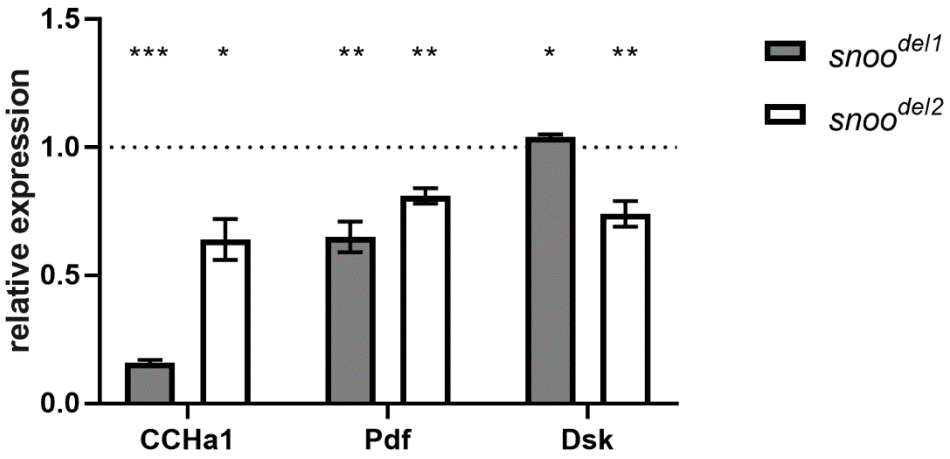

Fig 49. Snoo influences expression of neuropeptides involved in circadian rhythm and satiety.
The ΔΔCq method was used to calculate the relative expression of the genes. Mean values of the three replicates and standard error of the mean are shown. *t*-test was used to analyse the data. There is a significant reduction of the expression of CCHa1 in both deletion lines (*p*-values: $snoo^{del1} < 0.0001$, $snoo^{del2} = 0.0108$). The expression of Pdf is also reduced in both mutants (*p*-values: $snoo^{del1} = 0.0043$, $snoo^{del2} = 0.0032$). A significant effect was found for *dsk* in both deletion lines (*p*-values: $snoo^{del1} = 0.0161$, $snoo^{del2} = 0.0065$).

The reduced expression of the neuropeptides CCHa1, Pdf and both Dsks are differentially expressed in both deletion lines, $snoo^{del1}$ and $snoo^{del2}$, could be confirmed by qPCR (Fig 49).

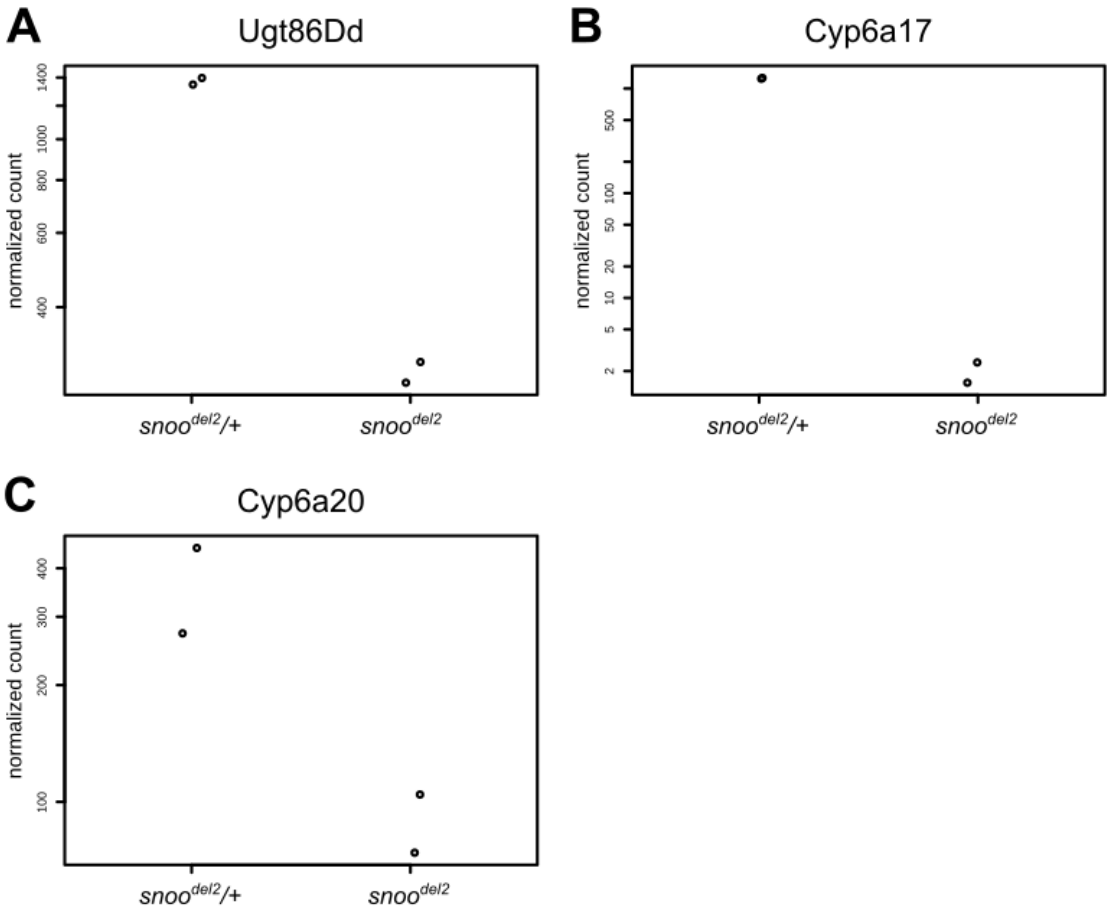

Fig 50. Detoxification enzymes are differentially expressed in *snoo*^{del2}.

In the RNAseq data of the mutants significantly less reads were found for the enzymes Ugt86Dd (fold change = -2.29; adjusted *p*-value < 0.0001), Cyp6a17 (fold change = -9.70; adjusted *p*-value < 0.0001) and Cyp6a20 (fold change = -2.02; adjusted *p*-value < 0.0001), which are involved in detoxification.

Some enzymes responsible for detoxification were found to be downregulated within the *snoo* mutants (Fig 50). These are the UDP-glucuronosyltransferase Ugt86Dd and the cytochrome P450 proteins Cyp6a17 and Cyp6a20.

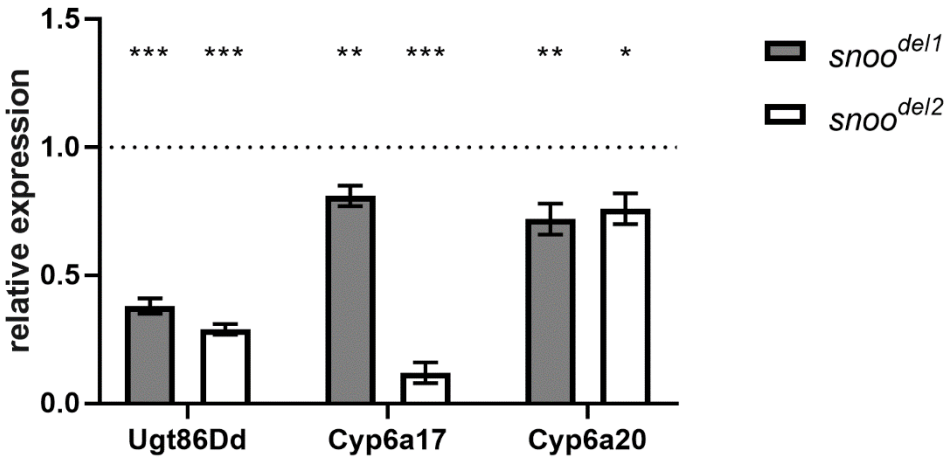

Fig 51. Expression of detoxification enzymes is impaired in *snoo* deletion lines.
The ΔΔCq method was used to calculate the relative expression of the genes. Mean values of the three replicates and standard error of the mean are shown. *t*-test was used to analyse the data. The expression of Ugt86Dd is significantly reduced in both deletion lines (*p*-value < 0.0001 in both cases). There is a significant reduction of Cyp6a17 in both deletion lines (*p*-values: $snoo^{del1}$ = 0.0090, $snoo^{del2}$ < 0.0001). Furthermore, a significant effect for Cyp6a20 could be found for both deletion lines (*p*-values: $snoo^{del1}$ = 0.0095, $snoo^{del2}$ = 0.0161).

The analysis with qPCR confirmed that the expression of the detoxification enzymes Ugt86Dd, Cyp6a17 and Cyp6a20 is decreased in both deletion lines (Fig 51) as the analysis of the RNAseq data had suggested.

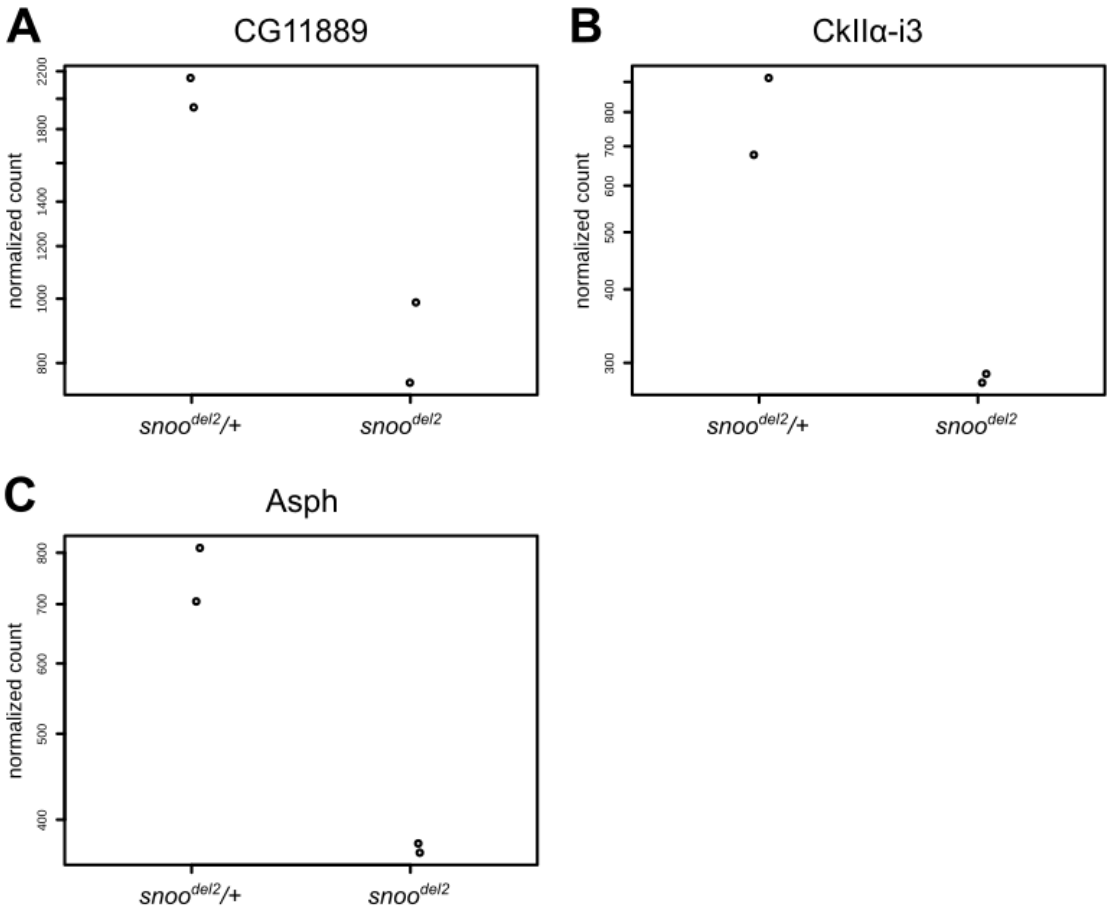

Fig 52. Further genes which are differentially expressed in *snoo^{del2}*.

Differential expression analysis revealed significant differences for CG11889 (fold change = -1.24; adjusted *p*-value < 0.0001), CkIIα-i3 (fold change = -1.49; adjusted *p*-value < 0.0001) and Asph (fold change = -1.03; adjusted *p*-value = 0,0002).

For three further genes a significant difference could be found in the RNAseq data (Fig 52). One of these is the yet unnamed gene CG11889. Another one is the CKII-α subunit interactor-3 (CKIIα-i3). The Casein Kinase 2 (CKII) is known to be involved in the regulation in a variety of processes, which includes the circadian rhythm (Allada & Meissner, 2005; Wairkar *et al*, 2013). The third one is the gene encoding Aspartyl β-hydroxylase (Asph).

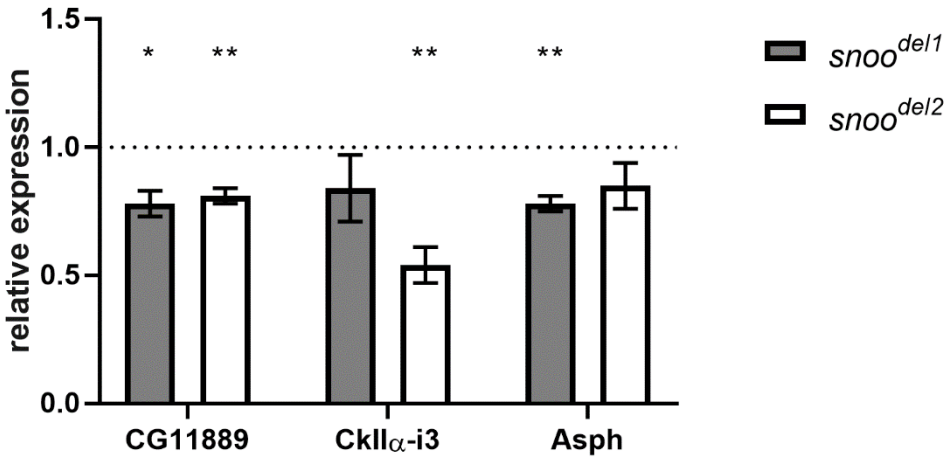

Fig 53. Differential Expression could be confirmed.

The ΔΔCq method was used to calculate the relative expression of the genes. Mean values of the three replicates and standard error of the mean are shown. *t*-test was used to analyse the data. There is a significant reduction of the expression of CG11889 in both deletion lines (*p*-values: $snoo^{del1}$ = 0.0117, $snoo^{del2}$ = 0.0032). The expression of CkIIα-i3 is significantly reduced in $snoo^{del2}$ (*p*-value = 0.0028) but not $snoo^{del1}$ (*p*-value = 0.2858). A significant effect for *asph* was found in $snoo^{del1}$ (*p*-value = 0.0018) but not $snoo^{del2}$ (*p*-value = 0.1709).

The analysis with qPCR confirmed the differential expression of the three genes *CG11889*, *CKIIα-i3* and *asph* (Fig 53).

2.8. Influence of nutrition on the phenotype of *snoo* deletion lines

The RNAseq and the qPCR assays showed that in *snoo* deletion mutants Ilp2 and Ilp5 were down regulated. Further qPCR experiments were performed to confirm these results and investigate if the expression of other genes involved in sugar metabolism is also affected (Fig 54). Virgins of the deletion lines $snoo^{del1}$ and $snoo^{del2}$ were crossed with males of w^{1118}. The male offspring of this cross was used as control.

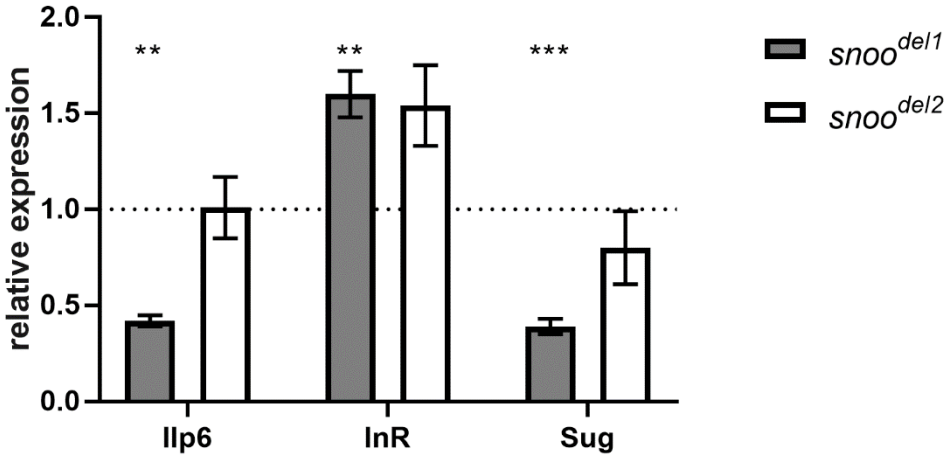

Fig 54. Genes involved in IIS are differentially expressed in *snoo* deletion lines.
The ΔΔCq method was used to calculate the relative expression of the genes. Mean values of the three replicates and standard error of the mean are shown. *t*-test was used to analyse the data. There is a significant reduction of the expression of *ilp6* in $snoo^{del1}$ (*p*-value = 0.0027) but not $snoo^{del2}$ (*p*-value = 0.9532). The expression of InR is significantly increased in $snoo^{del1}$ (*p*-value = 0.0075) but not in $snoo^{del2}$ (*p*-value = 0.0619). The expression of Sug is significantly reduced in $snoo^{del1}$ (*p*-value = 0.0001) but not in $snoo^{del2}$ (*p*-value = 0.3330).

In the qPCR experiments with the new controls a significant reduction of the expression of Ilp6 could be found for $snoo^{del1}$ (Fig 54). Furthermore, it could be shown that the expression of InR, the receptor of the IIS, is significantly increased in both deletion lines. Additionally, in $snoo^{del1}$ a significant reduction could be found for the expression of the gene *sugarbabe* (*sug*), which codes for a transcription factor that is expressed in the IPCs and is also involved in the metabolic homeostasis (Zinke *et al*, 2002; Varghese *et al*, 2010; Mattila *et al*, 2015; Luis *et al*, 2016). As IIS is an important regulator of energy consumption and storage, it was investigated in further experiments if the nutritional status influences the phenotype of the *snoo* deletion lines.

2.8.1. Starving weakens the lifespan phenotype of *snoo* deletion

As RNAseq and qPCR experiments suggest an influence of the deletion of *snoo* on members of the IIS in *Drosophila melanogaster*, the lifespan assay was repeated under different nutritional conditions (Fig 55). On the one hand, flies were fed with food consisting of 20 % sugar. On the other hand, flies were starved by keeping them on food containing only 0.1 % sugar.

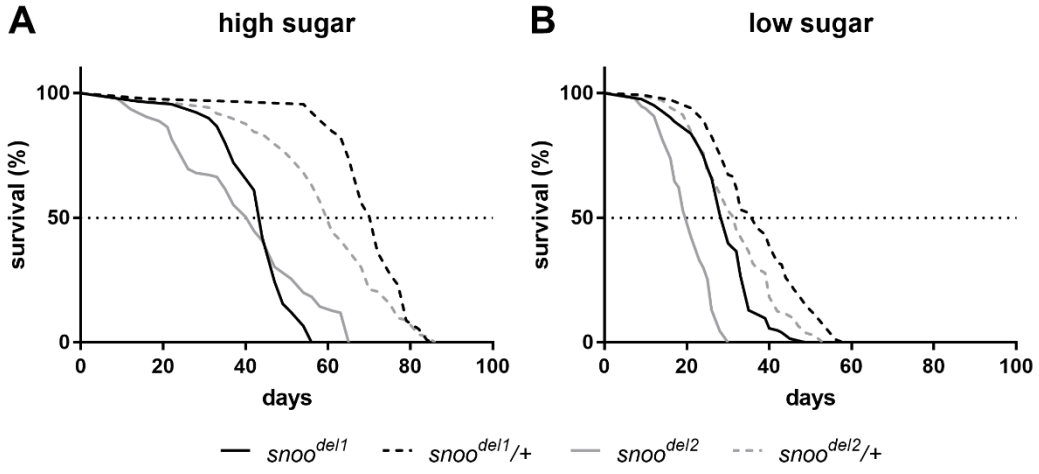

Fig 55. Starving weakens the lifespan phenotype of *snoo* deletion lines.

A. Lifespan assay of flies fed with 20 % sugar food. There is a significant reduction for both deletion lines, $snoo^{del1}$ and $snoo^{del2}$ (*p*-value < 0.0001 in both cases). Median survival: $snoo^{del1}$ = 44 d; $snoo^{del1}$/+ = 72 d; $snoo^{del2}$ = 40 d; $snoo^{del2}$/+ = 61 d. B. Lifespan assay of flies fed with 0.1 % sugar food. There is a significant reduction for both deletion lines, $snoo^{del1}$ and $snoo^{del2}$ (*p*-value < 0.0001 in both cases). Median survival: $snoo^{del1}$ = 30 d; $snoo^{del1}$/+ = 37 d; $snoo^{del2}$ = 21 d; $snoo^{del2}$/+ = 32 d.

In both cases, keeping the flies on a high sugar diet and starving them on a low sugar diet, the lifespan of the homozygous mutants is significantly reduced in comparison to the corresponding heterozygous controls (Fig 55), as it is the case for standard food (Fig 25). On the high sugar diet, the median survival of $snoo^{del1}$ is reduced by 28 days, $snoo^{del2}$ flies survive 21 days less. If the flies are starved by a low sugar diet, the median survival of $snoo^{del1}$ is reduced by 7 days in comparison to their heterozygous control and the $snoo^{del2}$ flies survive 11 days less. The difference between the homozygous flies and their heterozygous controls is much smaller on the low sugar diet if compared to the high sugar diet or standard food. This is mainly caused by the fact that the heterozygous flies have a shorter lifespan under starving conditions.

2.8.2. Nutrition does not influence the development of *snoo* mutants

To examine possible effects of the *snoo* deletion on development depending on the nutritional condition, an assay was performed to study the pupation time of the larvae (Fig 56). Again, this was tested on both, high and low sugar food.

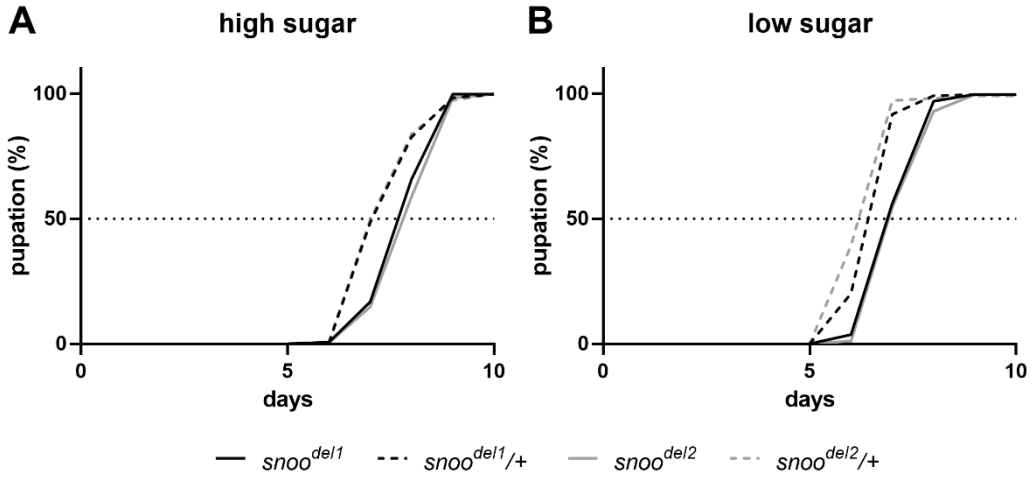

Fig 56. Pupation of the *snoo* deletion lines is slightly affected by starvation.

A. Pupation rate of individuals raised on 20 % sugar food. There is a significant difference for both deletion lines, $snoo^{del1}$ and $snoo^{del2}$ (p-value < 0.0001 in both cases). Median pupation time: $snoo^{del1}$ = 8 d; $snoo^{del1}/+$ = 8 d; $snoo^{del2}$ = 8 d; $snoo^{del2}/+$ = 8 d. B. Pupation rate of individuals raised on 0.1 % sugar food. There is a significant difference for both deletion lines (p-values: $snoo^{del1}$ = 0.0657, $snoo^{del2}$ < 0.0001). Median pupation time: $snoo^{del1}$ = 7 d; $snoo^{del1}/+$ = 7 d; $snoo^{del2}$ = 7 d; $snoo^{del2}/+$ = 7 d.

Under both feeding conditions, mutants and corresponding heterozygous controls show the same median pupation time (Fig 56). The median pupation time on high sugar is 8 days, on low sugar it is 7 days. Even if the Mantel-Cox test shows a significant difference between the curves, it seems to be very small and not really influenced by the feeding conditions.

2.8.3. Deletion of *snoo* has no clear influence on TAGs

Metabolic homeostasis does not only include the storage of energy in the form of carbohydrates, like glycogen or trehalose, but also as lipids. Therefore, changes in IIS can influence the abundance of TAGs. The concentration of TAGs was measured of homozygous and heterozygous individuals of both deletion lines (Fig 57).

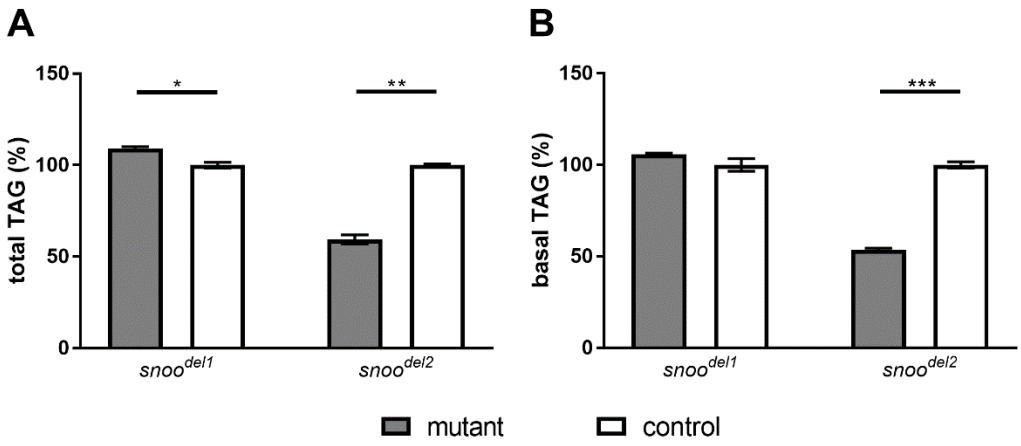

Fig 57. Deletion of *snoo* has no clear influence on TAG content.

The values have been normalised to the mean of the corresponding controls. *t*-test was used to compare the measured values of the homozygous deletion lines with their corresponding heterozygous controls. *p*-values: $snoo^{del1}$ = 0.0229, $snoo^{del2}$ = 0.0033.

There is a significant difference in the total amount of TAGs in both deletion lines (Fig 57). The effect found for $snoo^{del2}$ is considerably stronger than the effect found for $snoo^{del1}$. Furthermore, the effect is the opposite for the deletion lines as the total amount of TAGs is reduced in $snoo^{del2}$ but it is slightly increased in $snoo^{del1}$. A significant difference for the content of free glycerol could not be found for both deletion lines (*p*-values: $snoo^{del1}$ = 0.3436; $snoo^{del2}$ = 0.2211). No significant difference in basal TAGs could be found for $snoo^{del1}$ but there is a significant difference in the basal TAGs of $snoo^{del2}$. It is not clear if the reduction of total and basal TAG levels found in $snoo^{del2}$ is caused by the lack of *snoo* as it could not be found for $snoo^{del1}$.

2.8.4. Deletion of *snoo* has no influence on ATP concentration

As changes of the IIS can influence the availability of stores energy, the ATP concentration of $snoo^{del1}$ homozygous and heterozygous flies was measured (Fig 58).

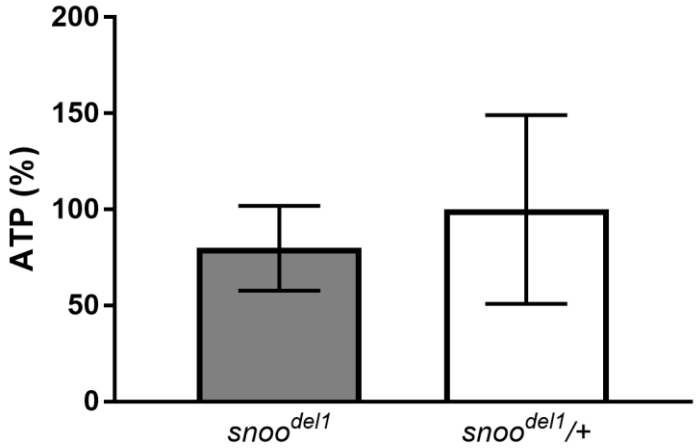

Fig 58. Deletion of *snoo* has no influence an ATP concentration.
The values have been normalised to the mean of the control $snoo^{del1}/+$. *t*-test was used to compare the homozygous mutant $snoo^{del1}$ with the heterozygous control. There is no significant difference (*p*-value = 0.3909).

There is no significant difference in the ATP levels between the mutants and the heterozygous controls (Fig 58).

2.9. Deletion of *snoo* does not influence neurodegeneration or autophagy

It was suspected that the reduced negative geotaxis and lifespan of *snoo* deletions could possibly be explained by neurodegeneration. To investigate if a lack of *snoo* results in increased neurodegeneration in the brain that would be visible as increased vacuolisation, heads of 30 days old male flies of the genotypes w^{1118}, $snoo^{del1}$, $snoo^{del1}/+$, $snoo^{del2}$, $snoo^{del2}/+$, $snoo^{del1}/snoo^{del2}$ were embedded in Epon and subjected to semithin sectioning (Fig 59).

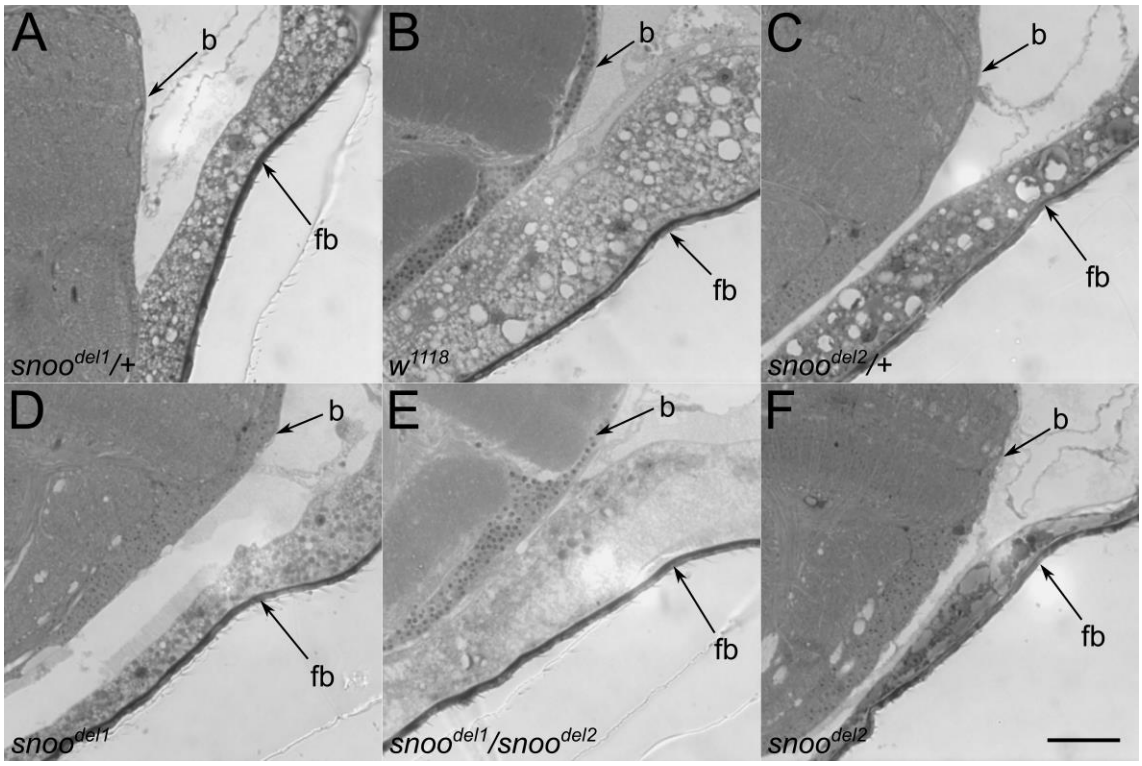

Fig 59. Deletion of *snoo* does not increase neurodegeneration.

The flies were aged for 30 days. Shown in each slide is a part of the brain (b) and the fat body (fb) under the cuticle. No increased vacuolisation is visible in the homozygous mutants, *snoo*^{del1} (D) and *snoo*^{del2} (F), and the transheterozygotes (E) if they are compared to the heterozygous controls, *snoo*^{del1}/+ (A) and *snoo*^{del2}/+ (C), or *w*^{1118} (B). Scale bar: 25 µm.

Enhanced neurodegeneration would be visible as increased vacuolisation in the brain. The homozygous *snoo* deletion lines and the transheterozygous flies do not show signs of increased vacuolisation in comparison to the heterozygous controls or the *w*^{1118} control (Fig 59). Therefore, it can be assumed that a deletion of *snoo* does not result in increased neurodegeneration. The layer of the fat body in the head of the homozygous mutant lines seems to be thinner than in the controls and the amount of lipid droplets, which appear as white bubbles in the sections, seems to be reduced in the deletion lines. Furthermore, the fat bodies of the homozygous mutants and the transheterozygotes appear less opaque than the fat bodies of the controls.

It could also be possible that the lack of *snoo* might result in increased autophagy. To address this question proteins were extracted from heads of the genotypes *w*^{1118}*; snoo*^{del1}, *w*^{1118}*; snoo*^{del1}/+, *w*^{1118}*; snoo*^{del2}, and *w*^{1118}*; snoo*^{del2}/+. 20 heads of 5 days old flies of each genotype were collected and homogenised in protein cracking buffer. The samples were analysed using SDS-PAGE and Western Blot. The blotting membrane was stained with an antibody for the autophagy marker p62 which is a marker for autophagy and for Tubulin as loading control (Fig 60).

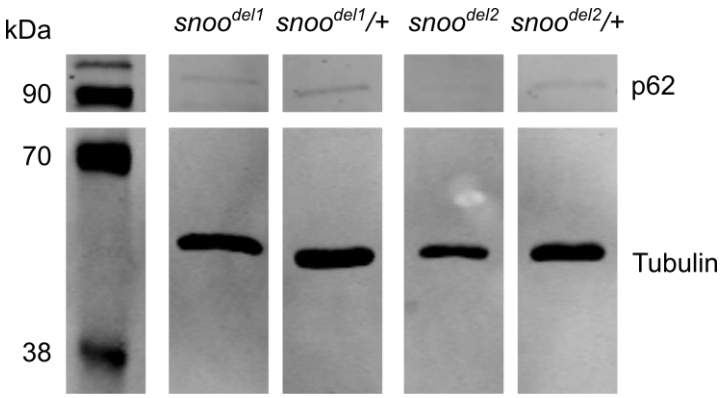

Fig 60. Deletion of *snoo* has no influence on autophagy.

The membrane was stained with antibodies for p62 and Tubulin (Tub). To quantify the amount of p62, the fluorescence signal of the antibody for this protein was normalised against the signal for Tubulin. There is no difference between the homozygous mutants and their corresponding heterozygous controls.

The fluorescence signal was quantified using the software Image Studio Lite by LI-COR Biosciences (Fig 60). No difference could be detected. Therefore, it can be assumed that a deletion of *snoo* has no influence on autophagy.

3. Discussion

3.1. Snoo expression pattern indicates a function in the CNS

The previously published expression patterns for *snoo* were of variable quality and partially contradictory. To get a consistent and reliable expression pattern throughout development and adulthood, two driver lines, *snoo-Gal4.2* and *snoo-T2A-Gal4*, were generated as part of this project using CRISPR/Cas9, which should represent authentic expression patterns and, due to the variety of reporter lines available, are superior to *in situ* hybridisations. Indeed, both driver lines show a seemingly identical expression pattern. Snoo is expressed during all stages of development. There is a ubiquitous but weak expression during early embryogenesis. The methods used in previous studies might not be sensitive enough to detect this weak expression.

The first peak of *snoo* expression appears at the beginning of nervous system formation at embryonal stage 14. At this stage, the first cells appear with a strong expression of Snoo and are localised outside of the developing nervous system. This is in concordance with previously published results that detected the first expression of *snoo* at embryonal stage 14 (Takaesu *et al*, 2006). In the mentioned study Snoo expression was further found to be restricted to the CNS towards the end of embryogenesis at stage 17. At this stage, the generated driver lines, *snoo-Gal4.2* and *snoo-T2A-Gal4*, reveal a moderate ubiquitous expression in the whole organism. Additionally, the CNS shows a much stronger expression at this stage, which might indicate that *snoo* has an important function during CNS development.

Similar to the ubiquitous *snoo* expression found by analysing *snoo-Gal4.2* and *snoo-T2A-Gal4*, *ski* expression in mice can be found in all embryonic and adult tissues at low levels (Nomura *et al*, 1989; Lyons *et al*, 1994; Pelzer *et al*, 1996; Pearson-White & Crittenden, 1997; Deheuninck & Luo, 2009; Jahchan & Luo, 2010). This *ski* expression is increased at different stages and tissues. The first peak of *ski* expression correlates with neural tube closure during embryogenesis. This is in concordance with the first peak of *snoo* expression in *Drosophila melanogaster* during nervous system formation.

Furthermore, the induction of the conditional knockout in different cell types revealed that the reduction of lifespan and geotaxis found for a deletion of *snoo* is mainly caused by the lack of the gene in neurons. The effect of the knockout could not be narrowed down to a specific type of neurons. A weak effect could be found in glutamatergic neurons. As the expression of the receptors of neurotransmitters begins relatively late in development, the weak effect found for a knockdown in glutamatergic neurons could rather be explained by a role of *snoo* in the development of these cells than in their function.

3.2. Comparison of *snoo* deletion phenotypes

Another aim of this project was the generation of precisely defined and validated *snoo* mutations, which would be able to help dissolving the contradictory results in the previously published results of different laboratories (Takaesu *et al*, 2006; Barrio *et al*, 2007; Ramel *et al*, 2007; Quijano *et al*, 2010). One of the main issues is the question of the lethality of these lines. Previously studied mutations of the *snoo* locus were lethal (Takaesu *et al*, 2006). However, studies with other mutations could not confirm this lethality (Barrio *et al*, 2007; Quijano *et al*, 2010). The lethal mutations consist of relatively large deletions and additionally affect other genes. The precisely defined deletions $snoo^{del1}$ and $snoo^{del2}$ generated as part of this project are clearly viable, except for a slightly increased developmental lethality during pupation. Additionally, the *snoo* deletion lines revealed that a lack of *snoo* does not result in any visible deformation resulting from developmental defects. Even though a deformation of wing veins found in $snoo^{del1}$ resembles a previously published phenotype (Ramel *et al*, 2007), it could be shown that this defect is only due to a second independent mutation in the genetic background of the deletion line.

It was previously proposed that one important issue of some *snoo* mutations being lethal and others being not could be explained by differences in the composition of the fly food used in different laboratories (Quijano *et al*, 2010). When assaying $snoo^{del1}$ and $snoo^{del2}$ for their pupation time no dramatic influences of the nutritional status on the development could be found. Therefore, it seems unlikely that the discrepancies between previous results can be explained by the different food compositions. The most likely explanation consists in the lethality found for some deletions being caused by other genes that are affected by the mutation.

3.3. Deciphering the genetic function of *snoo*

As the phenotypical analysis of the *snoo* deletion lines did not reveal any sever physiological or developmental effects despite for the reduction of the lifespan, the molecular approach of RNAseq should be used to search for significant differences in the transcriptome of the *snoo* deletion lines. On the one hand, this molecular approach could possibly enable the discovery of new genes and signalling pathways that might be impaired by a mutation of *snoo*. On the other hand, these results might bear a possible explanation for the reduction of the lifespan.

The bioinformatical analysis of the sequencing data begins with counting the reads that can be associated to specific genes (Patro *et al*, 2017). Using differential expression analysis, the read counts of the deletion line are compared to the control (Love *et al*, 2014). A set of genes with the highest fold change and lowest p-value was selected for further validation. Therefore, both deletion lines were investigated using qPCR with specific primer pairs for these genes. 12 genes could be identified that also showed a significant difference between mutant and control in these qPCR experiments, for at least one deletion line. These genes have different implication for possible functions of *snoo*.

3.4. A new role of *snoo* in metabolic homeostasis?

RNAseq and qPCR showed that in the *snoo* deletion lines the expression of the Ilp2, Ilp5 and Ilp6 is reduced. These are the orthologues of the mammalian Insulin and IGF (Brogiolo *et al*, 2001). Ilp2 and Ilp5 are produced in the 14 IPCs in the pars intercerebralis, while Ilp6 is produced in the fat body (Cao & Brown, 2001; Broughton *et al*, 2005; Okamoto *et al*, 2009). These neuropeptides are involved in the regulation of metabolic homeostasis (Saltiel & Kahn, 2001). Furthermore, the expression of the receptor of the Insulin signalling InR is significantly increased if *snoo* is absent. This might be due to a feedback loop to compensate for the lower abundance of the Ilps.

The Ilps are involved in the regulation of food consumption (Semaniuk *et al*, 2018). *dsk* is another gene differentially expressed in *snoo* mutants. The products of these gene, Dsk1 and Dsk2, are also produced in the IPCs and are known to induce satiety (Söderberg *et al*, 2012; Nässel & Williams, 2014). It might be possible that *snoo* mutants show differences in food consumption. This issue could be addressed in future experiments.

Previous studies showed that both, loss of IIS and mutation of *dsk*, result in an increased lifespan (Clancy *et al*, 2001; Tatar *et al*, 2001; Giannakou *et al*, 2004; Hwangbo *et al*, 2004; Broughton *et al*, 2005; Kenyon, 2005; Giannakou & Partridge, 2007; Söderberg *et al*, 2012). In contrast to these results, the *snoo* deletion lines, which show lower expression of *ilp2*, *ilp5* and *dsk*, have a decreased lifespan. On the one hand, the reduction of these gene products might be to weak to prolong the lifespan, as this effect is typically seen in the case of a complete absence of these proteins. On the other hand, the lifespan extension might be masked by the lifespan reducing effect of other differentially expressed genes. For example, it had previously been shown that the lifespan can be prolonged by an overexpression of *ilp6* (Bai *et al*, 2012) or a mutation of *inr* (Tatar *et al*, 2001). As the expression of *ilp6* is reduced in the *snoo* deletion lines, while the transcription of *inr* is increased, it can be hypothesised that this contributes to the reduction of the lifespan and antagonises the lifespan prolonging effect of the reduced expression of *ilp2*, *ilp5* and *dsk*.

The previously reported lifespan extension of an impaired IIS is associated with higher levels of stored energy and altered profiles of circulating carbohydrates (Broughton *et al*, 2005). In this study no evidence was found that the nutritional status influences the phenotype of a *snoo* deletion. The lifespan of the *snoo* mutants was reduced independently of the amount of sugar within the food of the flies and the development seemed not to be influenced by nutrition. The levels of the energy carrier ATP are also unchanged if Snoo is absent. In contrast, the amount of TAGs is significantly reduced in at least one deletion line. This could be explained by reduced expression of *ilp5* and *sug*, as it known that loss of these genes reduces TAG levels and Sugarbabe is essential for triglyceride homeostasis and fatty acid desaturation (Zinke *et al*, 2002; Varghese *et al*, 2010; Mattila *et al*, 2015; Luis *et al*, 2016; Semaniuk *et al*, 2018). Furthermore, the fat body in the head appears different in the *snoo* mutants. This could be further investigated in the future.

As Ilp2 influences haemolymph glucose levels (Broughton *et al*, 2005), measuring the glucose levels in future experiments could be a promising approach. Hr38 and both, Ilp2 and Ilp5, are involved in glycogen synthesis (Broughton *et al*, 2005; Ruaud *et al*, 2011). Therefore, the glycogen levels of the *snoo* deletion lines should also be investigated. As insects further store energy as trehalose, the levels of this metabolite should also be measured in *snoo* deletion mutants.

3.5. Deletion of *snoo* might impair circadian rhythm

RNAseq and qPCR revealed a set of differentially expressed genes in the *snoo* deletion lines which are involved in the regulation of the circadian rhythm. The basis of circadian rhythm is formed by molecular clocks that consists of transcription-based negative feedback loops (Mezan *et al*, 2016; Dubowy & Sehgal, 2017). The accumulation of certain clock proteins inhibits the transcription of their own mRNAs. As there is a delay between the translation and degradation of these proteins, these feedback loops result in the cycling accumulation of the proteins.

In *Drosophila melanogaster* the components of the molecular clock are expressed in ~ 150 neurons which are organised in a network of seven distinct clusters (Mezan *et al*, 2016; Dubowy & Sehgal, 2017). There are three clusters of dorsal neurons (DN1, 2, and 3) and four clusters of lateral neurons (LNs): the small and large ventrolateral neurons (sLNvs, and lLNvs), the dorsolateral neurons (LNds), and the lateral posterior neurons (LPNs).

The main modulator of the circadian neuronal network is the neuropeptide Pdf, which is expressed in the s-LNvs and l-LNvs (Dubowy & Sehgal, 2017; Fujiwara *et al*, 2018). It is part of different feedback loops and synchronises the molecular clocks in the different clusters. One of these negative feedback loops might also involve Hr38 (Mezan *et al*, 2016). Furthermore, Pdf seems to form another negative feedback loop together with CCHa1 (Fujiwara *et al*, 2018). CCHa1 is expressed in DN1 which signal the s-LNvs. Pdf secreted by the s-LNvs increases cAMP levels in the DN1. This feedback loop between Pdf and CCHa1 is necessary for the morning activity of the flies. Additionally, the Ilps are not only expressed in the IPCs but also in some clock neurons, the LNds, s-LNvs and l-LNvs (Cong *et al*, 2015). It has been shown that the Ilps are also involved in the regulation of sleep. Finally, CKII is also known to be involved in the regulation of the circadian rhythm (Allada & Meissner, 2005; Wairkar *et al*, 2013) and CKIIα-i3 is reduced in the *snoo* deletion lines.

In conclusion, several genes that are known to be involved in the regulation of the circadian rhythm, including the main modulator of the circadian neuronal network Pdf, were found to be differentially expressed in the *snoo* deletion lines. Furthermore, *snoo* was identified as a putative regulator of *pdf* in before (Mezan *et al*, 2016). Therefore, a role of *snoo* in the regulation of the circadian rhythm might be possible and should be investigated in future experiments.

Beyond its function in the circadian rhythm, Pdf might be involved in the regulation of reproductive diapause (Nagy *et al*, 2019). It has been found to antagonise this kind of dormancy in *Drosophila melanogaster*, possibly by enhancing the expression of Ilp2 and Ilp5 which are known as central regulators of reproductive diapause (Kubrak *et al*, 2014; Schiesari *et al*, 2016). As *snoo* seems to have an influence on the expression of all these genes, it could also be involved in the regulation of the reproductive diapause.

3.6. Deletion of *snoo* might impair xenobiotic resistance

Ugt86Dd, Cyp6a17, and Cyp6a20 are involved in the metabolism of xenobiotics and the resistance to different toxins, for example nicotine (Marriage *et al*, 2014; Highfill *et al*, 2017; Battlay *et al*, 2018; Duneau *et al*, 2018; Macdonald & Highfill, 2020). As these genes are differentially expressed in the *snoo* deletion lines, it can be hypothesised that *snoo* might also influence these processes. This would be in concordance with the observation that *snoo* is ubiquitously expressed as this fact might be indicative of a relatively fundamental function of the gene within the cellular metabolism.

An influence of *snoo* on the resistance to xenobiotics could also bear a further explanation for the observed reduction of the lifespan of a deletion of this gene. If a lack of Snoo impairs the degradation or excretion of toxins, detrimental chemicals would accumulate in the deletion lines as they age and worsen their overall health condition. This would then counteract the lifespan extending effect of the downregulation of IIS.

The resistance of *snoo* mutants to toxins should be tested in future experiments. An assay used in previous studies to investigate the resistance of Utg86Dd mutants to nicotine could be repeated with the *snoo* deletion lines (Marriage *et al*, 2014; Highfill *et al*, 2017; Macdonald & Highfill, 2020).

3.7. Snoo is important in neurons outside of the brain

As the phenotype of a general deletion of *snoo* is difficult to explain, a conditional knockout line for this gene was generated that can be expressed under the control of the Gal4/UAS system and therefore allows to mutate *snoo* in specific cell types or at a defined timepoint during development. This line was validated by inducing it in all cell types and thereby reproducing the results obtained with the deletion lines.

By inducing the conditional knockout of *snoo* in different tissues it could be shown that the lack of *snoo* in neurons is responsible for this lifespan reduction that can be observed in the *snoo* deletion lines. It was not possible to narrow down this effect to a specific type of neurons. The reduction of the lifespan could not be reproduced by a specific knockout of *snoo* in the brain. This implies that the lifespan phenotype might be due to the lack of *snoo* in the VNC. Additionally, it was not possible to completely reproduce the negative geotaxis phenotype of a *snoo* deletion by a specific knockout of the gene in the brain. This also argues for a possible function of Snoo in

the VNC. Furthermore, neurodegeneration in the brains of a *snoo* deletion or increased autophagy in the head could not be shown. In summary, the effects of a specific knockout of *snoo* in the VNC should be investigated in future experiments.

If the phenotypes can be attributed to the lack of *snoo* in the VNC, this could explain the relatively small number of differentially expressed genes found in the RNAseq of brains. In this case an RNAseq of the VNC of the *snoo* deletion lines would be worth considering. In this project, the RNAseq was performed simultaneously to the lifespan assays of the conditional knockout and at that moment, the brain seemed to be the most promising target of investigation.

4. Material

4.1. *Drosophila melanogaster* Stocks

Flies were reared in vials with standard food (0.8 % agar, 2.2 % sugar beet molasses, 8.0 % malt extract, 1.8 % yeast, 1.0 % soy flour, 8.0 % corn flour, 0.3 % nipagin) at 18 °C or 25 °C and 65 % relative humidity. Administrative illumination simulated a 12/12 h LD day-night-rhythm. All experiments were performed at 25 °C. The fly stocks used in this study, their genotype and origin are listed in Tab 1.

Name	Genotype	Origin
Act-Gal4	$y^1\ w^*;\ P\{Act5C\text{-}GAL4\}17bFO1/TM6B,\ Tb^1$	BDSC #3954
ChAT-Gal4	$w^*;\ Mi\{Trojan\text{-}GAL4.0\}ChAT^{MI04508\text{-}TG4.0}$ $CG7715^{MI04508\text{-}TG4.0\text{-}X}/TM6B,\ Tb^1$	BDSC #60317
CyO/Sco	CyO/sna^{Sco}	This project
CyO/Sco; UAS-t::sgRNA-snoo^{4x}	$w^{1118};\ CyO/sna^{Sco};\ M\{UAS\text{-}t::sgRNA\text{-}snoo^{4x}\}ZH\text{-}86Fb$	This project
D42-Gal4	$w^*;\ P\{GawB\}D42$	BDSC #8816
Da-Gal4	$w^*;\ P\{GAL4\text{-}da.G32\}UH1,\ Sb^1/TM6B,\ Tb^1$	BDSC #55851
Drgx-Gal4	$y^1\ w^*;\ Mi\{Trojan\text{-}GAL4.1\}Drgx^{MI11472\text{-}TG4.1}$	Laura Gizler
Elav-Gal4	$P\{GawB\}elav^{C155}$	BDSC #458
Elav-Gal4; Tsh-Gal80	$P\{GawB\}elav^{C155};\ Tsh\text{-}Gal80/CyO$	Laura Gizler
Gad1-Gal4	$TI\{2A\text{-}GAL4\}VGAT^{2A\text{-}GAL4}/CyO$	BDSC #84696
Glut-Gal4	$w^*;\ Mi\{Trojan\text{-}GAL4.2\}VGlut^{MI04979\text{-}TG4.2}/CyO$	BDSC #60312
Lsp-Gal4	$y^1\ w^{1118};\ P\{Lsp2\text{-}GAL4.H\}3$	BDSC #6357
Mhc-Gal4; UAS-Cas9	$w^*;\ P\{UAS\text{-}Cas9.P2\}attP40/CyO;\ P\{GAL4\text{-}Mhc.W\}Mhc\text{-}82/TM6B,\ Tb^1$	BDSC #67079
OK107-Gal4	$w^*;\ P\{GawB\}OK107\ ey^{OK107}/In(4)ci^D,\ ci^D\ pan^{ciD}$ $sv^{spa\text{-}pol}$	BDSC #854
Repo-Gal4	$w^{1118};\ P\{GAL4\}repo/\ TM6B,\ Tb^1$	Juan Navarro
snoo^{del1}	$w^{1118};\ snoo^{del1,dsRed}$	This project
snoo$^{del1,\text{-}dsRed}$	$w^{1118};\ snoo^{del1}$	This project
snoo^{del2}	$w^{1118};\ snoo^{del2,dsRed}$	This project
snoo$^{del2,\text{-}dsRed}$	$w^{1118};\ snoo^{del2}$	This project
snoo-Gal4.2	$w^{1118};\ snoo\text{-}Gal4.2/CyO$	This project
snoo-Gal4.2^{dsRed}	$w^{1118};\ snoo\text{-}Gal4.2^{dsRed}/CyO$	This project
snoo-T2A-Gal4	$w^{1118};\ snoo\text{-}T2A\text{-}Gal4/CyO$	This project
snoo-T2A-Gal4^{dsRed}	$w^{1118};\ snoo\text{-}T2A\text{-}Gal4^{dsRed}\ /CyO$	This project
UAS-Cas9	$P\{hsFLP\}12,\ y^1\ w^*;\ P\{UAS\text{-}Cas9.P2\}attP40$	BDSC #58985

Name	Genotype	Origin
UAS-Cas9; D3/TM3	*w^{*}; P{UAS-Cas9.P2}attP40; D3/TM3, Sb^{1}*	This project
UAS-Cas9; UAS-t::sgRNA-snoo^{4x}	*w^{1118}; UAS-Cas9; M{UAS-t::sgRNA-snoo^{4x}}ZH-86Fb*	This project
UAS-CD8::GFP	*y^{1} w^{*}; P{UAS-mCD8::GFP.L}LL5, P{UAS-mCD8::GFP.L}2*	BDSC #5137
UAS-GFP::NLS	*w^{*}; P{UAS-Stinger}2*	Lab collection
UAS-t::sgRNA-snoo^{4x}	*w^{1118}; M{UAS-t::sgRNA-snoo^{4x}}ZH-86Fb*	This project
UAS-β-Gal	*w^{1118}; P{UAS-lacZ.NZ}20b*	Lab collection
w^{-}; CyO/Sco	*w^{*}; CyO/sna^{Sco}*	Lab collection
w^{-}; CyO/Sco; D3/TM3	*w^{*}; CyO/sna^{Sco}; D3/TM3, Sb^{1}*	Lab collection
w^{-}; D3/TM3	*w^{*}; D3/TM3, Sb^{1}*	Lab collection
w^{-}; vas-Cas9	*w^{1118}; PBac{vas-Cas9}VK00027*	BDSC #51324
w^{1118}	*w^{1118}*	Juan Navarro
WTB	Wildtype Berlin	Lab collection
y^{-}, w^{-}, vas-Cas9	*y^{1} M{vas-Cas9.RFP-}ZH-2A w^{1118}*	BDSC #55821
y^{-}, w^{-}, vas-ΦC31; attP	*y^{1} M{vas-int.Dm}ZH-2A w^{*}; M{3xP3-RFP.attP}ZH-86Fb*	BDSC #24749
y^{-}, w^{-}; Sco/CyO,Cre	*y^{1} w^{67c23}; sna^{Sco}/CyO, P{Crew}DH1*	BDSC #1092

Tab 1. *Drosophila melanogaster* stocks used in this project.

If eggs had to be collected, flies were kept in cages on plates of apple juice agar (1.8 % agarose, 25 % apple juice, 2.5 % sucrose, 2.5 % ethanol, 0.375 % nipagin) for a defined period. Some experiments were performed on food containing high or low amount of sugar. The recipe for high sugar food (0.62 % agar, 6 % yeast, 6 % corn flour, 0.1 % apple juice, 20 % sucrose, 0.34 % nipagin) was taken from previously published study (Chng *et al*, 2017). Low sugar food (0.5 % agar, 10 % yeast, 0.7 % propionic acid, 0.34 % nipagin) contains a final concentration of only 0.1 % sugar. While other foods were prepared with water, this food was prepared by dissolving the ingredients in PBS. The recipe was taken from another study (Mattila *et al*, 2015).

4.2. Oligonucleotides

All used Oligonucleotides (Tab 2) were obtained from Thermo Fisher Scientific.

Name	Sequence
Asph qPCR forward	CCTCTGTCGGAGTCTAGGTTC
Asph qPCR reverse	CGTGACCATCATGCTCATCTC
CCHa1 qPCR forward	TGGTACAGCAAGTGCAGTTGG
CCHa1 qPCR reverse	CGAATGTCCGTATTCCAGGCA

Name	Sequence
CG11889 qPCR forward	CTGGCAGATTTCCATGCAG
CG11889 qPCR reverse	TTTTCAAAGATTCCCGGTTG
CkIIα-i3 qPCR forward	ATGCCATCCGCTACCTTAATG
CkIIα-i3 qPCR reverse	ACGCTTCGAGTTATTCTTCTCCT
cKO PCR1 forward	CGGCCCGGGTTCGATTCCCGGCCGATGCAAATCATTGGCGTC
cKO PCR1 reverse	ACGTATTGTTTCAGAGCTATGCTGGAAAC TTGGTGACTATGTCGAGGACTGCACCAGCCGGGAATCGAACC
cKO PCR2 forward	GTCCTCGACATAGTCACCAAGTTTCAGAGCTATGCTGGAAAC
cKO PCR2 reverse	GTGAACTATCGCAGCCGATTTGCACCAGCCGGGAATCGAACC
cKO PCR3 forward	AATCGGCTGCGATAGTTCACGTTTCAGAGCTATGCTGGAAAC
cKO PCR3 reverse	ATTTTAACTTGCTATTTCTAGCTCTAAAACACGGAGAAGCAT CCAATGGTTGCACCAGCCGGGAATCGAACC
Cyp6a17 qPCR forward	TGAGAATCGGGGAGTCTTCTAC
Cyp6a17 qPCR reverse	TCCAACTTTCACAACAATCGGAA
Cyp6a20 qPCR forward	CTGACGGACCATTTGTGGGTT
Cyp6a20 qPCR reverse	CGAATCAGTACGGTCTTAGCGA
Dsk qPCR forward	TCATTCTCTCTATTCGGGGACAG
Dsk qPCR reverse	GCGTGAAATTAGTGGCACTCTG
Gal4.2 forward	GCCTCTAGACAAAATGAAGCTGCTGAGT
Gal4.2 reverse	CGGCGGTCGACTAAGATACATTGATGAGTTTGGACAAAC
homology 1 forward	GCGGCGGCCGCAGGGCAGTCAAATCTGCTTA
homology 1 reverse	GCCCATATGATTGGGATCCATAATATTGATTACTTTAAAGG

Name	Sequence
homology 2 forward	GCCAGATCTAATTGGAGCATAAGAAAAGAAAGGTGCG
homology 2 reverse	GCCCTCGAGCGGAAAGCTAAAAATAAGCTCTCCAT
homology 3 forward	CGTAGAATTCCGTCCGTCGTCTG
homology 3 reverse	TGACCATATGTTATCCAATGGTCTTGCC
homology 4 forward	TGACAGATCTCCGATGCGGAACG
homology 4 reverse	TGACCTCGAGGCCAGCGGTG
homology 5 forward	TGACACCGGTCGTGCTTTCCGC
homology 5 reverse	CAGTTCTAGACGGGGTGGCG
homology 6 forward	TGACCTCGAGCGTGAACTATCGCAGC
homology 6 reverse	ACGTGGTACCAGGCTGTGGATACTGAAA
Hr38 qPCR forward	CGGCCACTTCAATGCCATC
Hr38 qPCR reverse	TGCGGAAACACCATTATATTCGT
Ilp2 qPCR forward	CGAGGTGCTGAGTATGGTGTG
Ilp2 qPCR reverse	CCCCAAGATAGCTCCCAGGA
Ilp5 qPCR forward	GAGGCACCTTGGGCCTATTC
Ilp5 qPCR reverse	CATGTGGTGAGATTCGG
Pdf qPCR forward	CGCAAGGAGTACAATCGGGA
Pdf qPCR reverse	GATAGCGACAGAGAGTGGCC
Snoo qPCR forward	ACTGGAGGGCAAGACCATTG
Snoo qPCR reverse	AGCTGATCGTGCGTACACTG
target 1 antisense	AAACAATCGTCGTACTCCTATCAC
target 1 sense	CTTCGTGATAGGAGTACGACGATT
target 2 antisense	AAACATTCCCGCTGCGCCTTGTGC
target 2 sense	CTTCGCACAAGGCGCAGCGGGAAT
target 3 antisense	AAACTTGGATGCTTCTCCGTGGGC
target 3 sense	CTTCGCCCACGGAGAAGCATCCAA
target 4 antisense	AAACGAACCGATGCGGAACGCCTC
target 4 sense	CTTCGAGGCGTTCCGCATCGGTTC
target 5 antisense	AAACCCCCGTGAACTATCGCAGCC
target 5 sense	CTTCGGCTGCGATAGTTCACGGGG
Ugt86Dd qPCR forward	GGCAGCTAAGGGTCATCAGG
Ugt86Dd qPCR reverse	TCAGCAAACTCATCATCTCGTC

Tab 2. List of used Oligonucleotides.

4.3. Plasmids

The plasmids that were used for this project and their origin are listed in Tab 3.

Name	Origin
pCFD6	Addgene #73915 (Port & Bullock, 2016)
pCFD6-t::sgRNA-snoo^{4x}	This project
pHD-DsRed-attP	Addgene #51019
pHD-snoo^{hom01}-DsRed-attP-snoo^{hom02}	This project
pHD-snoo^{hom03}-DsRed-attP-snoo^{hom04}	This project
pT-GEM(0)	Addgene #62891 (Diao *et al*, 2015)
pT-GEM-snoo^{hom05}-snoo^{hom06}	This project
pU6-BbsI-gRNA	Addgene #45946 (Gratz *et al*, 2013)
pU6-snoo^{target01}-gRNA	This project
pU6-snoo^{target02}-gRNA	This project
pU6-snoo^{target03}-gRNA	This project
pU6-snoo^{target04}-gRNA	This project
pU6-snoo^{target05}-gRNA	This project
pBPGAL4.2Uw-2	Addgene #26227 (Pfeiffer *et al*, 2010)
pT-GEM-Gal4.2	This project
pT-GEM-snoo^{hom01}-Gal4.2-snoo^{hom02}	This project

Tab 3. List of used plasmids.

4.4. Antibodies

The used antibodies are listed in Tab 4 with the species of their origin, the fluorophore if one is coupled to them. The name indicates the antigen the antibody is binding to.

Name	Source	Fluorophore	Origin
anti Elav	Rat	-	DSHB (7E8A10)
anti FasII	Mouse	-	DSHB (34B3)
anti Ilp5	Rabbit	-	Patrick Callaerts
anti mouse 488	Goat	Alexa Fluor 488	Invitrogen (A-11029)
anti mouse 594	Goat	Alexa Fluor 594	Invitrogen (A-11032)
anti mouse 680	Goat	IRDye 680 LT	LI-COR Biosciences
anti p62	Rabbit	-	Gabor Juhasz
anti pH3	Rabbit	-	Sigma-Aldrich (H0412)
anti pMAD	Mouse	-	NEB (9516P)
anti rabbit 800	Goat	IRDye 800 CW	LI-COR Biosciences
anti rat 555	Goat	Alexa Fluor 555	Invitrogen (A-21434)

Name	Source	Fluorophore	Origin
anti tub	Mouse	-	Sigma-Aldrich (B-5-1-2)
anti β-Gal	Mouse	-	DSHB (JIE7)

Tab 4. List of used antibodies.

4.5. Solutions and buffers

The composition of solutions and buffers that were used in this study can be found in Tab 5.

Solution	Ingredients	Concentration
Injection Buffer	KCl	5 mM
	phosphate buffer (pH 6.8)	0.1 mM
10 x Low Salt Buffer	Tris/HCl (pH 8.75)	200 mM
	KCl	100 mM
	$(NH_4)_2SO_4$	100 mM
	$MgSO_4$	20 mM
	BSA	1 mg/ml
	Triton-X 100	1 % (v/v)
0.1 M phosphate buffer (pH 6.8)	Na_2HPO_4	49 mM
	NaH_2PO_4	51 mM
0.1 M phosphate buffer (pH 7.4)	Na_2HPO_4	75.4 mM
	NaH_2PO_4	24.6 mM
Phosphate buffered saline (PBS)	NaCl	137 mM
	KCl	2.7 mM
	Na_2HPO_4	10 mM
0.1 % PBS with Tween20 (PBST)	NaCl	137 mM
	KCl	2.7 mM
	Na_2HPO_4	10 mM
	Tween-20	0.1 % (v/v)
Protein Cracking Buffer	Urea	6 M
	SDS	1 % (w/v)
	Bromophenol blue	0.01 % (w/v)
	2-Mercaptoethanol	0.05 % (w/v)
	$NaPO_4$ buffer (pH 7.2)	10 mM
5 x SDS Sample Buffer	Tris/HCl (pH 6.8)	1.25 mM
	2-Mercaptoethanol	12.5 % (w/v)
	SDS	5 % (w/v)
	Bromophenol blue	0.05 % (w/v)
	Glycerol	25 % (w/v)

Solution	Ingredients	Concentration
Semi-Dry Blotting Buffer (SDBB)	Tris	48 mM
	Glycine	39 mM
	Methanol	30 % (v/v)
	SDS	0.04 %
Sodium Chloride-Tris-EDTA (STE)	NaCl	100 mM
	Tris/HCl (pH 8.0)	10 mM
	EDTA	1 mM
Tris-Acetate-EDTA (TAE)	Tris/Acetate (pH 8.2 – 8.4)	40 mM
	EDTA	1 mM
Tris buffered saline (TBS)	Tris/HCl (pH 7.5)	10 mM
	NaCl	150 mM
0.1 % TBS with Tween20 (TBST)	Tris/HCl (pH 7.5)	10 mM
	NaCl	150 mM
	Tween20	0.1 % (v/v)

Tab 5. List of used solutions and buffers.

4.6. Media

The composition of media that were used in this study is given in Tab 6.

Solution	Ingredients	Concentration
Lysogeny broth (LB_0)	Tryptone	10 g/l
	Yeast extract	5 g/l
	NaCl	10 g/l
	NaOH	3 mM
LB_0 plates	Tryptone	10 g/l
	Yeast extract	5 g/l
	NaCl	10 g/l
	NaOH	3 mM
	Bacto-Agar	1 % (w/v)

Tab 6. List of used media.

By supplementing LB_0 with 100 µg/ml of the selection antibiotic Ampicillin the medium LB_{Amp} is prepared.

4.7. Chemicals and consumable materials

Chemicals and consumable materials were purchased from the following suppliers: Abcam, Bioline, BioRad, Biozym, DSHB, Fermentas, Fluka, Balur, Hartenstein, Kimberley-Clark,

LiCor, Menzel, Merck, New England Biolabs, Pall, Pierce, Pharmacia, PeqLab, Polysciences, Qiagen, Roche, Rockland, Roth, Sarstedt, Schleicher & Schuell, SemperMed, Serva, Stratagene, Sigma-Aldrich, ThermoFisher Scientific.

5. Methods

5.1. Immunohistochemistry

5.1.1. Preparation of embryos

The parental generation was kept on apple juice agar plates in cages for a defined period. The eggs on the plates were loosened with a pencil and rinsed with water into a plastic strainer. To remove the chorion, the eggs were incubated in chlorine bleach for 2 minutes, washed with water, covered with heptane and transferred into a snap lid glass. To fixate the embryos, they were shaken for 20 minutes in a mixture of 4 ml heptane, 1 ml PBS and 100 µl formaldehyde (37 %). After transfer into a microcentrifuge tube the embryos were covered with 0.5 ml heptane and 0.5 ml ice cold methane and vortexed for 60 seconds. The embryos were washed three times with methanol by vortexing for 30 seconds. The embryos were rehydrated by incubation in a 1:1 mixture of 0.1 % PBST and methanol for 10 minutes. After washing three times by incubation in 0.1 % PBST for 20 minutes at room temperature, the samples could be stained with antibodies. The samples were mounted on object slides.

5.1.2. Dissection of larval tissue

3rd Instar larvae were used for dissection. The posterior half of the larvae was removed, and the anterior part was turned inside-out. For fixation, the tissue was incubated in 4 % PFA in PBS for 20 to 30 minutes at room temperature. After washing three times in 0.1 % PBST for 20 minutes at room temperature, the samples were stained with antibodies. The desired tissues were dissected and mounted on object slides.

5.1.3. Dissection of wing muscles

Heads and abdomens of the flies were removed. The thoraces were cut in sagittal halves. For fixation, the tissue was incubated in 4 % PFA in PBS for 20 to 30 minutes at room temperature. After washing three times by incubation with 0.1 % PBST for 20 minutes at room temperature, the samples were stained with phalloidin in 0.1 % PBST supplemented with phalloidin in a 1:1000 dilution overnight. After washing three times by incubation in 0.1 % PBST for 20 minutes at room temperature, the halves of thoraces were mounted on object slides.

5.1.4. Dissection of adult brains

Whole flies were fixated by incubation in 4 % PFA in PBST for 3 hours at room temperature. After washing three times in 0.1 % PBST for 20 minutes at room temperature, the brains of the flies were dissected. The brains were stained with antibodies. The brains were mounted on object slides.

5.1.5. Immunostaining of tissue

The fixated tissue samples were incubated in a solution of the primary antibody with the desired dilution in 0.1 % PBST supplemented with 5 % Normal Goat Serum overnight at 4 °C. The samples were washed three times with 0.1 % PBST for 20 minutes. The samples were incubated in a solution of the secondary antibody with the desired dilution in 0.1 % PBST supplemented with 5 % Normal Goat Serum overnight at 4 °C. The samples were washed three times with 0.1 % PBST for 20 minutes.

5.1.6. Collection of heads of adult flies

50 adult male flies were collected and frozen in liquid nitrogen. To detach the heads from the rest of the bodies, the samples were vortexed 12 times for 3 seconds. A stainless-steel sieve (mesh size: 710 µm) was used to separate the heads from the bodies and the heads were collected in another stainless-steel sieve (mesh size: 400 µm). During the whole process thawing of the samples was prevented by constant cooling with liquid nitrogen.

5.1.7. Mounting and microscopy of tissue samples

Using DPX Mountant for Histology (Sigma-Aldrich) two coverslips (32 mm x 24 mm, Carl Roth) were glued onto a third one while leaving a gap with a width of a few millimetres between the top coverslips. After complete hardening of the mountant, dissected tissue was placed in the gap, overlaid with Vectashield Antifade Mounting Medium (Vector Laboratories), covered with a coverslip (18 mm x 18 mm, VWR) and sealed using nail polish. A LSM510 (Zeiss) confocal microscope was used to record the samples. The resulting files were edited using the ImageJ distribution Fiji (Schindelin *et al*, 2012). The figures included in this document were creating using the software Inkscape 0.92.4.

5.1.8. Embedding in Epon and semithin sectioning

Flies were prepared in 0.1 M phosphate buffer (pH 7.4) on ice. The flies were fixed in 5 % glutaraldehyde in phosphate buffer at 4 °C overnight. After washing three times for 10 minutes with phosphate buffer the flies were fixed a second time with 1 % OsO_4 in phosphate buffer for 1 hour and washed again three times for 10 minutes with phosphate buffer.

To dehydrate the samples, they were incubated in solutions with increasing concentrations of ethanol (30 %, 50 %, 70 %, 80 %, 95 %, 99.5 %) for 10 minutes each. The samples were washed twice with pure ethanol for 10 minutes and subsequently incubated twice in propylene oxide on ice for 10 minutes. After incubation in a 1:1 mixture of propylene oxide and Epon overnight, the samples were incubated in Epon for 1 hour. The samples were incubated in Epon at 37 °C overnight. The embedded sample were cut using a microtome and the sections were mounted on object slides using DPX Mountant for Histology (Sigma-Aldrich).

5.2. Molecular biological methods – nucleic acids

5.2.1. Determination of nucleic acid concentration

The concentration of DNA or RNA in solution was determined using a NanoDrop 1000 Spectrophotometer (Thermo Fisher Scientific).

5.2.2. Extraction of DNA

5.2.2.1. Mini Prep

To extract small amounts of a plasmid, transformed bacteria were inoculated in 5 ml LB selection medium and incubated at 37 °C overnight. The DNA was extracted using the mi-Plasmid Miniprep Kit (Metabion) following the instructions of the manufacturer.

5.2.2.2. Midi Prep

To extract greater amounts of a plasmid, transformed bacteria were inoculated in 25 ml LB selection medium and incubated at 37 °C overnight. The DNA was extracted using the Qiafilter Midi-Kit (QIAGEN) following the instructions of the manufacturer.

5.2.2.3. Extraction from Agarose gels

The band containing the DNA fragment of interest was cut out from the gel. The DNA was extracted using the E.Z.N.A. Gel Extraction Kit (VWR/Omega) following the instructions of the manufacturer.

5.2.3. Agarose gel electrophoresis

The size dependent electrophoretic separation of DNA is used for analysis or purification. The DNA samples were supplemented with an appropriate amount of 5 x Loading Dye (6 x Loading Dye supplemented with an appropriate amount of 30 x GelRed) and loaded onto a gel of 0.8 % (w/v) agarose in TAE. The electrophoresis was performed at 120 V. After an appropriate time, the separation of the DNA fragments was screened using UV light to visualise the DNA bands stained by the GelRed contained in the Loading Dye. In case of a preparative agarose gel electrophoresis the band of the desired DNA fragment was cut out from the gel and the contained DNA was purified.

5.2.4. Ligation

This method is used to generate plasmids from DNA fragments with compatible sticky ends. T4 DNA Ligase (NEB) was used. The composition of the reaction mix is given in Tab 7.

Ingredient	Amount
10 x T4 Ligase Buffer	2 µl
Vector DNA	50 ng
Insert DNA	Molar ratio to vector = 3:1
T4 DNA Ligase	1 µl
H_2O	ad 20 µl

Tab 7. Reaction mix for ligation.

This reaction mix was incubated at room temperature for 1 hour.

5.2.5. Restriction digest

Restriction enzymes and buffers were obtained from NEB. One or more restriction enzymes were used together with a suitable restriction buffer to prepare the reaction mix given in Tab 8.

Ingredient	Amount
Restriction Buffer (10 x)	2 µl
Restriction enzyme	1 µl
DNA	1 µg
H_2O	ad 50 µl

Tab 8. Reaction mix for restriction digest.

The reaction mix was incubated at the temperature optimum of the enzymes for 1 hour.

5.2.6. Annealing of oligonucleotides

Complementary oligonucleotides were phosphorylated and hybridised to generate double stranded DNA fragments. T4 Polynucleotide Kinase (PNK, NEB) was used for phosphorylation. The reaction mix given in Tab 9 was prepared.

Ingredient	Amount
Sense oligonucleotide (100 µM)	1 µl
Antisense Oligonucleotide (100 µM)	1 µl
10 x T4 Ligase Buffer	1 µl
T4 PNK	1 µl
H_2O	ad 10 µl

Tab 9. Reaction mix for annealing of oligonucleotides.

The reaction mix was incubated at 37 °C for 30 minutes for phosphorylation of the oligonucleotides. The PNK was inactivated by heating to 95 °C for 5 minutes. For hybridisation of the oligonucleotides the temperature was decreased by 0.1 °C per second to 25 °C.

5.2.7. Cloning

5.2.7.1. Restriction Cloning

This cloning method is based on the digestion of DNA fragments with restriction enzymes that produce compatible sticky ends followed by ligation. The insert was either generated by PCR or annealing of oligonucleotides. If PCR was used, specific primers were designed with overhangs containing suitable restriction sites. The PCR product was purified using preparative agarose gel electrophoresis and digested with restriction enzymes. The insert was purified again using preparative agarose gel electrophoresis. If annealing of oligonucleotides was used, these oligonucleotides were designed with overhangs that generate sticky end.

The vector was digested with restriction enzymes and purified using preparative agarose gel electrophoresis. 50 ng of this vector were used with either 3 times molar surplus of a PCR generated insert or 1 µl of annealed oligonucleotides for ligation. The ligated DNA was used for heat shock transformation of *E. coli* stock DH5α (Thermo Fisher Scientific). Positive colonies were identified by colony PCR.

5.2.7.2. Gibson Assembly

The NEBuilder HiFi DNA Assembly Master Mix (NEB) was used to assemble plasmids from DNA fragments. A suitable amount of DNA was used, and the reaction was performed according to the instructions of the manufacturer.

5.2.8. Polymerase Chain Reaction (PCR)

5.2.8.1. Standard PCR

Polymerase Chain Reaction (PCR) was used to amplify a specific DNA sequence. The reaction mix was prepared as described in Tab 10. If the template DNA was genomic, 50 ng – 250 ng were used. If the template DNA consisted of a plasmid, 1 pg – 10 ng were used.

Ingredient	Amount
Template DNA	variable
Forward primer (10 µM)	2.5 µl
Reverse primer (10 µM)	2.5 µl
dNTPs (10 µM)	1 µl
5x Phusion Buffer	10 µl
Phusion DNA Polymerase	0.5 µl
H_2O	ad 50 µl

Tab 10. Reaction mix for PCR.

PCR was performed in a thermocycler using the program described in Tab 11. This is the standard program. The temperature for primer hybridisation, the time for elongation and the number of cycles were adjusted for each PCR.

Step	Temperature	Time	Cycles
Denaturation	98 °C	30 s	1 x
Denaturation	98 °C	10 s	
Primer hybridisation	60 °C	30 s	25 – 35 x
Elongation	72 °C	60 s	
Elongation	72 °C	2 min	1 x
Storage	10 °C	∞	1 x

Tab 11. Thermocycling program for PCR.

The outcome of the PCR was validated by agarose gel electrophoresis and subsequently the PCR product was purified if necessary.

5.2.8.2. Colony PCR

Colony PCR was used to identify correct colonies of transformed bacteria on agar plates. For each colony that should be analysed the reaction mix in Tab 12 and a culture tube with 5 ml of LB selection medium were prepared.

Ingredient	Amount
10 x Low Salt Buffer	2 µl
Forward primer (10 mM)	1 µl
Reverse primer (10 mM)	1 µl
dNTPs (10 mM)	1 µl
Taq polymerase	1 µl
H_2O	ad 20 µl

Tab 12. Reaction mix for colony PCR.

A PCR mix and a culture tube were inoculated with each colony. The PCR program in Tab 13 was performed in a thermocycler.

Step	Temperature	Time	Cycles
Denaturation	95 °C	5 min	1 x
Denaturation	95 °C	25 s	
Primer hybridisation	60 °C	30 s	30 x
Elongation	72 °C	60 s	
Elongation	72 °C	10 min	1 x
Storage	10 °C	∞	1 x

Tab 13. Thermocycling program for colony PCR.

The outcome of the PCR was validated using analytical agarose gel electrophoresis. Culture tubes of positive colonies were incubated at 37 °C overnight.

5.2.8.3. Quantitative Real Time PCR (qPCR)

The Sso QuantiTect SYBR® Green Kit (QIAGEN) was used for quantitative real time PCR (qPCR). Each cDNA sample was investigated using primer pairs for specific target genes. These reactions were performed as triplicates. For each cDNA sample a duplicate of qPCRs using a primer pair for the target Rp49 was performed. This housekeeper gene was used as reference during the analysis of the qPCR data. For each primer pair one negative control without cDNA was performed. The composition of one reaction is given in Tab 14.

Ingredient	Amount
2x SYBR Green Master Mix	5 µl
cDNA	1 µl
10 mM forward primer	0.5 µl
10 mM reverse primer	0.5 µl
H_2O	ad 10 µl

Tab 14. Reaction mix for qPCR.

The qPCR was performed in a Bio-Rad CFX Connect Real-Time PCR Detection System using the program in Tab 15.

Step	Temperature	Time	Cycles
Denaturation	95 °C	2 min	1 x
Denaturation	95 °C	10 s	
Primer hybridisation	60 °C	10 s	40 x
Elongation, measurement	65 °C	30 s	
Denaturation	95 °C	10 s	1 x
Melting curve, measurement	65 °C – 95 °C	+ 0.5 °C / 5s	1x

Tab 15. Thermocycling program for qPCR.

The qPCR data was analysed using the ΔΔCq method. The mean Cq values of the replicates were calculated. The ΔCq value was calculated as the difference of the mean values for the target genes of a cDNA sample and the corresponding Rp49 reference. The ΔΔCq value was calculated as difference of the ΔCq values of a cDNA sample of interest and a corresponding control sample. The relative expression of the target gene within the cDNA sample of interest was calculated as $2^{-\Delta\Delta Cq}$.

5.2.9. Heat Shock Transformation

Plasmids were transformed into *E. coli* bacteria of the strain DH5α (Thermo Fisher Scientific). A 200 µl aliquot of heat shock competent cells was thawed on ice. The DNA was added to the aliquot. After further incubation on ice for 10 minutes the cells were treated by a heat shock at 42 °C for 45 seconds. The cells were incubated on ice for 2 minutes. 800 µl of LB_0 medium were added and the cells were incubated at 37 °C for 60 minutes. The bacteria were plated on a suitable LB selection medium and incubated at 37 °C overnight.

5.2.10. Microinjection of DNA into embryos

DNA was purified by Midi prep and eluted in Ampuwa® (Fresenius Kabi Deutschland GmbH). It was diluted to the needed concentration and supplemented with a suitable amount of 10 x Injection Buffer. 30 to 60 minutes after laying the chorion was removed from eggs. Embryos were fixed on an object slide. The diluted DNA was injected into the posterior end of the embryos. Embryos were overlaid with oil to prevent dehydration. The object slides with the embryos were incubated on apple agar plates at 18 °C. The hatched larvae were transferred into vials with standard food and reared at standard conditions.

5.2.11. Sequencing

The Sanger sequencing was performed by Eurofins Genomics. Samples were prepared according to the instructions of the service provider. DNA was diluted to a suitable concentration in 7.5 µl and supplemented with 2.5 µl primer (10 µM).

5.2.12. Genotyping

To validate the success of genomic editing of a fly strain genomic DNA was extracted and used for PCR with a specific primer pair for the desired modification. Up to 5 flies were homogenised in 50 µl STE supplemented with 2 µl Proteinase K (20 mg/ml, Thermo Fisher Scientific) and incubated at 37 °C for 30 minutes. The proteinase was inactivated by heating the samples to 95 °C for 5 minutes. The lysate was cleared of insoluble components by centrifugation and 1 µl was used for PCR according to the Colony PCR protocol. The success of the PCR was validated by agarose gel electrophoresis.

5.2.13. Extraction of RNA

For extraction of RNA peqGOLD TriFast™ (VWR) was used following the protocol of the manufacturer. The RNA was eluted in nuclease free water.

5.2.14. Reverse Transcription

The OneStep RT-PCR Kit (QIAGEN) was used to generate cDNA. To remove residual genomic DNA from the template RNA the mix in Tab 16 was prepared.

Ingredient	Amount
7x gDNA wipe out buffer	1 µl
Template RNA	500 ng
H_2O	ad 7 µl

Tab 16. Reaction mix for removal of genomic DNA.

The reaction mix was incubated at 42 °C for 2 minutes and supplemented with the reagents given in Tab 17.

Ingredient	Amount
5x Quantiscript RT buffer	2 µl
Quantiscript reverse transcriptase	0.5 µl
Oligo(dT) primer	0.5 µl

Tab 17. Reaction mix for reverse transcription.

The reverse transcription was performed at 37 °C for 30 minutes and the reverse transcriptase was inactivated by heating the reaction to 95 °C for 3 minutes. The generated cDNA was diluted 1:10 with nuclease free water and analysed using qPCR.

5.3. Molecular biological methods – proteins

5.3.1. Bradford Assay

To determine protein concentrations Bradford assay with the Pierce Coomassie Plus Protein Assay (Thermo Fisher Scientific) was used. 20 µl of the sample were mixed with 1 ml Bradford Reagent and incubated for 5 minutes at room temperature. 300 µl were transferred into a well of a transparent 96-well plate and the absorbance at 595 nm was measured in a TECAN Spark Infinity plate reader. By plotting the absorbance against a standard curve, the amount of protein was determined.

5.3.2. SDS Polyacrylamide gel electrophoresis (SDS-PAGE)

Polyacrylamide gel electrophoresis (PAGE) was used to separate proteins by their size. The resolving gel was prepared according to Tab 18. By addition of TEMED the polymerisation reaction

was started and 5 ml the gel was poured into the cast. The resolving gel was overlaid with 1 ml isopropanol.

Ingredient	Amount
H_2O	2.94 ml
Tris (1.5 M, pH 8.8)	1.5 ml
Rotiphorese Gel 40	1.5 ml
SDS (20 %)	30 µl
APS (10 %)	30 µl
TEMED	6 µl

Tab 18. Composition of the resolving gel.

After completion of the polymerisation the isopropanol was removed. The stacking gel was prepared according to Tab 19. By addition of TEMED the polymerisation reaction was started, and the gel was poured into the cast. A comb was placed in the cast to produce wells for the addition of the samples.

Ingredient	Amount
H_2O	2.22 ml
Tris (1.0 M, pH 6.8)	375 µl
Rotiphorese Gel 40	375 µl
SDS (20 %)	15 µl
APS (10 %)	15 µl
TEMED	3 µl

Tab 19. Composition of the stacking gel.

After completion of the polymerisation the comb was removed, and the gel was placed in the electrophoresis chamber. The protein samples were supplemented with an appropriate amount of 5 x SDS Sample Buffer, denatured by heating to 95 °C for 5 minutes and loaded onto the gel. Electrophoresis was performed at 150 V until the bromophenol blue band had left the gel.

5.3.3. Western blot

The semi-dry method was used for Western blotting. After SDS-PAGE the gel was washed with Semi-Dry Blotting Buffer (SDBB) and placed on three layers of Whatman filter paper (5.5 cm x 8.5 cm, GE Healthcare) rinsed in SDBB. An Amersham Protran 0.45 µm nitrocellulose membrane (5.5 cm x 8.5 cm, GE Healthcare) was activated by rinsing with SDBB and placed on the gel. Three layers of Whatman filter paper (5.5 cm x 8.5 cm, GE Healthcare) rinsed with SDBB were placed on top of the setup. The Blot was performed at 400 mA for 1 hour.

The membrane was washed two times with TBS for 10 minutes. The blocking of the membrane was performed by incubation in 1:1 mixture of Odyssey Blocking Buffer (OBB) and TBS at room temperature for one hour. The blocked membrane was incubated in a 1:1 mixture of OBB and 0.1 % TBST supplemented with the primary antibodies at 4 °C overnight. The membrane was washed two times with 0.1 % TBST for 10 minutes and incubated in a 1:1 mixture of OBB and 0.1 % TBST supplemented with the secondary antibodies at room temperature for 2 hours. The membrane was washed two times with 0.1 % TBST for 10 minutes and documented using an Odyssey Infrared Imager (LI-COR Biosciences). The software Image Suite Lite from LI-COR Bioscience was used to quantify the fluorescence signal of the antibodies.

5.4. Behavioural and lifespan assays

5.4.1. Lifespan assay

Around 25 males were transferred into vials 2 to 3 days after eclosion. Every 2 to 3 days the flies were transferred into new vials by shaking. The number of dead flies that remained in the used vials was documented. The software GraphPad Prism was used to analyse the data using the Mantel-Cox test.

5.4.2. Survival assay

Flies were kept on apple agar plates for a defined period. The number of eggs was documented, and the plates were incubated at 25 °C for 24 hours. The number of hatched larvae was documented. The larvae were transferred into vials with standard food and reared at standard conditions. The number of resulting pupae and adults was documented. The proportion of eggs developing up to a specific developmental stage was calculated and the data was analysed using *t*-test.

5.4.3. Fecundity assay

Flies were kept on apple agar plates for a defined period. The number of females and of laid eggs were documented. The fecundity rate was calculated by dividing the number of eggs by the number of females and the time in hours. The data was analysed using *t*-test.

5.4.4. Negative geotaxis assay

Up to 15 males were transferred individually into 25 cm long vials labelled with height marks. The flies were transferred to the bottoms of the vial by shaking and the maximal height the flies had reached within 12 seconds was documented. Each fly was tested 3 times with a pause of at least 2 minutes between the iterations.

By dividing the average maximally reached height of each fly by 12 seconds the average climbing speed was calculated. *t*-test or ANOVA was used to analyse the data in combination with Tuckey's post hoc test if necessary.

5.4.5. Buridan's Paradigm assay

Buridan's Paradigm assay can be used to investigate the overall locomotor behaviour of flies (Colomb *et al*, 2012). The wings of 3 to 5 days old flies were clipped. After recovery overnight the flies were transferred into the arena. The arena consisted of a circular platform where flies could walk freely surrounded by water. Two opposing vertical black stripes functioned as optical cues. The motion of the flies was tracked for 10 minutes using a digital camera and the software Buritrack. The data was analysed with the software Centroid Trajectory Analysis (CeTrAn) which extracts eleven metrics. The metrics of different genotypes were compared using ANOVA in combination with Tuckey's post hoc test.

5.5. Metabolic assays

5.5.1. Measuring ATP concentration

To measure ATP levels the ATP Bioluminescence Assay Kit HS II (Sigma-Aldrich) was used. 5 flies were homogenised in 200 µl boiling ATP buffer. After incubation at 95 °C for 5 minutes and centrifugation (3000 RPM, 3 min) 25 µl of the supernatant was diluted 1:5 with ATP dilution buffer. 50 µl of the diluted sample was mixed with 50 µl luciferase in a well of a 96-well plate (Greiner Flat Bottom Black Polystyrol). The luminescence was measured in a TECAN Spark Infinity plate reader (integration time: 10,000 ms, settle time: 1000 ms, attenuation: automatic). By plotting the luminescence values against an ATP standard curve the concentration of ATP was determined. The ATP concentration was normalised against the protein concentration determined by Bradford assay.

5.5.2. Measuring triacylglyceride (TAG) concentration

To determine TAG concentrations the Serum Triglyceride Determination Kit (Sigma-Aldrich) was used. 10 flies were homogenised in 300 µl PBS supplemented with 0.5 % Tween-20. The homogenised sample was incubated at 70 °C for 5 minutes. A 40 µl aliquot of the sample was mixed with 40 µl PBS, another 40 µl aliquot was mixed with 40 µl Triglyceride Reagent. The samples were incubated at 37 °C for 30 minutes and centrifuged (10,000 RPM, 5 min). 60 µl of the supernatant was mixed with 200 µl Free Glycerol Reagent in a well of a 96-well plate (Greiner Flat Bottom Black Polystyrol). The samples were incubated at 37 °C for 5 minutes and the absorbance at 540 nm was measured in a TECAN Spark Infinity plate reader. The TAG levels were normalised against protein levels determined by Bradford assay of the homogenised sample. The measurement of the sample treated with Triglyceride Reagent allowed the determination of the total amount of TAGs. The measurement of the sample treated with PBS allowed the determination of basal TAG levels. The free glycerol level could be determined by subtracting basal TAG levels from the total amount of the TAGs.

5.6. Generation of mutant lines – Genomic editing

5.6.1. Genomic Editing

To generate mutant lines the CRISPR/Cas9 method was used in combination with HDR. Plasmids coding for sgRNAs were injected in embryos of a *Drosophila melanogaster* stock expressing the Cas9 protein in germ line cells. The sgRNAs interact with the Cas9 and guide it to specific target sequences of 20 bp in the genome. The Cas9 introduced DSBs in the genomic DNA at the target sequences. These target sequences were identified using the online tool flyCRISPR Target Finder (Gratz *et al*, 2014).

Together with the sgRNA plasmids a template plasmid for the HDR was injected into the embryos. This plasmid contains 2 sequences of around 1 kb that are homologous to the genomic regions upstream and downstream of the introduced DSBs. The DSBs induce the endogenous HDR mechanism of the cells to repair the genomic DNA. The sequence of the template plasmid flanked by the homologous sequences was introduced into the genomic DNA in between the DSBs.

The sgRNA plasmids were cloned by annealing sense and antisense oligonucleotides and ligating them into the vector pU6-BbsI-gRNA that was linearized with the restriction enzyme BbsI. The template plasmid was generated by amplifying the homologous sequences from genomic DNA using PCR and cloning them into a suitable vector using restriction cloning. 500 ng/µl of the template plasmid and 100 ng/µl of each sgRNA plasmid were injected into embryos on a fly stock expressing the Cas9 protein in germ lines cells.

5.6.2. Conditional knockout

The method used here for a conditional knockout of a gene is based on the Gal4 driven expression of Cas9 protein and specific sgRNAs, thus inducing indel mutations resulting in a frame shift within this locus in the Gal4 expressing cells. A fly line was generated containing 4 sgRNAs interspaced and flanked by sequences of tRNAs under the control of a UAS promotor. The multiplex of tRNAs and sgRNAs is expressed as a single transcript. The processing of the tRNA sequences liberates the functional sgRNAs.

To generate the UAS construct for the conditional knockout three different PCRs were performed to amplify the sgRNA and tRNA scaffold from the plasmid pCFD6. The primers used for these PCRs contained the target sequences for the conditional knockout within their overhangs. These target sequences were identified using the online tool flyCRISPR Target Finder (Gratz *et al*, 2014). The overhangs of the primers also contained overlapping sequences to enable Gibson Assembly of the PCR products and the vector pCFD6 which was linearized with the restriction enzyme BbsI.

100 ng of the resulting plasmid were injected into embryos of the stock y^-, w^-, *vas-ΦC31; attP*. The resulting flies were crossed to the balancer w^-*; D3/TM3* and transformant flies within the

offspring of this cross were identified using the mini-white marker of the cloned construct. Homozygous stocks were established by back crossing.

5.7. RNAseq of adult brains

An RNAseq was performed to analyse gene expression in the brains of mutant flies. Homozygous mutants of *snoo*^{del2} were used. Virgins of *snoo*^{del2} were crossed with males of the stock *y*$^{-}$, *w*$^{-}$, *vas-Cas9* and the offspring was used as control. Two to three days after eclosion the brains of male flies were dissected in ice cold PBS supplemented with Thermo Scientific™ RiboLock RNase-Inhibitor and immediately frozen in liquid nitrogen. 40 brains per genotype were pooled for RNA extraction using the RNeasy Mini Kit from Qiagen. After determining the concentration of the RNA by Qubit Fluorometric Quantification (Thermo Fisher Scientific) it was used to produce the libraries for sequencing with the NEBNext Ultra II Directional RNA Library Prep Kit. The DNA concentration of the libraries was determined using Qubit Fluorometric Quantification. The whole procedure was performed twice to produce two replicate samples. The Illumina® sequencing of the libraries was performed in the laboratory of Prof. Dr. Michael Rehli.

The bioinformatic analysis of the data was performed by Dr. Mathias Raß. The transcript abundance was quantified with the R package Salmon (Patro *et al*, 2017) using the release of the *Drosophila melanogaster* genome BDGP6.22. The data was imported using tximeta (Love *et al*, 2020) and investigated by differential expression analysis with DESeq2 (Love *et al*, 2014).

6. Appendix

6.1. References

Abdollah S, Macías-Silva M, Tsukazaki T, Hayashi H, Attisano L & Wrana JL (1997) TbetaRI phosphorylation of Smad2 on Ser465 and Ser467 is required for Smad2-Smad4 complex formation and signaling. *J Biol Chem* 272: 27678–27685

Allada R & Meissner R-A (2005) Casein kinase 2, circadian clocks, and the flight from mutagenic light. *Mol Cell Biochem* 274: 141–149

Arndt S, Poser I, Moser M & Bosserhoff A-K (2007) Fussel-15, a novel Ski/Sno homolog protein, antagonizes BMP signaling. *Mol Cell Neurosci* 34: 603–611

Arndt S, Poser I, Schubert T, Moser M & Bosserhoff A-K (2005) Cloning and functional characterization of a new Ski homolog, Fussel-18, specifically expressed in neuronal tissues. *Lab Invest* 85: 1330–1341

Bai H, Kang P & Tatar M (2012) Drosophila insulin-like peptide-6 (dilp6) expression from fat body extends lifespan and represses secretion of Drosophila insulin-like peptide-2 from the brain. *Aging Cell* 11: 978–985

Barrio R, López-Varea A, Casado M & de Celis JF (2007) Characterization of dSnoN and its relationship to Decapentaplegic signaling in Drosophila. *Dev Biol* 306: 66–81

Battlay P, Leblanc PB, Green L, Garud NR, Schmidt JM, Fournier-Level A & Robin C (2018) Structural Variants and Selective Sweep Foci Contribute to Insecticide Resistance in the Drosophila Genetic Reference Panel. *G3 Bethesda Md* 8: 3489–3497

Bonni S & Bonni A (2012) SnoN signaling in proliferating cells and postmitotic neurons. *FEBS Lett* 586: 1977–1983

Brogiolo W, Stocker H, Ikeya T, Rintelen F, Fernandez R & Hafen E (2001) An evolutionarily conserved function of the Drosophila insulin receptor and insulin-like peptides in growth control. *Curr Biol CB* 11: 213–221

Broughton SJ, Piper MDW, Ikeya T, Bass TM, Jacobson J, Driege Y, Martinez P, Hafen E, Withers DJ, Leevers SJ, *et al* (2005) Longer lifespan, altered metabolism, and stress resistance in Drosophila from ablation of cells making insulin-like ligands. *Proc Natl Acad Sci* 102: 3105–3110

Brummel T, Abdollah S, Haerry TE, Shimell MJ, Merriam J, Raftery L, Wrana JL & O'Connor MB (1999) The Drosophila activin receptor baboon signals through dSmad2 and controls cell proliferation but not patterning during larval development. *Genes Dev* 13: 98–111

Cao C & Brown MR (2001) Localization of an insulin-like peptide in brains of two flies. *Cell Tissue Res* 304: 317–321

Caubit X, Thangarajah R, Theil T, Wirth J, Nothwang HG, Rüther U & Krauss S (1999) Mouse Dac, a novel nuclear factor with homology to Drosophila dachshund shows a dynamic expression in the neural crest, the eye, the neocortex, and the limb bud. *Dev Dyn Off Publ Am Assoc Anat* 214: 66–80

Chan HM & La Thangue NB (2001) p300/CBP proteins: HATs for transcriptional bridges and scaffolds. *J Cell Sci* 114: 2363–2373

Chen C-R, Kang Y, Siegel PM & Massagué J (2002) E2F4/5 and p107 as Smad cofactors linking the TGFbeta receptor to c-myc repression. *Cell* 110: 19–32

Chen X, Chanda A, Ikeuchi Y, Zhang X, Goodman JV, Reddy NC, Majidi SP, Wu DY, Smith SE, Godec A, *et al* (2019) The Transcriptional Regulator SnoN Promotes the Proliferation of Cerebellar Granule Neuron Precursors in the Postnatal Mouse Brain. *J Neurosci* 39: 44–62

Chng WA, Koch R, Li X, Kondo S, Nagoshi E & Lemaitre B (2017) Transforming Growth Factor β/Activin signaling in neurons increases susceptibility to starvation. *PLOS ONE* 12: e0187054

Clancy DJ, Gems D, Harshman LG, Oldham S, Stocker H, Hafen E, Leevers SJ & Partridge L (2001) Extension of life-span by loss of CHICO, a Drosophila insulin receptor substrate protein. *Science* 292: 104–106

Colomb J, Reiter L, Blaszkiewicz J, Wessnitzer J & Brembs B (2012) Open Source Tracking and Analysis of Adult Drosophila Locomotion in Buridan's Paradigm with and without Visual Targets. *PLoS ONE* 7

Cong X, Wang H, Liu Z, He C, An C & Zhao Z (2015) Regulation of Sleep by Insulin-like Peptide System in Drosophila melanogaster. *Sleep* 38: 1075–1083

Deheuninck J & Luo K (2009) Ski and SnoN, potent negative regulators of TGF-β signaling. *Cell Res* 19: 47–57

Derynck R, Akhurst RJ & Balmain A (2001) TGF-beta signaling in tumor suppression and cancer progression. *Nat Genet* 29: 117–129

Diao F, Ironfield H, Luan H, Diao F, Shropshire WC, Ewer J, Marr E, Potter CJ, Landgraf M & White BH (2015) Plug-and-play genetic access to drosophila cell types using exchangeable exon cassettes. *Cell Rep* 10: 1410–1421

Djabrayan NJ-V & Casanova J (2016) Snoo and Dpp Act as Spatial and Temporal Regulators Respectively of Adult Progenitor Cells in the Drosophila Trachea. *PLOS Genet* 12: e1005909

Doudna JA & Charpentier E (2014) Genome editing. The new frontier of genome engineering with CRISPR-Cas9. *Science* 346: 1258096

Dubowy C & Sehgal A (2017) Circadian Rhythms and Sleep in Drosophila melanogaster. *Genetics* 205: 1373–1397

Duneau D, Sun H, Revah J, San Miguel K, Kunerth HD, Caldas IV, Messer PW, Scott JG & Buchon N (2018) Signatures of Insecticide Selection in the Genome of Drosophila melanogaster. *G3 Bethesda Md* 8: 3469–3480

Ferreiro MJ, Pérez C, Marchesano M, Ruiz S, Caputi A, Aguilera P, Barrio R & Cantera R (2018) Drosophila melanogaster White Mutant w1118 Undergo Retinal Degeneration. *Front Neurosci* 11

Fischer S, Bayersdorfer F, Harant E, Reng R, Arndt S, Bosserhoff A-K & Schneuwly S (2012) fussel (fuss)--A negative regulator of BMP signaling in Drosophila melanogaster. *PloS One* 7: e42349

Fujiwara Y, Hermann-Luibl C, Katsura M, Sekiguchi M, Ida T, Helfrich-Förster C & Yoshii T (2018) The CCHamide1 Neuropeptide Expressed in the Anterior Dorsal Neuron 1 Conveys a Circadian Signal to the Ventral Lateral Neurons in Drosophila melanogaster. *Front Physiol* 9

Gasiunas G, Barrangou R, Horvath P & Siksnys V (2012) Cas9–crRNA ribonucleoprotein complex mediates specific DNA cleavage for adaptive immunity in bacteria. *Proc Natl Acad Sci* 109: E2579–E2586

Giannakou ME, Goss M, Jünger MA, Hafen E, Leevers SJ & Partridge L (2004) Long-lived Drosophila with overexpressed dFOXO in adult fat body. *Science* 305: 361

Giannakou ME & Partridge L (2007) Role of insulin-like signalling in Drosophila lifespan. *Trends Biochem Sci* 32: 180–188

Graca LS da, Zimmerman KK, Mitchell MC, Kozhan-Gorodetska M, Sekiewicz K, Morales Y & Garth I. Patterson (2004) DAF-5 is a Ski oncoprotein homolog that functions in a neuronal TGFβ pathway to regulate C. elegans dauer development. *Development* 131: 435–446

Gratz SJ, Cummings AM, Nguyen JN, Hamm DC, Donohue LK, Harrison MM, Wildonger J & O'Connor-Giles KM (2013) Genome Engineering of Drosophila with the CRISPR RNA-Guided Cas9 Nuclease. *Genetics* 194: 1029–1035

Gratz SJ, Ukken FP, Rubinstein CD, Thiede G, Donohue LK, Cummings AM & O'Connor-Giles KM (2014) Highly specific and efficient CRISPR/Cas9-Catalyzed Homology-Directed repair in Drosophila. *Genetics* 196: 961–971

Grönke S, Clarke D-F, Broughton S, Andrews TD & Partridge L (2010) Molecular Evolution and Functional Characterization of Drosophila Insulin-Like Peptides. *PLoS Genet* 6

Heanue TA, Reshef R, Davis RJ, Mardon G, Oliver G, Tomarev S, Lassar AB & Tabin CJ (1999) Synergistic regulation of vertebrate muscle development by Dach2, Eya2, and Six1, homologs of genes required for Drosophila eye formation. *Genes Dev* 13: 3231–3243

Highfill CA, Tran JH, Nguyen SKT, Moldenhauer TR, Wang X & Macdonald SJ (2017) Naturally Segregating Variation at Ugt86Dd Contributes to Nicotine Resistance in Drosophila melanogaster. *Genetics* 207: 311–325

Hwangbo DS, Gershman B, Gersham B, Tu M-P, Palmer M & Tatar M (2004) Drosophila dFOXO controls lifespan and regulates insulin signalling in brain and fat body. *Nature* 429: 562–566

Jahchan NS & Luo K (2010) SnoN in mammalian development, function and diseases. *Curr Opin Pharmacol* 10: 670–675

Jakowlew SB (2006) Transforming growth factor-beta in cancer and metastasis. *Cancer Metastasis Rev* 25: 435–457

Ji M, Ding Y, Li X, Mao N & Chen J (2019) Computational investigation of a ternary model of SnoN-SMAD3-SMAD4 complex. *Comput Biol Chem* 83: 107159

Jinek M, Chylinski K, Fonfara I, Hauer M, Doudna JA & Charpentier E (2012) A programmable dual-RNA-guided DNA endonuclease in adaptive bacterial immunity. *Science* 337: 816–821

Kenyon C (2005) The Plasticity of Aging: Insights from Long-Lived Mutants. *Cell* 120: 449–460

Kozmik Z, Pfeffer P, Kralova J, Paces J, Paces V, Kalousova A & Cvekl A (1999) Molecular cloning and expression of the human and mouse homologues of the Drosophila dachshund gene. *Dev Genes Evol* 209: 537–545

Kretzschmar M, Liu F, Hata A, Doody J & Massagué J (1997) The TGF-beta family mediator Smad1 is phosphorylated directly and activated functionally by the BMP receptor kinase. *Genes Dev* 11: 984–995

Kubrak OI, Kučerová L, Theopold U & Nässel DR (2014) The sleeping beauty: how reproductive diapause affects hormone signaling, metabolism, immune response and somatic maintenance in Drosophila melanogaster. *PloS One* 9: e113051

Lagna G, Hata A, Hemmati-Brivanlou A & Massagué J (1996) Partnership between DPC4 and SMAD proteins in TGF-β signalling pathways. *Nature* 383: 832–836

Li Y, Turck CM, Teumer JK & Stavnezer E (1986) Unique sequence, ski, in Sloan-Kettering avian retroviruses with properties of a new cell-derived oncogene. *J Virol* 57: 1065–1072

Love MI, Huber W & Anders S (2014) Moderated estimation of fold change and dispersion for RNA-seq data with DESeq2. *Genome Biol* 15: 550

Love MI, Soneson C, Hickey PF, Johnson LK, Pierce NT, Shepherd L, Morgan M & Patro R (2020) Tximeta: Reference sequence checksums for provenance identification in RNA-seq. *PLOS Comput Biol* 16: e1007664

Luis NM, Wang L, Ortega M, Deng H, Katewa SD, Li PW-L, Karpac J, Jasper H & Kapahi P (2016) Intestinal IRE1 Is Required for Increased Triglyceride Metabolism and Longer Lifespan under Dietary Restriction. *Cell Rep* 17: 1207–1216

Lyons GE, Micales BK, Herr MJ, Horrigan SK, Namciu S, Shardy D & Stavnezer E (1994) Proto-tooncogene c-ski is expressed in both proliferating and postmitotic neuronal populations. *Dev Dyn* 201: 354–365

Macdonald SJ & Highfill CA (2020) A naturally-occurring 22-bp coding deletion in Ugt86Dd reduces nicotine resistance in Drosophila melanogaster. *BMC Res Notes* 13: 188

Macías-Silva M, Abdollah S, Hoodless PA, Pirone R, Attisano L & Wrana JL (1996) MADR2 is a substrate of the TGFbeta receptor and its phosphorylation is required for nuclear accumulation and signaling. *Cell* 87: 1215–1224

Mardon G, Solomon NM & Rubin GM (1994) dachshund encodes a nuclear protein required for normal eye and leg development in Drosophila. *Development* 120: 3473–3486

Marriage TN, King EG, Long AD & Macdonald SJ (2014) Fine-mapping nicotine resistance loci in Drosophila using a multiparent advanced generation inter-cross population. *Genetics* 198: 45–57

Massagué J (1990) The transforming growth factor-beta family. *Annu Rev Cell Biol* 6: 597–641

Mattila J, Havula E, Suominen E, Teesalu M, Surakka I, Hynynen R, Kilpinen H, Väänänen J, Hovatta I, Käkelä R, *et al* (2015) Mondo-Mlx Mediates Organismal Sugar Sensing through the Gli-Similar Transcription Factor Sugarbabe. *Cell Rep* 13: 350–364

Mezan S, Feuz JD, Deplancke B & Kadener S (2016) PDF Signaling Is an Integral Part of the Drosophila Circadian Molecular Oscillator. *Cell Rep* 17: 708–719

Miyazono K, Suzuki H & Imamura T (2003) Regulation of TGF-β signaling and its roles in progression of tumors. *Cancer Sci* 94: 230–234

Nagy D, Cusumano P, Andreatta G, Anduaga AM, Hermann-Luibl C, Reinhard N, Gesto J, Wegener C, Mazzotta G, Rosato E, *et al* (2019) Peptidergic signaling from clock neurons regulates reproductive dormancy in Drosophila melanogaster. *PLoS Genet* 15: e1008158

Nässel DR, Liu Y & Luo J (2015) Insulin/IGF signaling and its regulation in Drosophila. *Gen Comp Endocrinol* 221: 255–266

Nässel DR & Williams MJ (2014) Cholecystokinin-Like Peptide (DSK) in Drosophila, Not Only for Satiety Signaling. *Front Endocrinol* 5: 219

Ng HH & Bird A (2000) Histone deacetylases: silencers for hire. *Trends Biochem Sci* 25: 121–126

Nomura N, Sasamoto S, Ishii S, Date T, Matsui M & Ishizaki R (1989) Isolation of human cDNA clones of ski and the ski-related gene, sno. *Nucleic Acids Res* 17: 5489–5500

Okamoto N, Yamanaka N, Yagi Y, Nishida Y, Kataoka H, O'Connor MB & Mizoguchi A (2009) A fat body-derived IGF-like peptide regulates postfeeding growth in Drosophila. *Dev Cell* 17: 885–891

Patro R, Duggal G, Love MI, Irizarry RA & Kingsford C (2017) Salmon provides fast and bias-aware quantification of transcript expression. *Nat Methods* 14: 417–419

Pearson-White S & Crittenden R (1997) Proto-oncogene Sno expression, alternative isoforms and immediate early serum response. *Nucleic Acids Res* 25: 2930–2937

Pelzer T, Lyons GE, Kim S & Moreadith RW (1996) Cloning and characterization of the murine homolog of the sno proto-oncogene reveals a novel splice variant. *Dev Dyn Off Publ Am Assoc Anat* 205: 114–125

Pfeiffer BD, Ngo T-TB, Hibbard KL, Murphy C, Jenett A, Truman JW & Rubin GM (2010) Refinement of tools for targeted gene expression in Drosophila. *Genetics* 186: 735–755

Port F & Bullock SL (2016) Augmenting CRISPR applications in *Drosophila* with tRNA-flanked sgRNAs. *Nat Methods* 13: 852

Pot I & Bonni S (2008) SnoN in TGF-beta signaling and cancer biology. *Curr Mol Med* 8: 319–328

Quijano JC, Stinchfield MJ, Zerlanko B, Gibbens YY, Takaesu NT, Hyman-Walsh C, Wotton D & Newfeld SJ (2010) The Sno Oncogene Antagonizes Wingless Signaling during Wing Development in Drosophila. *PLoS ONE* 5

Raftery LA & Sutherland DJ (1999) TGF-beta family signal transduction in Drosophila development: from Mad to Smads. *Dev Biol* 210: 251–268

Ramel M-C, Emery CS, Foulger R, Goberdhan DCI, van den Heuvel M & Wilson C (2007) Drosophila SnoN modulates growth and patterning by antagonizing TGF-β signalling. *Mech Dev* 124: 304–317

Rass M, Oestreich S, Guetter S, Fischer S & Schneuwly S (2019) The Drosophila fussel gene is required for bitter gustatory neuron differentiation acting within an Rpd3 dependent chromatin modifying complex. *PLOS Genet* 15: e1007940

Ruaud A-F, Lam G & Thummel CS (2011) The Drosophila NR4A nuclear receptor DHR38 regulates carbohydrate metabolism and glycogen storage. *Mol Endocrinol Baltim Md* 25: 83–91

Saltiel AR & Kahn CR (2001) Insulin signalling and the regulation of glucose and lipid metabolism. *Nature* 414: 799–806

Schiesari L, Andreatta G, Kyriacou CP, O'Connor MB & Costa R (2016) The Insulin-Like Proteins dILPs-2/5 Determine Diapause Inducibility in Drosophila. *PloS One* 11: e0163680

Schindelin J, Arganda-Carreras I, Frise E, Kaynig V, Longair M, Pietzsch T, Preibisch S, Rueden C, Saalfeld S, Schmid B, *et al* (2012) Fiji: an open-source platform for biological-image analysis. *Nat Methods* 9: 676–682

Semaniuk UV, Gospodaryov DV, Feden'ko KM, Yurkevych IS, Vaiserman AM, Storey KB, Simpson SJ & Lushchak O (2018) Insulin-Like Peptides Regulate Feeding Preference and Metabolism in Drosophila. *Front Physiol* 9

Shravage BV, Altmann G, Technau M & Roth S (2007) The role of Dpp and its inhibitors during eggshell patterning in Drosophila. *Development* 134: 2261–2271

Söderberg JAE, Carlsson MA & Nässel DR (2012) Insulin-Producing Cells in the Drosophila Brain also Express Satiety-Inducing Cholecystokinin-Like Peptide, Drosulfakinin. *Front Endocrinol* 3: 109

Souchelnytskyi S, Tamaki K, Engström U, Wernstedt C, ten Dijke P & Heldin CH (1997) Phosphorylation of Ser465 and Ser467 in the C terminus of Smad2 mediates interaction with Smad4 and is required for transforming growth factor-beta signaling. *J Biol Chem* 272: 28107–28115

Takaesu NT, Hyman-Walsh C, Ye Y, Wisotzkey RG, Stinchfield MJ, O'connor MB, Wotton D & Newfeld SJ (2006) dSno facilitates baboon signaling in the Drosophila brain by switching the affinity of Medea away from Mad and toward dSmad2. *Genetics* 174: 1299–1313

Takaesu NT, Stinchfield MJ, Shimizu K, Arase M, Quijano JC, Watabe T, Miyazono K & Newfeld SJ (2012) Drosophila CORL is required for Smad2-mediated activation of Ecdysone Receptor expression in the mushroom body. *Dev Camb Engl* 139: 3392–3401

Tatar M, Kopelman A, Epstein D, Tu MP, Yin CM & Garofalo RS (2001) A mutant Drosophila insulin receptor homolog that extends life-span and impairs neuroendocrine function. *Science* 292: 107–110

Tecalco-Cruz AC, Ríos-López DG, Vázquez-Victorio G, Rosales-Alvarez RE & Macías-Silva M (2018) Transcriptional cofactors Ski and SnoN are major regulators of the TGF-β/Smad signaling pathway in health and disease. *Signal Transduct Target Ther* 3: 15

Ten Dijke P, Goumans M-J, Itoh F & Itoh S (2002) Regulation of cell proliferation by Smad proteins. *J Cell Physiol* 191: 1–16

Varghese J, Lim SF & Cohen SM (2010) Drosophila miR-14 regulates insulin production and metabolism through its target, sugarbabe. *Genes Dev* 24: 2748–2753

Wairkar YP, Trivedi D, Natarajan R, Barnes K, Dolores L & Cho P (2013) CK2α regulates the transcription of BRP in Drosophila. *Dev Biol* 384: 53–64

Waite KA & Eng C (2003) From developmental disorder to heritable cancer: it's all in the BMP/TGF-β family. *Nat Rev Genet* 4: 763–773

Walldén K, Nyman T & Hällberg BM (2017) SnoN Stabilizes the SMAD3/SMAD4 Protein Complex. *Sci Rep* 7

Wrana JL, Attisano L, Cárcamo J, Zentella A, Doody J, Laiho M, Wang XF & Massagué J (1992) TGF beta signals through a heteromeric protein kinase receptor complex. *Cell* 71: 1003–1014

Wrana JL, Attisano L, Wieser R, Ventura F & Massagué J (1994) Mechanism of activation of the TGF-β receptor. *Nature* 370: 341–347

Wu K, Yang Y, Wang C, Davoli MA, D'Amico M, Li A, Cveklova K, Kozmik Z, Lisanti MP, Russell RG, *et al* (2003) DACH1 inhibits transforming growth factor-beta signaling through binding Smad4. *J Biol Chem* 278: 51673–51684

Zhu Q, Chang A, Xu A & Luo K (2018) The regulatory protein SnoN antagonizes activin/Smad2 protein signaling and thereby promotes adipocyte differentiation and obesity in mice. *J Biol Chem* 293: 14100–14111

Zinke I, Schütz CS, Katzenberger JD, Bauer M & Pankratz MJ (2002) Nutrient control of gene expression in Drosophila: microarray analysis of starvation and sugar-dependent response. *EMBO J* 21: 6162–6173

6.2. Figures

6.3. Tables

6.4. Abbreviations

ANOVA	Analysis of variance
Asph	Aspartyl β-hydroxylase
b	brain
BMP	Bone Morphogenetic Protein
Cas9	CRISPR-associated 9
CCHa1	CCHamide1
CKII	Casein Kinase 2
CKIIα-i3	CKII-α subunit interactor-3
CNS	central nervous system
Co-Smad	common mediator Smad
CRISPR	Clustered Regularly Interspaced Short Palindromic Repeats
Cyp6a17	cytochrome P450 protein 6a17
Cyp6a20	cytochrome P450 proteins 6a20
Dac	Dachshund
Dach	Dachshund Homolog
D-Box	Destruction Box
DHD	Dachshund domain
DN	dorsal neurons
Dpp	Decapentaplegic
DSB	double strand break
Dsk	Drosulfakinin
FasII	Fasciclin II
fb	fat body
Fig	Figure
Fussel	Functional Smad Suppressing Element
GFP	Green Fluorescent Protein
HDR	homology-directed repair
Hr38	Hormone receptor-like 38
IGF	Insulin-like Growth Factor
IIS	Insulin/IGF signalling
Ilp	Insulin-like peptide
indel	insertion/deletion
InR	Insulin receptor
IPCs	Insulin producing cells
Kc	Kenyon cells
l-LNv	large ventral-lateral neurons

LN	lateral neurons
LNd	dorsal-lateral neurons
LPN	lateral posterior neurons
Mad	Mother Against Dpp
mb	mushroom bodies
mNSC	median neurosecretory cell
NHEJ	non-homologous end joining
NLS	nuclear localisation sequence
OBB	Odyssey Blocking Buffer
ol	optic lobes
PAGE	Polyacrylamide gel electrophoresis
PAM	protospacer adjacent motif
PBS	Phosphate buffered saline
PBST	PBS with Tween20
PCR	Polymerase Chain Reaction
Pdf	Pigment-dispersing factor
pH3	phosphorylated Histone 3
pMAD	phosphorylated MAD
PNK	Polynucleotide Kinase
qPCR	quantitative real time PCR
R-Smad	receptor associated Smad
SAND	Sp100, AIRE1, NucP41/75 and DEAF1
SDBB	Semi-Dry Blotting Buffer
sgRNA	single guide RNA
Ski	Sloan-Kettering Institute
s-LNv	small ventral-lateral neurons
Smox	Smad on X
SnoN	Ski novel gene
Snoo	Sno oncogene
STE	Sodium Chloride-Tris-EDTA
Sug	Sugarbabe
Tab	Table
TAE	Tris-Acetate-EDTA
TAG	triacylglyceride
TBS	Tris buffered saline
TBST	TBS with Tween20
TGFβ	Transforming Growth Factor β

tRNA	transfer RNA
UAS	Upstream Activation Sequence
Ugt86Dd	UDP-glucuronosyltransferase 86Dd
VNC	ventral nerve cord
β-Gal	β-Galactosidase

Acknowledgements

Ich möchte mich bei meinem Doktorvater Prof. Dr. Stephan Schneuwly für die Möglichkeit bedanken dieses Projekt durchzuführen.

Vielen Dank an meine beiden Mentoren und Prüfer Prof. Dr. Eugen Kerkhoff und Prof. Dr. Frank Sprenger.

Besonderen Dank auch an Prof. Dr. Micheal Rehli und seine Arbeitsgruppe für die Kooperation beim RNAseq.

I want to thank Ottavia Palazzo and the whole lab of Prof. Dr. Björn Brembs for the help with the Buridan's paradigm assay.

Besonders bedanken möchte ich mich vor allem bei Dr. Mathias Raß für die umfassende Unterstützung während der gesamten Promotion und für die Auswertung der RNAseq-Daten.

I want to kindly thank Dr. Juan Navarro for the help with many experiments and with statistics.

Vielen Dank an Renate Reng für die Unterstützung bei den Mikroinjektionen und Ursula Roth für die Anfertigung der Semidünnschnitte.

Darüber hinaus bedanke ich mich bei Maximilian Hauck, Ramona Pawlak, Julia Pable, Larissa Kalb, Michael Schletter, Delila Aslouj, Katharina Schneider, Christian Schwarz und Andreas Berger, die im Rahmen von Laborpraktika oder Abschlussarbeiten an diesem Projekt beteiligt waren.

Vielen Dank an Dr. Susanne Fischer, Gudrun Karch, Dr. José Botella-Munoz, Anneliese Götz, Christa Preischl und Eva Köppl für die schöne Zeit am Lehrstuhl.

Ich bedanke mich insbesondere bei Svenja Oestreich und Laura Gizler, weil ihr mir immer das Gefühl gegeben habt kompetent zu sein und für die Wärme, die ihr mir entgegengebracht habt.

Schließlich möchte ich mich bei meiner Familie, meinen Freunden und meinem Freund bedanken, weil ihr mich immer unterstützt habt, indem ihr euch mein Gejammer über die Arbeit angehört habt und bei persönlichen Problemen immer für mich da wart.